The role of CRAC channel inhibitor CM4620 in pancreatic acinar cells as a potential therapy for acute pancreatitis

Thesis submitted in accordance with the requirements of Cardiff University for the degree of Master of Philosophy (MPhil)

Siân Lewis

May 2020

Summary

Introduction. Acute pancreatitis (AP) is a life-threatening disorder with significant morbidity, mortality and no specific therapy available in the clinic. Excessive alcohol consumption and gallstone biliary disease are the leading causative factors of AP. Excessive release of Ca^{2+} from intracellular stores and subsequent activation of Ca^{2+} release-activated Ca^{2+} (CRAC) channels instigates cytosolic Ca^{2+} overload, mitochondrial dysfunction, necrosis and premature activation of digestive enzymes. Currently, a novel selective CRAC channel inhibitor CM4620 (developed by CalciMedica) has reached phase III human trials. However, this inhibitor has a very short therapeutic window due to its profound effects on immune cells. Recently, another approach has emerged where cells are supplied with energy supplement galactose, reducing AP effects *in vitro* and *in vivo*. This thesis aimed to combine these two approaches *in vitro* and *in vivo.*

Methods. The effect of 1 μM and 10 μM CM4620 on calcium entry was recorded, using fluorescence imaging, by depleting intracellular calcium stores and activating calcium influx. Different concentrations of CM4620 (100 nM, 50 nM, 10 nM, 1 nM, 200 pM) were administered in the presence or absence of galactose (1 mM) and the effects on cellular necrosis levels, elicited by AP-inducing agents, was also measured using confocal microscopy. Additionally, the effect of nanomolar concentrations of CM4620 in alcohol-induced *in vivo* models of AP was investigated.

Results. The data presented in this thesis shows that CM4620 markedly protects against acinar cell necrosis *in vitro* at much lower concentrations (100 nM, 50 nM, 10 nM, 1 nM, 200 pM) than reported previously, following exposure to bile acids, alcohol metabolites and asparaginase. Combining CM4620 and galactose (1 mM) provided a higher degree of protection, reducing the extent of necrosis to near-control levels. Administering 0.1 mg/kg CM4620 significantly diminished pancreatic histopathology in alcohol-induced *in vivo* mouse models of AP.

Conclusions. As a potential therapy for the incurable disease AP, the protective capability of low concentrations of CM4620 could also diminish side effects resulting from CRAC channel inhibition. The novel combination of CM4620 with galactose increases the effectiveness of treatments and is therefore a very promising therapeutic future avenue.

Table of Contents

Table of Figures

Abbreviations

AAP	Asparaginase-associated Pancreatitis
ACH	Acetylcholine
ADH	Alcohol Dehydrogenase
ALL	Acute Lymphoblastic Leukaemia
AP	Acute Pancreatitis
ASNase	L-Asparaginase
ATP	Adenosine Triphosphate
BA	Bile Acid
BCL	B-cell Lymphoma
BH	B-cell Lymphoma-homology
Ca^{2+}	Calcium Ion
$CaCl_2$	Calcium Chloride
CAD	CRAC Activation Domain
cADPR	Cyclic Adenosine Diphosphate-Ribose
CALP	Ca^{2+}-like Peptide
CBD	Common Bile Duct
CCK	Cholecystokinin
CICR	Calcium-induced Calcium Release
CP	Chronic Pancreatitis
CPA	Cyclopiazonic Acid
CRAC	Ca^{2+} Release-activated Ca^{2+} Current
CYP 2E1	Cytochrome P450 2E1
DAG	Diacylglycerol
DMSO	Dimethyl Sulfoxide
E. Coli	Escherichia Coli
EGTA	Ethylene Glycol Tetraacetic Acid
ER	Endoplasmic Reticulum
EV	Endocytic Vacuoles
FA	Fatty Acid
FAEE	Fatty Acid Ethyl Ester
FAEE-AP	Fatty Acid Ethyl Ester Acute Pancreatitis
FDA	Food and Drug Administration
GSK-7975A	2,6-Difluoro-N-1(1-(4-Hydroxy-2-(Trifluoromethyl)Benzyl)-1H-Pyrazol-3-Yl)Benzamide
H&E	Haematoxylin-eosin
HEPES	4-(2-Hydroxyethyl)Piperaxine-1-Ethanesulfonic Acid
IMM	Inner Mitochondrial Membrane
IP	Intraperitoneal

IP_3	1,4,5-trisphosphate
IP_3R	IP_3 Receptor
IV	Intravenous
MCU	Mitochondrial Ca^{2+} Uniporter
MPTP	Mitochondrial Permeability Transition Pore
NAADP	Nicotinic Acid Adenine Dinucleotide Phosphate
NAOH	Sodium Hydroxide
NCE	Na^{+}- Ca^{2+} Exchanger
NTCP	Na^{+} Taurocholate Co-transporting Polypeptide
OATP	Organic Anion Transporting Polypeptide
PAC	Pancreatic Acinar cell
PAR	Protease-activated Receptor
PASC	Pancreatic Stellate Cell
PBS	Phosphate-buffered Saline
PI	Propidium Iodide
PLC	Phospholipase C
PM	Plasma Membrane
PMCA	Plasma Membrane Ca^{2+}-ATPase
POA	Palmitoleic Acid
POAEE	Palmitoleic Acid Ethyl Ester
PP	Pancreatic Polypeptide
RBL	Rat Basophilic Leukaemia
ROS	Reactive Oxygen Species
RyR	Ryanodine Receptor
SAM	Sterile α-motif Domain
SCID	Severe Combined Immunodeficiency
SERCA	Sacro/Endoplasmic Reticulum Ca^{2+}-activated
siRNA	Small Interfering RNA
SOCE	Store-operated Calcium Entry
STIM	Stromal Interaction Molecule
TL	Transmitted Light
TLC-S	Taurolithocholic Acid 3-Sulfate
TM	Transmembrane
TPC	Two-pore Channel
TRPC	Transient Receptor Potential
US	United States
ZG	Zymogen Granule

Acknowledgements

Firstly, I would like to thank my supervisors, Dr Julia Gerasimenko and Dr Oleg Gerasimenko, for their kindness, wisdom, inspiration and guidance that helped to shape this entire project. Secondly, I would like to thank Professor Ole Petersen for his invaluable advice and considerable scientific thinking. Special thanks to Dr Oleksiy Gryshchenko, Dr Tetyana Tsugorka Dr Shuang Peng and David for their technical support, knowledge and positivity throughout my project. I also owe a great deal of gratitude to my office colleagues, Lucy, Beth, Rich and Ping, for their time and constant encouragement during my studies.

Many thanks to the staff in the JBIOS animal unit, especially Mr Rhys Perry, Mrs Veronica Walker and Miss Helen Read for their training and advice. I would also like to thank the staff in the Bioimaging Hub for microscopy technical support as well as their assistance with histological slide preparing and sample processing.

I would like to thank the James Pantyfedwen Foundation for funding my tuition fees. Also, many thanks to CalciMedica for providing CM4620.

Finally, thank you to all my family and friends, especially Mum, Dad, Gareth and William, for their eternal support and motivation every step of the way.

CHAPTER 1: INTRODUCTION

CHAPTER 1: Introduction

1.1 Acute pancreatitis

Acute pancreatitis (AP) is a life-threatening, inflammatory disorder in which pancreatic tissue and its surroundings are digested. This process of autodigestion is caused by premature activation of digestive proenzymes inside pancreatic acinar cells (PACs) (as opposed to normal activation occurring when they are secreted into the gut). This results in necrosis and inflammation (Petersen *et al.,* 2011). AP can vary considerably in its presentation, from a mild, self-limiting disorder, to a more severe disease coupled with significant mortality. Unfortunately, there is no specific pharmacological therapy available for this devastating disease (Pandol *et al.,* 2007; Petersen and Sutton, 2006).

AP sufferers typically present with a wide range of symptoms, including severe upper abdominal pain, vomiting, nausea, fever, jaundice, diarrhoea, back pain and weight loss (Manohar *et al.,* 2017). Incidence rates of up to 100 people per 100,000 per annum have been reported for AP and have been continually increasing, on a global basis, for the past 40 years (Pandol *et al.,* 2007; Spanier *et al.,* 2008; Hamada *et al.,* 2014). An increase in the number of cases of paediatric AP has also been documented during the past 20 to 25 years (Lopez, 2002; Nydegger *et al.,* 2007; Park *et al.,* 2009b; Morinville *et al.,* 2010). Although the majority of AP cases are mild to moderate and tend to resolve spontaneously with supportive care, AP generally has a sudden onset and carries a significant mortality rate of around 5% (Petersen and Sutton, 2006; Pandol *et al.,* 2007). Furthermore, it is approximated that the disease state of 20% of patients will advance, with prolonged hospitalisation and more severe complications characterised by significant PAC necrosis, a systemic inflammatory response, multiple organ failure and an increased mortality of 30% (Pandol *et al.,* 2007; Petersen *et al.,* 2011; Krishnan, 2017). With 270,000 hospital admissions and an annual inpatient cost of $2.6 billion, AP was the single most common specific gastrointestinal diagnosis in the United States (US), in 2009 (Peery *et al.,* 2012). Furthermore, between 2017 and 2018, there were over 28,000 hospital admissions recorded for AP in England (Hospital Admitted Patient Care Activity, 2018). This devastating disease is consequently creating an increasing burden on healthcare services.

It is well established in the literature that repeated attacks of AP can lead to Chronic pancreatitis (CP). This condition is characterised by progressive fibrosis, inflammation and scarring of the exocrine pancreas, ultimately causing damage and failure of the gland and its cellular contents (Sankaran *et al.,* 2015; Ahmed *et al.,* 2016; Majumder and Chari, 2016). This chronic syndrome also markedly increases the risk of developing pancreatic cancer, by up to 100-fold (Petersen and Sutton, 2006; Criddle *et al.,* 2007; Petersen *et al.,* 2009). With a devastating 5-year survival rate of 8% and an estimated 44,330 deaths in the US in 2018, pancreatic cancer is described as one of the most intractable, rapidly progressive and fatal malignancies (Siegel *et al.,* 2018). The silent nature, relatively common and nonspecific symptoms of pancreatic cancer (including weight loss, abdominal pain, light-coloured stools and vomiting), account for its poor prognosis. Less than 10% of patients are diagnosed in the early stages of pancreatic cancer where symptoms are seldom as prominent (Kamisawa *et al.,* 2016; Kikuyama *et al.,* 2018).

Gallstone biliary disease and excessive alcohol consumption are the leading causative factors of AP, responsible for approximately 70-80% of cases (Spanier *et al.,* 2008; Nesvaderani *et al.,* 2015; Forsmark *et al.,* 2016). Transient blockage of either the bile duct, pancreatic duct, or both by gallstone migration out of the gallbladder is the most common cause of AP. This obstruction can result in bile reflux into the pancreatic duct or an increase in pressure, exposing the pancreas to biliary components thus inducing pancreatic acinar cell injury (Petersen and Sutton, 2006; Perides *et al.,* 2010b; Yadav and Lowenfels, 2013). Although the second most common cause of AP and the leading cause of CP, alcohol abuse is less well understood as only a fraction of heavy drinkers (2 to 5%) are at risk of developing pancreatitis. Significant alcohol use over a prolonged period i.e., four to five drinks per day over 5 years, is required for ethanol-induced pancreatitis (Coté *et al.,* 2011). The mechanisms underlying alcohol-induced pancreatitis are highly complex. It is thought that alcohol and both its oxidative and non-oxidative metabolites predispose the exocrine pancreas to toxic effects, resulting in autodigestive damage or more chronic forms of pancreatitis (Apte *et al.,* 2010). Other causes of AP include smoking, medication, hyperlipidemia, hypercalcemia, hyperparathyroidism, surgical complications, trauma, obesity and environmental toxins (Badalov *et al.,* 2007; Pandol *et al.,* 2007; Sadr-Azodi *et al.,* 2012; Manohar *et al.,* 2017). Another cause of AP is L-asparaginase (ASNase), a treatment received by

patients suffering with acute lymphoblastic leukaemia (ALL). This is defined as asparaginase-associate pancreatitis (AAP). Although ALL is the most common type of cancer affecting children, antileukemic drugs based on ASNase have been used since the 1960s and are an essential element in treatments used in the clinic currently. The use of ASNase has markedly increased survival rates of childhood ALL (Wolthers *et al.,* 2017). The most common purpose for ending ASNase treatment, however, is the development of AP as a serious adverse reaction which occurs in up to 10% of cases (Alvarez and Zimmerman, 2000; Silverman *et al*., 2001; Knoderer *et al.,* 2007; Flores-Calderon *et al.,* 2009; Kearney *et al.,* 2009; Treepongkaruna *et al.,* 2009; Raja *et al.,* 2012). The pathophysiological mechanisms underlying this well-recognised complication have not been intensely investigated and are poorly understood. Despite a concerted research effort to significantly improve our knowledge of the pathogenesis and pathophysiology underlying AP, there is still no licensed therapeutic available. Developing an effective treatment for AP is vital to mitigate the suffering of individuals and minimise the burden of this life-threatening disease on global healthcare systems.

1.2 The pancreas

The human pancreas is a vital digestive and endocrine gland, lying retroperitoneally on the posterior abdominal wall, within the left upper abdominal cavity (Ellis, 2013; Vishy, 2016). It has a slight irregular shape, measuring around 15 cm in length and 5 cm wide, with a weight varying from 82 to 117 g. For descriptive purposes, the pancreas is divided into four parts: the head, neck, body and tail (Fig. 1.1). The head and neck of the pancreas lie marginally to the right of the midline. The body of the pancreas passes to the left, arching anterior to the aorta and the vertebral column (at the level of L1), before verging upwards to become continuous with the tail which lies to the left of the midline, adjoining the hilus of the spleen. Physical examination of the pancreas is not possible due to its deep location, posterior to numerous abdominal viscera. The pancreas comprises a main pancreatic duct (duct of Wirsung) and an accessory pancreatic duct (duct of Santorini). The main pancreatic duct runs the length of the pancreas and unites with the common bile duct (CBD) to open into the duodenum through the ampulla of Vater, at the major duodenal papilla (Fig. 1.1). The accessory pancreatic duct opens approximately 2 cm proximal to the main duct opening, at the minor papilla

(Vishy, 2016). Macroscopically, the pancreas has a lobulated appearance and is enclosed within a fibrous capsule (Ellis, 2013).

The pancreas has a fundamental dual function, executing a variety of multifaceted endocrine and exocrine functions (Ellis, 2013). The endocrine component consists of around one million islets of Langerhans which are small, clustered alpha (α), beta (β), delta (δ) and pancreatic polypeptide (PP) cells that constitute for only 1-2% of the developed pancreas (Chandra and Liddle, 2009) (Fig. 1.1). The islets secrete hormones such as glucagon (α cells), insulin (β cells), somatostatin and gastrin (δ cells) and PP cells, thus functioning in blood glucose homeostasis (Leung and Ip, 2006). The focus of this study however, the exocrine pancreas, accounts for 95-99% of the entire organ and primarily comprises PACs and ductal cells (Fig. 1.1). The exocrine pancreas is responsible for the organ's finely lobulated exterior. Within these lobules are acinar cell units which individually contain multiple PACs, interconnected by tight junctions. Digestive enzymes required for nutrient digestion (such as trypsinogen, chymotrypsinogen, amylase and lipase) are secreted from the acinar cell units into a highly elaborate, branched ductal network which eventually opens into the second part of the duodenum. Whereas the duct cells secrete an alkaline bicarbonate-rich fluid that neutralises the acidic chime and gastric acid existing in the duodenum (Johansson and Grapin-Botton, 2002).

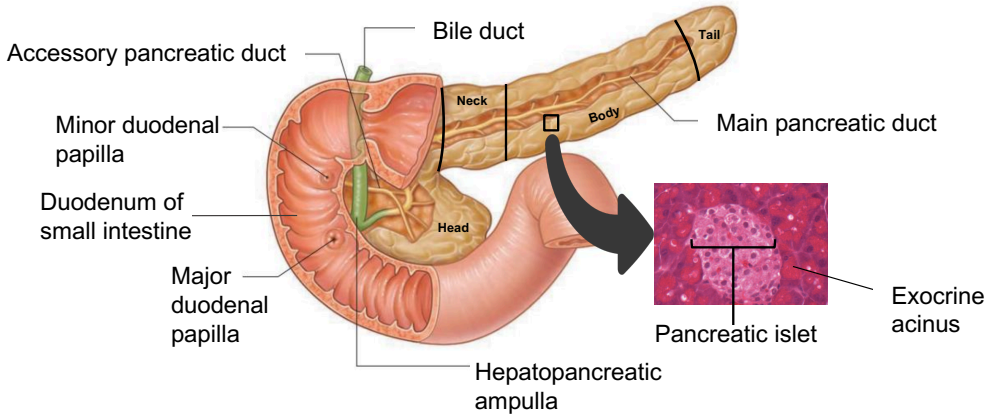

Figure 1.1. The pancreas. The exocrine component of the pancreas consists of highly specialised pancreatic acinar cells (PACs). These cells secrete digestive enzymes into the second part of the duodenum, through the pancreatic duct system, for nutrient digestion. The endocrine function is mediated by a variety of hormones secreted into the bloodstream from cell types, including α and β cells within the islets of Langerhans. The micrograph demonstrates mouse pancreatic islets, surrounded by pancreatic acinar cells. Micrograph taken with x20 objective on an Olympus BX41 brightfield microscope (adapted from Drake *et al.,* 2014; Röder *et al.,* 2016).

1.2.1 Structure and function of the pancreatic acinar cell

The tightly polarised PAC is a terminally differentiated epithelial cell type with a round pyramid-like appearance (Low *et al.,* 2010). PACs are highly specialised and each cell consists of two plasma membrane domains: the large basolateral membrane situated at the acinar periphery and the apical membrane which forms the boundary of the acinar lumen that abuts a small intercalated duct. Groups of intercalated ducts directly connect the acinar lumen to larger intralobular ducts which subsequently converge into extralobular ducts, forming the main collecting pancreatic duct that drains into the duodenum (Leung and Ip, 2006; Logsdon and Baoan, 2014). Organelles are distinctly located in PACs due to the high polarisation which is sustained by tight and adherens junctions to adjacent cells. Specific secretory granules, namely zymogen granules (ZGs), function as a storage unit for digestive enzymes. These granules are highly concentrated near the apical pole of the cell, which is in close proximity to the duct of the exocrine pancreas for efficient secretion (Fig. 1.2) (Low *et al.,* 2010). Three main areas in the acinar cell accommodate mitochondria in order for the organelle to perform specific functions: 1) the nuclear region; 2) the sub-plasma membrane; 3) mainly around the ZG area, in the perigranular portion (Fig. 1.2) (Tinel *et al.,* 1999; Park *et al.,* 2001; Petersen, 2012). The basolateral region of the acinar cell comprises the majority of the endoplasmic reticulum (ER) which surrounds the nucleus. The ER, however, also significantly extends into the apical region of the cell where strands of ER actually surround each ZG (Park *et al.,* 2000; Gerasimenko *et al.,* 2002).

The exocrine pancreas was originally utilised as a model to discover the structural and functional organisation of the mammalian secretory pathway and has been extensively studied subsequently (Palade, 1975). PACs primarily mediate the synthesis, storage and regulated secretion of hydrolytic digestive enzymes required for food digestion and absorption within the small intestine (Williams, 2008; Husain and Thrower, 2009; Logsdon and Baoan, 2014). Carbohydrates, fats and proteins are hydrolysed by α-amylase, lipase and proteases, respectively. These three classes of digestive enzymes are specifically secreted by PACs (Leung and Ip, 2006). The initial process of digestive enzyme synthesis transpires in the rough ER, forming the first secretory pathway compartment. This is followed by the sorting and packing of these inactive proenzymes into large, optically dense secretory (zymogen) granules, at the trans-Golgi network. Lastly, food ingestion initiates both the PAC secretion process as well as endocrine, neurocrine and paracrine

pathways that control the release of appropriate quantities of digestive enzymes to closely match dietary need. Food ingestion also evokes the release of particular secretagogues such as acetylcholine (ACh) and cholecystokinin (CCK) (Fig. 1.2). Upon binding of these secretagogues to their corresponding receptors on the acinar cell basolateral membrane, digestive enzyme secretion into the pancreatic ductal system ensues via exocytosis. Fusion of the granule membrane with the apical cell membrane permits movement of zymogens into the acinar lumen. A neutral chloride- and bicarbonate-rich fluid secretion from acinar cells and small ducts, respectively, enables zymogen movement from the ductal system into the gut (Leung and Ip, 2006). Under physiological conditions, inactive precursor forms of digestive enzymes (such as trypsinogen as the precursor of trypsin) are then solely activated extrapancreatically after their release into the duodenal lumen. Enteropeptidase, an enzyme secreted by small intestinal epithelial cells, converts trypsinogen into active trypsin which subsequently triggers an activation cascade of other proteolytic enzymes (Case, 1978; Petersen and Sutton, 2006). Therefore, the intermediate storage process of these harmful proenzymes in acidic ZGs is vital in preventing their premature activity and significant damage to pancreatic tissue (Leung and Ip, 2006).

A

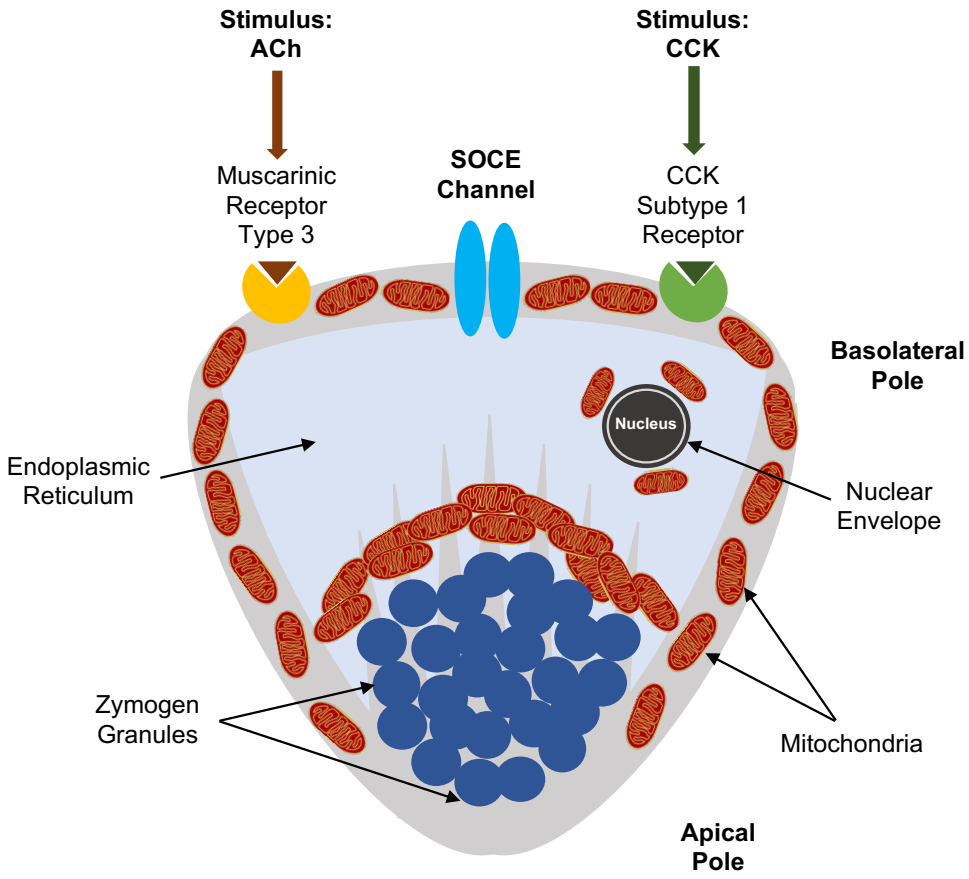

B

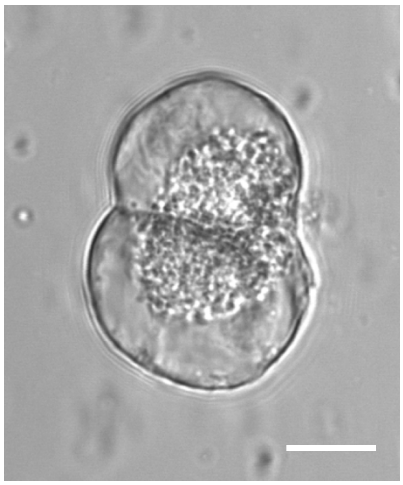

Figure 1.2. Structure of a pancreatic acinar cell. (A) Schematic diagram of a highly polarised, pyramid-shaped acinar cell. The bulk of the endoplasmic reticulum is situated in the basolateral pole, with small projections into the apical region. The zymogen granules are found in the apical pole of the cell. Cell surface receptors are mainly located on the basal membrane of the cell. Mitochondria are localised into three main, sub-cellular areas: sub-plasmalemmal, perigranular and perinuclear (image adapted from Gerasimenko *et al.,* 2006). **(B)** Transmitted light image of a typical doublet acinar cell, freshly isolated from a mouse pancreas. Dark zymogen granules are tightly clustered. Scale bar: 10 μm.

1.3 Physiological calcium signalling in pancreatic acinar cells

As a universal, versatile intracellular messenger, the calcium ion (Ca^{2+}) participates in the dynamic regulation of a myriad of key cellular functions in excitable and non-excitable cells (Berridge *et al.,* 2000). These include gene expression, fertilisation, muscular contraction, neurotransmitter release, exocytosis and cell death (including apoptosis, autophagy and necrosis) thus accompanying cells throughout their lifespan. Ca^{2+} can operate from within microseconds at synaptic endings to driving cell proliferation processes over minutes to hours (Berridge *et al.,* 2000; Li *et al.,* 2014). In order to characterise these functions, it is essential for each cell type to have a specific Ca^{2+} signalling system with various spatio-temporal aspects that are derived from a unique Ca^{2+} signalling toolkit (Berridge *et al.,* 2003). Under normal resting conditions within a eukaryotic cell, the cytosolic Ca^{2+} concentration ($[Ca^{2+}]_i$) is rigorously controlled at around 55 - 100 nM, compared with up to 1 mM in the extracellular fluid depending on the cell type (Chakrabarti and Chakrabarti, 2006). This intracellular Ca^{2+} regulation depends on an equilibrium between the basic “on” reactions that introduce Ca^{2+} signals into the cytoplasm and the “off” reactions that remove signals through the action of buffers, pumps and exchangers (Berridge *et al.,* 2003). Dysregulation of Ca^{2+} signalling, however, is the hallmark of multiple human pathologies such as Alzheimer’s disease, cancer, cardiac disease and in relation to this thesis: acute pancreatitis (Ashby and Tepikin, 2002; Berridge, 2011; Cartwright *et al.,* 2011; Stewart *et al.,* 2015; Gerasimenko *et al.,* 2018).

PACs have been widely used as models of non-excitable cells to investigate the role of Ca^{2+} signalling in the synthesis, processing, vectorial transport and secretion of proteins (Palade, 1975; Mikoshiba *et al.,* 2008; Petersen and Tepikin, 2008; Ambudkar, 2012). Increases in cytosolic Ca^{2+} signals are essential for these PAC functions and are mostly transient and localised in the apical region of the acinar cell, under physiological conditions (Ashby and Tepikin, 2002). Stimulants acting on the outside of the acinar plasma membrane serve as triggers in activating this highly sophisticated Ca^{2+} signalling toolkit. These stimulants include the circulating hormone CCK, produced by intestinal endocrine cells and the neurotransmitter ACh which is released from vagal nerve endings (Iwatsuki and Petersen, 1977; Philpott and Petersen, 1979; Wakui and Petersen, 1990). The intestinal phase of digestion triggers the release of CCK which binds to its G-protein linked

transmembrane receptor, CCK subtype 1 (CCK1) (Owyang, 1996). This interaction activates adenosine diphosphate-ribosyl cyclase which subsequently produces cyclic adenosine diphosphate-ribose (cADPR) and the Ca^{2+}-releasing agent, nicotinic acid adenine dinucleotide phosphate (NAADP) (Yamasaki *et al.,* 2005; Li *et al.,* 2014). ACh is released during all stages of digestion and binds to the G-protein-coupled receptor, muscarinic receptor type 3 (M3) (Petersen, 1992; Nakamura *et al.,* 2013). Upon receptor ligand binding, phospholipase C (PLC) is activated which then hydrolyses phosphatidylinositol 4,5-bisphosphate into the Ca^{2+}-releasing messengers inositol 1,4,5-trisphosphate (IP_3) and diacylglycerol (DAG) which mobilise Ca^{2+} and activate protein kinase C respectively (Fig. 1.5) (Williams, 2001; Li *et al.,* 2014).

1.3.1 Ca^{2+} release from intracellular stores

Release of Ca^{2+} from intracellular stores in PACs is caused by the three second messengers, IP_3, cADPR and NAADP. Although the main intracellular store of Ca^{2+} in PACs is the ER, acidic Ca^{2+} stores are present in the apical pole of the cell, namely the ZGs, late endosomes and lysosomes (Christensen *et al.,* 2002; Lloyd-Evans *et al.,* 2008; Lloyd-Evans and Platt, 2011). The ZGs have previously been shown to release Ca^{2+} via Ca^{2+}-releasing messengers (Gerasimenko *et al.,* 1996a; Yoo et al., 2000; Quesada et al., 2001; Mitchell et al., 2001; Quesada et al., 2003). It is also possible that other acidic organelles such as the Golgi, endosomes or lysosomes contribute towards the liberation of Ca^{2+} in response to Ca^{2+}-releasing messengers (Hirano, 1991; Grondin, 1996; Cerny et al., 2004; Yamasaki et al., 2004; Malosio et al., 2004). Overall, the acidic store demonstrates a high sensitivity to IP_3, cADPR and NAADP signalling pathways (Fig. 4). Ca^{2+} is liberated following binding of these second messengers to specific Ca^{2+} sensitive ligand-gated Ca^{2+} channels (Petersen, 2005; Petersen and Tepikin, 2008; Petersen, 2012). There are two main types of regulated Ca^{2+}-release channels located on the ER membrane: the IP_3 receptors (IP_3Rs) and ryanodine receptors (RyRs).

The IP_3R is a tetrameric intracellular IP_3-gated Ca^{2+} release channel, expressed in almost all cell types with various isoforms (Foskett *et al.,* 2007; Mikoshiba, 2007). IP_3R type 1 is primarily present in the nervous system whilst type 2 and 3 isoforms are expressed in a wide variety of organs, functioning in secretory regulation and proliferation (Futatsugi *et al.,* 2005). IP_3Rs in PACs are predominantly concentrated within the apical region and

require binding of both IP_3 and Ca^{2+} for their activation (Thorn *et al.,* 1993; Nathanson *et al.,* 1994). Stimulation of a PLC-coupled cell surface receptor, such as the muscarinic ACh receptor through ACh binding, activates the IP_3R which releases Ca^{2+} from the ER lumen. IP_3R activation permits the movement of Ca^{2+} into the cytosol, down the concentration gradient (Fig. 1.5). This potential difference across the ER membrane is sustained by the ER luminal free Ca^{2+} concentration (around 100 – 300 μM) (Mogami *et al.,* 1998).

RyRs exist in three isoforms (RYR 1, 2 and 3) and are expressed in a variety of tissues. RyR1 and RyR2 were first found in skeletal and cardiac muscle, respectively and RyR3 was first detected in the brain (Takeshima *et al.,* 1989; Nakai *et al.,* 1990; Hakamata *et al.,* 1992). In contrast to the localisation of IP_3Rs, RyRs are evenly dispersed in both apical and basolateral regions of the PAC. RyRs are also, like IP_3Rs, activated by Ca^{2+} but require second messengers such as cADPR and NAADP (Cancela *et al.,* 2000; Yamasaki *et al.,* 2005; Gerasimenko *et al.,* 2015). Although IP_3R activation requires the dual action of both IP_3 and Ca^{2+}, RyR-dependent Ca^{2+} release from intracellular stores can result from Ca^{2+} alone (Leite *et al.,* 1999). It is thought that NAADP is a potential accessory protein for the activation of two-pore channels (TPCs) which are present on the membrane of acidic Ca^{2+} stores (Calcraft *et al.,* 2009). The subsequent liberation of Ca^{2+} and the ensuing small increases in cytosolic Ca^{2+} concentration further activates additional IP_3Rs and RyRs, inducing additional Ca^{2+} release from intracellular stores. This process is known as calcium-induced calcium release (CICR) (Gerasimenko *et al.,* 2006; Gerasimenko *et al.,* 2015).

Physiological concentrations of ACh and CCK evoke repetitive, local cytosolic Ca^{2+} spiking that originates and is generally confined to the apical region of the cell, despite stimuli acting on receptors at the basolateral plasma membrane (Gerasimenko *et al.,* 2003; Orabi *et al.,* 2013). This Ca^{2+} signalling pattern is due to the dispersal of Ca^{2+} release channels in the acinar cell and CICR which permits propagation of a whole cell Ca^{2+} signal originating from RyRs in the basolateral region of the cell. These increases in $[Ca^{2+}]_i$, due to Ca^{2+} release from the ER in the apical pole, stimulates the secretion process. Secretory granules comprising digestive proenzymes are all situated at the apical pole of the cell, thus aiding the functional purpose of Ca^{2+} release.

1.3.2 Ca^{2+} extrusion and uptake mechanisms from the cytosol

Although cytosolic Ca^{2+} spiking plays an essential role in physiological Ca^{2+} signalling mechanisms and the activation of digestive enzyme exocytosis, the effect of sustained global $[Ca^{2+}]_i$ elevations on PACs can be fatal (Reed *et al.,* 2011). In order to clear Ca^{2+} from the cytosol and maintain a resting $[Ca^{2+}]_i$ level, eukaryotic cells employ a combination of extrusion mechanisms which involve components situated at both the plasma membrane and ER (Fig. 3) (Guerini *et al.,* 2005). These extrusion mechanisms are activated whenever there is an increase in $[Ca^{2+}]_i$ above 100 nM and include the sarcoplasmic/endoplasmic reticulum Ca^{2+}-activated adenosine triphosphate (ATP)ase (SERCA) and plasma membrane Ca^{2+}-ATPase (PMCA) pumps (Fig. 1.5) (Lytton *et al.,* 1992; Carafoli, 1994; Brini and Carafoli, 2011).

The SERCA pump, in PACs, is found on the ER membrane and is therefore predominantly situated at the basal pole of exocrine cells (Lee *et al.*, 1997; Gerasimenko *et al.,* 2002). Under normal, physiological conditions, SERCA actively re-uptakes Ca^{2+} from the cytosol into the ER lumen. This is to compensate for Ca^{2+} release evoked by physiological receptor stimulation whilst also allowing intracellular stores to refill (Petersen and Sutton, 2006; Garside *et al.,* 2010). Once the cell surface receptor stimulation ceases and the ER Ca^{2+} release channels subsequently close, SERCA has a more profound effect on removing Ca^{2+} from the cytosol (Petersen and Tepikin, 2008). In contrast, during unphysiological, sustained receptor stimulation, the ability of SERCA pumps to clear Ca^{2+} from the cytosol through re-uptake into the ER is insignificant due to the opening of Ca^{2+} release channels. Under these circumstances, the PMCA pumps are primarily accountable for Ca^{2+} clearance (Tepikin *et al.,* 1992).

Dissimilar to many excitable cells, PACs do not express functional Na^+-Ca^{2+} exchangers (NCEs). The NCE is an important antiporter situated in the plasma membrane which removes Ca^{2+} out of the cell in exchange for Na^+ ions entering the cell (Blaustein and Lederer, 1999). For example, following an action potential in electrically excitable cardiac cells, NCE is the principle mechanism to extrude Ca^{2+} from the cytosol in order to maintain and restore low $[Ca^{2+}]_i$ levels (Berberián *et al.,* 2012). In non-excitable PACs, however, the only process available for Ca^{2+} extrusion across the plasma membrane is PMCA (Fig. 1.5) (Zylińska and Soszyński, 2000; Ferdek *et al.,* 2012; Gerasimenko *et al.,* 2014a). In the majority of eukaryotic cells, the PMCA

pump is universally expressed throughout the plasma membrane (Carafoli, 1994). However, in order to actively pump Ca^{2+} into the extracellular environment from the region where it is largely liberated, PMCA pumps are primarily situated and confined to the apical part of PACs. Although there are low levels of PMCA expression on the basolateral membrane, the concentration of PMCA in the apical region is necessary for tightly regulating $[Ca^{2+}]_i$ and preventing unwarranted and potentially harmful signal propagation of Ca^{2+} (Lee *et al.,* 1997). The ATP-dependent PMCA pump has a high affinity for Ca^{2+} and is rapidly activated following any oscillation in cytosolic Ca^{2+}. Under physiological conditions, it is estimated that PMCA-mediated Ca^{2+} extrusion is activated at an agonist-elicited cytosolic concentration of 100-300 nM (Mangialavori *et al.,* 2010; Brini and Carafoli, 2011). The maintenance and restoration of $[Ca^{2+}]_i$ is therefore fine-tuned due to the limited capacity of PMCA (Petersen and Sutton, 2006).

Further to these processes, it is known that an additional Ca^{2+} store, the mitochondrion, also contributes towards cytosolic Ca^{2+} uptake and homeostasis in PACs (Tinel *et al.,* 1999; Park *et al.,* 2001; Voronina *et al.,* 2002b). Following increases in $[Ca^{2+}]_i$ by physiological stimulation, mitochondria have the ability to limit rises in $[Ca^{2+}]_i$ by taking up Ca^{2+} released from the ER or Ca^{2+} entering from the external environment (Bultynck and Parys, 2018). This is a rapid process, with the peak increase in mitochondrial Ca^{2+} concentration occurring soon after the peak cytosolic Ca^{2+} concentration (Szabadkai *et al.,* 2003). Mitochondrial Ca^{2+} uptake occurs via a Ca^{2+}-selective ion channel, the mitochondrial Ca^{2+} uniporter (MCU) and the driving force behind this uptake mechanism is the membrane potential across the inner mitochondrial membrane (Fig. 1.5) (Kirichok *et al.,* 2004; Leo *et al.,* 2005; De Stefani *et al.,* 2011). As mentioned previously, mitochondria are located in specific regions of the PAC, such as beneath the plasma membrane and surrounding the nucleus. Mitochondria also separate zymogen granules from the basolateral region of the cell by forming a distinct perigranular belt in the apical part of the cell (Tinel *et al.,* 1999; Park *et al.,* 2001; Ashby and Tepikin, 2002; Voronina *et al.,* 2002b; Bano *et al.,* 2005; Reed *et al.,* 2011). Following release of Ca^{2+} from the ER in the apical region, this mitochondrial belt functions as a Ca^{2+} buffer barrier by immediately taking up Ca^{2+} into the mitochondrial matrix thus confining cytosolic Ca^{2+} signals to the secretory region of the cell (Tinel *et al.,* 1999; Straub *et al.,* 2000; Petersen and Sutton, 2006). This perigranular belt also prevents spreading of Ca^{2+} to the basolateral part of the cell where the nucleus is situated (Fig. 1.2). Furthermore, mitochondrial Ca^{2+} uptake

results in activation of the dehydrogenase enzymes of the Krebs cycle, driving ATP production. ATP production via the metabolic pathway of glycolysis and oxidative phosphorylation is imperative for physiological operations of the pancreas. The ATP produced is also required for SERCA-mediated Ca^{2+} re-uptake into the ER and PMCA-mediated Ca^{2+} extrusion (Leo *et al.,* 2005; Mukherjee *et al.,* 2008; Reed *et al.,* 2011).

1.3.3 Store-operated Ca^{2+} entry

Excitable cells such as neurones, myocytes and endocrine cells possess voltage-gated Ca^{2+} channels which open to allow Ca^{2+} entry, following membrane depolarisation by an action potential. Ca^{2+} influx, down the concentration gradient, results in $[Ca^{2+}]_i$ elevations which activates the exocytotic machinery of these cells (Boquist *et al.,* 1995). The plasma membrane in non-excitable cells, such as the PAC, however, is not electrically excitable and so does not possess these voltage-gated Ca^{2+} channels (Petersen, 1992). In further contrast, during stimulation of PACs with physiological concentrations of secretagogues, the cytosolic Ca^{2+} responses driving exocytotic enzyme or fluid secretion are repetitive, short-lasting elevations. These elevations are primarily confined to the apical region and largely depend on Ca^{2+} release from intracellular stores (Yule *et al.,* 1991). The secretory processes will eventually cease, however, after several minutes because not all Ca^{2+} released from the ER is taken up again, rendering these stores finite (Petersen and Ueda, 1976). A substantial portion of Ca^{2+} will be extruded out of the cell by PMCA pumps on the plasma membrane which are activated whenever $[Ca^{2+}]_i$ increases. Therefore, all cytosolic Ca^{2+} signals are associated with an inevitable loss of Ca^{2+} from the cell. In order to replenish these intracellular stores with the Ca^{2+} required for cellular functions, a specific compensatory pathway must exist whereby Ca^{2+} from the external environment enters the cell. In non-excitable cells, this Ca^{2+} entry is known as store-operated calcium entry (SOCE) and provides an almost limitless supply of Ca^{2+} to the ER from the basal pole, through SERCA-mediated pumping (Putney, 1986; Park *et al.,* 2000; Putney, 2007; Petersen and Tepikin, 2008; Parekh, 2010).

The notion of SOCE was first defined by Putney in 1986. This concept stemmed from several experiments using lacrimal and parotid acinar cells which demonstrated that Ca^{2+} entry refilled internal stores, independent of cell surface receptor stimulation (Putney, 1977; Parod and Putney, 1978; Putney, 1986). It was hypothesised that in non-excitable cells, the amount of

Ca^{2+} entry is dependent on the quantity of Ca^{2+} within the stores and this was initially termed “capacitative calcium entry” (Putney, 2007). A later study readily demonstrated the SOCE pathway with the use of thapsigargin, a specific SERCA pump inhibitor (Takemura *et al.,* 1989). Ca^{2+} replenishment of the ER was blocked by thapsigargin, therefore resulting in store depletion, due to passive leak of Ca^{2+} from the ER. This in turn, activated Ca^{2+} influx via SOCE (Fig. 1.5). Thapsigargin and other inhibitors, such as cyclopiazonic acid (CPA), are still used as reagents for investigating SOCE currently (Michelangeli and East., 2011). Direct evidence demonstrating the SOCE concept was provided by Hoth and Penner in 1992 using extensive electrophysiological studies. A combination of patch-clamp and Ca^{2+} imaging techniques were used to observe membrane currents in mast cells, following emptying of internal stores. The authors revealed that a sustained Ca^{2+} inward current was activated following intracellular store depletion (Hoth and Penner, 1992). This non-voltage activated, inward rectifying current was named calcium release-activated calcium (CRAC) channel or I_{CRAC} (Zweifach and Lewis, 1993; Parekh and Penner, 1997). Loss of this I_{CRAC} through CRAC channels across the plasma membrane occurred when extracellular Ca^{2+} was removed (Hoth and Penner, 1992).

1.4 The calcium release-activated calcium (CRAC) channel

Several unique characteristics belonging to the CRAC channel as well as its distinctive activation by intracellular store depletion differentiate this channel from the numerous other known Ca^{2+}-permeable channels. The CRAC channel has a remarkably high selectivity for Ca^{2+} with a permeability ratio for Ca^{2+}:Na^{+} of >1,000 compared to the most selective Ca^{2+} channels documented, such as the voltage-gated L-type Ca^{2+} channel (Hoth, 1995). Furthermore, the channels can distinguish between monovalent and divalent cations as well as between differing divalent cations (Hoth and Penner, 1992). Although the single channel Ca^{2+} conductance of the CRAC channel has to be measured indirectly as it is so small (estimated between 10 – 35 fS), it is highly likely that these channels will open and therefore conduct Ca^{2+} after store depletion (Zweifach and Lewis, 1993; Prakriya and Lewis, 2006). CRAC channels also display intracellular Ca^{2+}-dependent inactivation and extracellular Ca^{2+}-dependent enhancement of channel activity (Hoth and Penner, 1992; Hoth and Penner, 1993).

Although CRAC-mediated SOCE is the principle pathway through which Ca^{2+} enters PACs, non-selective cation channels, or transient receptor potential (TRPC) channels also contribute towards store-operated acinar Ca^{2+} influx (Kim *et al.,* 2009; Lur *et al.,* 2011; Dingsdale *et al.,* 2012; Gerasimenko *et al.,* 2013). The store-operated nature of TRPC channels is, however, still highly debated in the field (Clapham, 2003; DeHaven *et al.,* 2009; Choi *et al.,* 2014). TRPC1 knockdown studies in mouse salivary glands resulted in a reduction in SOCE evoked by thapsigargin-induced store depletion, providing supporting evidence for TRPCs as subunits of SOC channels (Liu *et al.,* 2000; Liu *et al.,* 2007). Several confounding factors, however, pose significant difficulties in the acceptance of TRPCs as store-operated channels. TRPC channels respond to diverse stimuli (such as G proteins, Ca^{2+} and redox compounds) and numerous TRPC proteins form heteromultimers with other TRPC members which modifies their mode of activation (Yuan *et al.,* 2007). The resulting Ca^{2+} selectivity and conductance of TRPCs fails to contend with the capability of I_{CRAC} (Voets *et al.,* 2001; Gross *et al.,* 2009; Choi *et al.,* 2014). Although the CRAC channel is the most well established and investigated SOCE channel, for almost two decades, the molecular components, biophysical properties and the mechanisms underpinning the opening of these channels, following store depletion, remained an unsolved mystery (Parekh, 1997; Prakriya and Lewis, 2004; Parekh and Putney, 2005).

1.4.1 Stromal interaction molecule (STIM), an endoplasmic reticulum Ca^{2+} sensor

The molecular identification of the ER Ca^{2+} sensor STIM (stromal interaction molecule) and the CRAC channel subunit Orai in 2005 and 2006 respectively, paved the way for major advances in revealing the molecular mechanisms, components and functions of SOCE (Fig. 1.3) (Liou *et al.,* 2005; Roos *et al.,* 2005; Feske *et al.,* 2006; Vig *et al.,* 2006; Zhang *et al.,* 2006; Prakriya and Lewis, 2015). Through the use of small interfering RNA (siRNA) screening in Drosophila S2 and HeLa cells, the STIM protein was discovered as a fundamental component in the SOCE pathway (Liou *et al.,* 2005; Feske *et al.,* 2006). Two homologs of the protein exist in mammals, STIM1 and STIM2 with 61% homology. After knockdown of STIM1, the siRNA screens demonstrated suppression of SOCE and I_{CRAC} in both Ca^{2+} imaging and electrophysiological experiments, thus strongly associating STIM1 to CRAC channel function. This dramatic reduction in store-operated

Ca^{2+} influx was also shown in Jurkat T and HEK293 cells following STIM1 knockdown (Roos *et al.,* 2005). As type I single-pass ER membrane proteins, both STIM1 and STIM2 have an amino terminus situated inside the ER lumen and a cytoplasmic carboxy-terminal region with molecular weights of 77 kDa and 85 kDA, respectively (Collins and Meyer, 2011; Stathopulos and Ikura, 2013). Although STIM1 is predominantly dispersed throughout the ER in resting cells, STIM1 was shown (through fluorescent labelling) to translocate into clusters or "puncta" near the plasma membrane (PM) upon ER store depletion (Fig. 1.4) (Liou *et al.,* 2005; Zhang *et al.,* 2005). This was the first indication of an ER Ca^{2+} sensing role for STIM proteins which was further reinforced by the intracellular location and the organisation of STIM1 functional domains. The luminal, amino terminus of STIM1, which lies within the ER lumen, comprises a Ca^{2+}-binding motif known as an EF-hand domain (Fig. 1.4). The EF hand has a typical helix-loop-helix structure that binds to one calcium ion between loops 1 and 2. This domain permits STIM1 to sense the ER luminal Ca^{2+} concentration and the content of the stores. Mutations of Ca^{2+}-binding residues within this EF hand domain results in SOCE, regardless of the content of ER Ca^{2+} stores (Liou *et al.,* 2005; Zhang *et al.,* 2005). A non-binding Ca^{2+} ER hand structure acts to stabilise the Ca^{2+}-binding domain via hydrogen bonding at this terminus. This region of the protein also comprises a sterile α-motif domain (SAM), enabling protein-protein interactions. This SAM domain is stabilised by, and interacts with, a hydrophobic cleft which is formed from amino acids belonging to both EF hands (Stathopulos *et al.,* 2008). On the cytoplasmic side, the most critical parts for SOCE include the coiled-coil CRAC activation domain (CAD) and a polybasic domain which both interact at the plasma membrane (Parekh, 2010).

1.4.2 Orai, a subunit of the CRAC channel

Despite the integral Ca^{2+}-sensing role of STIM1, its actions alone are not sufficient for CRAC channel function. One year after the identification of STIM1, several groups discovered the transmembrane domain channel protein, Orai1, which forms the subunit of the CRAC channel pore (Fig. 1.3). This resulted, initially, from human genetic linkage analysis of patients with a rare form of inherited severe combined immunodeficiency (SCID) as well as their families (Feske *et al.,* 2006). Through this linkage analysis approach and positional cloning, the authors identified mutations in a gene localised on chromosome 12, covering approximately 74 genes, which was associated with the absence of SOCE and CRAC channel function. This abrogation of

I_{CRAC} resulted from a single point mutation in Orai1 in the SCID patients, despite normal STIM1 expression. Furthermore, the wild-type expression of Orai1 in T cells isolated from the SCID sufferers fully re-established I_{CRAC} and store-operated Ca^{2+} entry (Feske *et al.,* 2006). The use of siRNA studies to test 23,000 genes for their contribution towards SOCE was conducted simultaneously in Drosophila cells. CRACM1 (CRAC modulator 1, also known as Orai1) was identified as an essential component of store-operated influx machinery (Vig *et al.,* 2006). These conclusions were further reinforced from experiments by Zhang and colleagues in Drosophila S2 cells. They demonstrated almost complete inhibition of I_{CRAC} following knockdown of Orai1, compared to control cells (Zhang *et al.,* 2006). Although these studies implied that Orai1/CRACM1 is the structural CRAC channel component/gene, its role remained uncertain and there was still a possibility of an encoded, plasma membrane bound accessory protein controlling channel opening (Liou *et al.,* 2005; Feske *et al.,* 2006; Vig *et al.,* 2006; Zhang *et al.,* 2006). Several groups therefore carried out mutagenesis studies of highly conserved acidic residues in the transmembrane domains of Orai1. Orai1, and other members of its protein family (Orai2 and Orai3), consist of four transmembrane-spanning domains (TM1-TM4) and intracellular NH_2 and COOH termini facing the cytoplasm. In all three proteins, the C terminus has a coiled-coil domain which participates in protein-protein interactions (Fig. 1.3) (Hou *et al.,* 2012). Following alterations of these acidic residues in HEK293 and Drosophila cells, the sensitivity of CRAC channels for Ca^{2+} was significantly reduced or the CRAC channel conduction was blocked, thus establishing Orai1 as the pore forming subunit of the CRAC channel (Prakriya *et al.,* 2006; Vig *et al.,* 2006; Yeromin *et al.,* 2006). No other ion channel proteins are known to share homology with all three isoforms of Orai (Roberts-Thomson *et al.,* 2010). Although Orai2 is predominantly expressed in the brain, lung, spleen and intestine, the ubiquitous expression of Orai1, Orai3 and STIM1 throughout the whole body highlights their functional importance (Gross *et al.,* 2007).

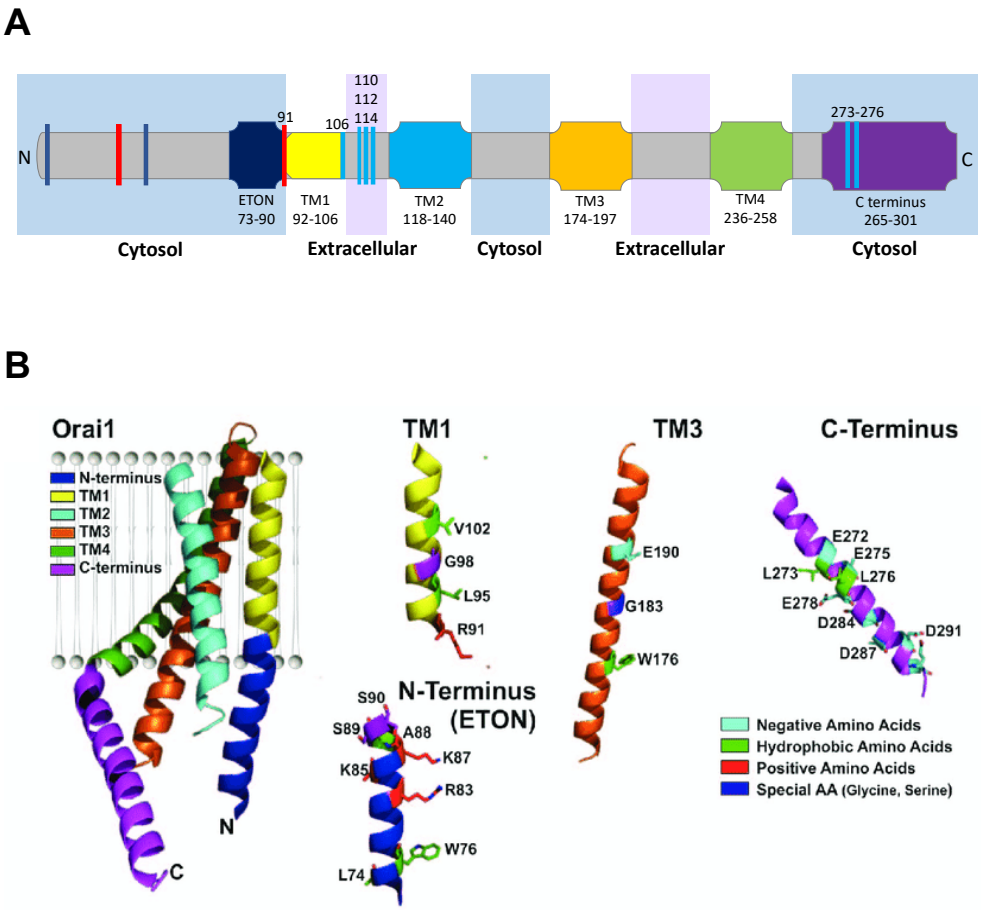

Figure 1.3. Structure of Orai1. (A). Schematic diagram of the full-length, human Orai1 which shows the 4 transmembrane (TM) domains, the N- and C-terminal. **(B).** Diagram demonstrating a single Orai1 subunit, present within the plasma membrane with the 4 TM regions, terminal elongated N- and C- termini. Amino acid numbering signifies human Orai1 (adapted and taken from Fahrner *et al.,* 2013).

1.4.3 CRAC channel-mediated Ca^{2+} entry

The mechanism of CRAC channel activation is a highly dynamic event that involves translocation of membrane proteins between two different cell compartments, the ER and the PM. Under resting conditions when internal Ca^{2+} stores are filled, STIM1 is homogeneously dispersed throughout the ER membrane (Fig. 1.4) (Baba *et al.,* 2006; Park *et al.,* 2009a; Covington *et al.,* 2010). Loss of Ca^{2+} from stores causes release of Ca^{2+} from the luminal Ca^{2+}-binding EF hand of STIM1 (Liou *et al.,* 2005; Zhang *et al.,* 2005). The subsequent weakening of intramolecular connections between the SAM domain and the two EF hands on the protein's luminal terminus causes unfolding of STIM1. These conformational changes lead to the formation of STIM1 oligomers (Luik *et al.,* 2008; Stathopulos *et al.,* 2008). The oligomers

then re-distribute to specific ER-PM junctions where they co-accumulate in clusters, situated within 10 – 25 nm of the PM (Wu *et al.,* 2006; Liou *et al.,* 2007; Varnai *et al.,* 2007). This close localisation to the PM permits binding of STIM1 to Orai1, opening the CRAC channel which initiates Ca^{2+} entry into the cell (Fig. 1.4). Although STIM1 oligomers can form and accumulate without the cytosolic domain of the STIM1 protein, this is not sufficient to activate Orai1. The presence of the CRAC activation domain stabilises these STIM1 aggregates and binds directly to both the N- and C- termini of Orai1 thus playing an essential role in CRAC channel activation (Park *et al.,* 2009a; Zhou *et al.,* 2010). Upon refilling of stores, SOCE concludes as STIM1 and Orai1 return to their original, highly dispersed distributions (Liou *et al.,* 2005; Prakriya and Lewis, 2015).

The physiological importance of CRAC channels is highlighted by the impact of CRAC channel dysregulation on human health as well as their high degree of conservation, from yeast to humans. CRAC channels are widely distributed in PACs as they are concentrated in both apical and basolateral membranes, thus traversing around 95% of the PAC surface (Lur *et al.,* 2011). In recent years, various human diseases have also been associated with abnormal CRAC channel activity, including severe disorders of the immune system, allergies, myocardial infarction, thrombosis, Alzheimer's disease and cancer (Vig *et al.,* 2008; Yang *et al.,* 2009; Parekh, 2010; Kim *et al.,* 2014; Sun *et al.,* 2014; Lacruz and Feske, 2015).

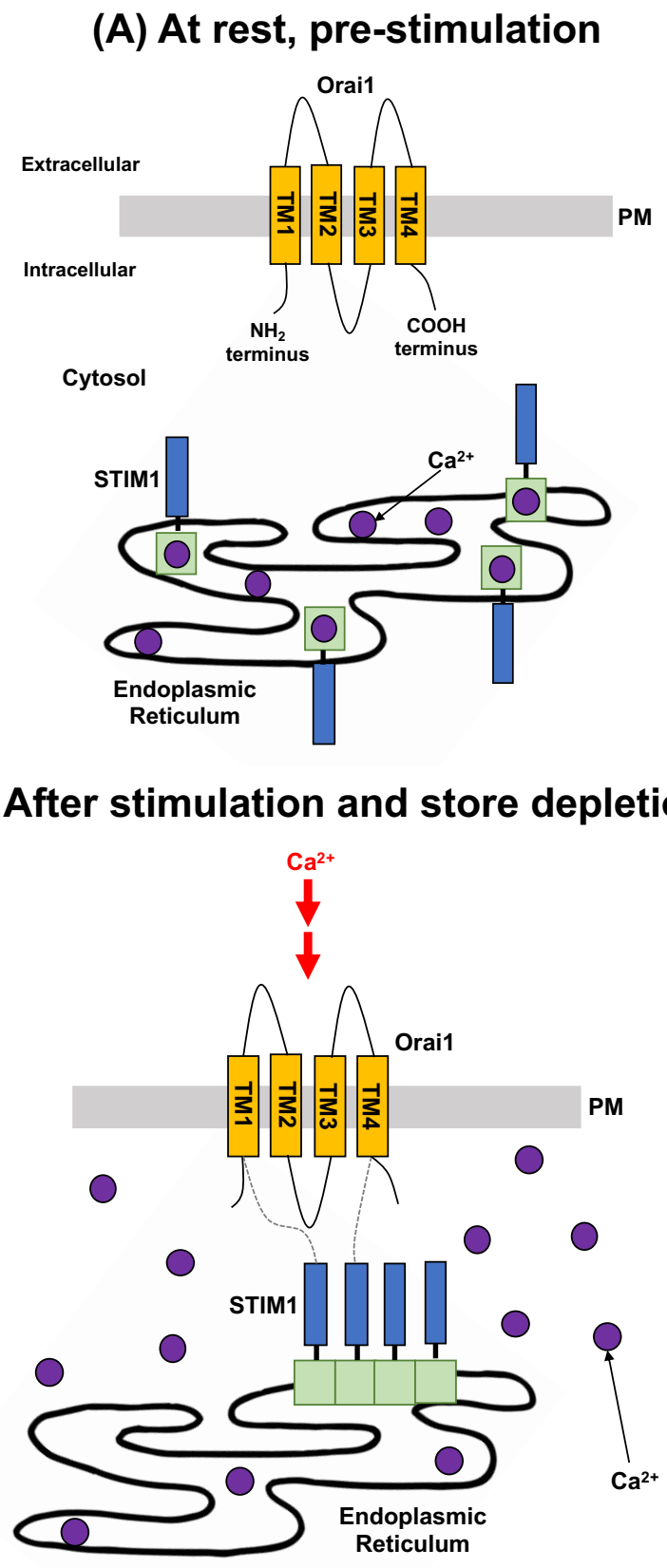

Figure 1.4. Activation of the Ca^{2+} release-activated Ca^{2+} (CRAC) channel. **(A)** At resting state, when stores are filled with Ca^{2+}, stromal interaction molecule 1 (STIM1) is uniformly distributed throughout the endoplasmic reticulum (ER) membrane with its EF hand motif occupied with Ca^{2+}. The channel protein Orai1 is comprised of four transmembrane domains with both NH_2 and COOH termini facing the cytoplasm and the pore-forming subunit of the CRAC channel distributed within the plasma membrane (PM). **(B)** During store depletion, Ca^{2+} is released from the ER and is sensed by STIM1, which oligomerises and migrates to ER-plasma membrane junctions. At these locations, STIM1 puncta form and interact with Orai1, inducing CRAC channel activation and subsequent Ca^{2+} influx from the extracellular environment (adapted from Roberts-Thomson *et al.,* 2010).

1.5 Pathological Ca^{2+} signalling in acute pancreatitis

The overall agreement, hypothetically proposed in 1995, is that a disruption in Ca^{2+} signalling within the PAC leads to excessive cytosolic Ca^{2+} signals which in turn, initiates almost all pathological hallmarks of AP (Fig. 1.5) (Ward *et al.,* 1995; Raraty *et al.,* 2000; Krüger *et al.,* 2000; Voronina *et al.,* 2002a; Petersen and Sutton, 2006; Gerasimenko *et al.,* 2014b). As mentioned previously, short-lasting, repetitive, transient oscillations in cytosolic Ca^{2+} confined to the apical pole of the acinar cell cause normal exocytosis of digestive enzymes (Maruyama *et al.,* 1993; Thorn *et al.,* 1993). Under pathophysiological conditions, however, sustained, global elevations of $[Ca^{2+}]_i$ in PACs are the most damaging and result from pathological agents such as alcohol, bile, various drugs as well as high concentrations of ACh or CCK secretagogues (Petersen and Sutton, 2006; Gerasimenko *et al.,* 2013). These stimuli instigate excessive release of Ca^{2+} from internal stores followed by excessive Ca^{2+} entry, or impair mechanisms acting to restore physiological levels of $[Ca^{2+}]_i$ (Fig. 1.5). The toxic overload in cytosolic Ca^{2+} prematurely activates digestive enzymes intracellularly which results in the molecular cannibalism that digests the pancreas and triggers acute pancreatitis (Ward *et al.,* 1995; Krüger *et al.,* 2000; Raraty *et al.,* 2000; Petersen *et al.,* 2011).

1.5.1 Alcohol-induced acute pancreatitis

The close correlation between alcohol intake and AP has been acknowledged for some time. In 1788, an association between excessive alcohol consumption and diseases of the pancreas was made, with the first description of the Drunkard's Pancreas by Friedrich ensuing a century later (Cawley, 1788). Increases in binge drinking and chronic alcohol intake has, in more recent decades, mirrored a dramatic elevation in hospital admissions for AP (Roberts *et al.,* 2008). Furthermore, a population-based cohort study in 2008 demonstrated an increased risk of individuals developing AP after consuming more than 14 drinks per week (Kristiansen *et al.,* 2008). A subsequent meta-analysis indicated that the risk of pancreatitis occurring is more than doubled when individuals imbibe in excess of 4 drinks per day (Irving *et al.,* 2009). Interestingly, however, only a minority (less than 10%) of heavy drinkers actually develop AP (Pandol *et al.,* 2011). Clarification of the pathobiology of alcoholic AP has been further complicated by the inability of alcohol ingestion to cause AP in experimental animal models. In this case, additional agents such as CCK are required to

induce alcoholic AP (Siech *et al.,* 1991; Pandol *et al.,* 1999; Lerch and Gorelick, 2013). Moreover, the direct application of high concentrations of ethanol (850 mM) to isolated PACs typically generates only modest increases in cytosolic Ca^{2+} (Criddle *et al.,* 2004). Therefore, it is evident that other elements play a role in the mechanisms underlying alcohol-induced pancreatitis.

The exocrine pancreas utilises both oxidative and non-oxidative routes to metabolise ethanol (Gukovskaya *et al.,* 2002; Criddle, 2015). The oxidative metabolism of alcohol involves the catalysation actions of alcohol dehydrogenase (ADH) and cytochrome P450 2E1 (CYP 2E1) which yield reactive oxygen species (ROS) and acetaldehyde (Gukovskaya *et al.,* 2002). ROS are highly reactive, short-lived compounds and are potentially injurious to cellular components including lipid membranes, DNA and intracellular proteins. Cells have the ability under physiological conditions to effectively clear ROS within the cell through the actions of proteins (such as catalase, peroxidases, superoxide dismutase, glutathione and glutathione peroxidase). Oxidative stress, however, can result from an imbalance between these protective protein mechanisms and ROS production, instigating pancreatic cell death (Vonlaufen *et al.,* 2008). Both ADH and CYP 2E1 enzymes are expressed in the pancreas, however, their expression is significantly higher in the liver. As a result, the capacity for oxidative metabolism of ethanol by the pancreas is substantially less than that of the liver (Haber *et al.,* 1998; Norton *et al.,* 1998; Clemens *et al.,* 2016). The non-oxidative metabolism of ethanol involves the esterification of free fatty acids (FAs) to produce highly lipophilic fatty acid ethyl esters (FAEEs) via FAEE synthases such as carboxylester lipase. The generation of these FAEE synthase enzymes occurs in the human pancreas at rates of approximately 54 nmol/min/g tissue. This level is higher than any other organ (Hamamoto *et al.,* 1990; Diczfalusy *et al.,* 2001; Haber *et. al.,* 2004). Moreover, post-mortem studies of intoxicated patients reported that accumulations of FAEEs in the pancreas were higher than any other organ analysed. The capacity for non-oxidative metabolism of ethanol in the pancreas is therefore highly due to significant FAEE synthase activity (Laposata and Lange, 1986). Compared to oxidative metabolism of ethanol, non-oxidative alcohol metabolism by FAEE synthases and the generation of FAEEs likely has a more predominant contribution to the damaging effects of alcohol-induced pancreatitis (Criddle *et al.,* 2006b; Criddle *et al.,* 2007; Shalbueva *et al.,* 2013; Mukherjee *et al.,* 2016).

The significance of PAC organellar dysfunction, particularly in mitochondria and in the ER, in the initiation of AP has been emphasised through recent advances in the mechanisms underlying alcohol-induced damage. Non-oxidative alcohol metabolites, FAEEs, induce global, sustained elevations in cytosolic Ca^{2+} concentration in pancreatic acinar cells thus prematurely activating digestive proenzymes and initiating AP (Criddle *et al.,* 2004). This toxic effect has been demonstrated in both *in vitro* and *in vivo* experiments. The non-oxidative ethanol metabolite palmitoleic acid (POA) ethyl ester (POAEE), which is produced by hydrolysis of its parent FAEE, was administered to PACs and resulted in persistent and damaging increases in cytosolic Ca^{2+}, in a concentration-dependent manner (Criddle *et al.,* 2004; Criddle *et al.,* 2006b). Activation of IP_3Rs and subsequent Ca^{2+} liberation from the ER gives rise to these excessive increases in $[Ca^{2+}]_i$ (Fig. 1.5). The successive activation of store-operated Ca^{2+} influx mechanisms is significant, pathologically, as it sustains cytosolic Ca^{2+} elevations (Criddle *et al.,* 2006b; Gerasimenko *et al.,* 2013). In addition to these damaging *in vitro* effects, FAEEs have induced protease (trypsinogen) activation, pancreatic oedema and vacuolisation in animal models. Intracellular vacuolisation involves the destabilisation and conversion of zymogen granules into empty-looking vacuoles in the apical secretory granular pole of the acinar cell (Werner *et al.,*1997). These processes lead to digestion of the acinar cell and its surrounding tissue, thereby releasing cell contents and digestive enzymes, causing further digestion of PACs, namely autodigestion (Pandol *et al.,* 2007). In general, it has been shown that trypsinogen activation, an early event in the initiation of AP, occurs within endocytic vacuoles (EV) which assemble in PACs following AP induction. Intracellular rupture and fusion of EVs to the plasma membrane can enable both the targeting of cytoplasmic and extracellular structures by trypsin as well as the release of digestive enzymes into the cytosol of PACs (Sherwood *et al.,* 2007; Chvanov *et al.,* 2018; De Faveri *et al.,* 2019). These findings highlight the importance of depicting the intracellular processing of EVs which could improve our understanding of early events in AP pathology and potentially result in new therapeutic molecular targets being identified.

Together with Ca^{2+} overload, loss of ATP is also a principle feature of alcohol-induced acute pancreatitis and leads to the induction of massive cellular necrosis (Criddle *et al.,* 2004; Criddle *et al.,* 2007; Mukherjee *et al.,* 2008; Gukovsky *et al.,* 2011). In recent years, evidence has demonstrated that sustained rises in cytosolic Ca^{2+} in PACs, due to non-oxidative ethanol metabolites, causes excessive mitochondrial Ca^{2+} uptake which opens the

mitochondrial permeability transition pore (MPTP). This MPTP opening triggers mitochondrial dysfunction (Shalbueva *et al.,* 2013; Mukherjee *et al.,* 2016). MPTP formation, as a result of mitochondrial Ca^{2+} overload and oxidative stress, occurs within the inner mitochondrial membrane (IMM). Opening of this multi-protein channel permeabilises the IMM and permits free movement of protons and substances weighing up to 1.5 kDA into the mitochondria. Therefore, the development of the MPTP dissipates the membrane potential and the proton gradient required for ATP production (Criddle *et al.,* 2015). The subsequent mitochondrial ATP depletion within PACs, compromises ATP-dependent pumps such as SERCA and PMCA (Fig. 1.5) (Criddle *et al.,* 2006b). SERCA pumps cannot replenish ER stores with Ca^{2+} and PMCA is unable to stabilise the effect of SOCE by extruding Ca^{2+} across the plasma membrane thus inadequately clearing elevated cytosolic Ca^{2+}. This mitochondrial malfunction further contributes towards acinar necrosis, the extent of which, is a principle determinant of disease severity in AP (Gerasimenko and Gerasimenko, 2012). The prognosis of pancreatitis largely relies on whether apoptosis or necrosis cell death pathways occur (Criddle *et al.,* 2007; Gukovskaya and Gukovsky, 2011). The plasma membrane remains intact during the tightly regulated "physiological" cell death process, apoptosis, which is a mechanism of programmed cell death. However, as the necrosis processes abolish the integrity of the plasma membrane, cellular constituents are expelled into the interstitial fluid which induces a detrimental inflammatory response. ATP is required for apoptosis thus in AP, where mitochondrial dysfunction ensues, necrosis is the only available cell death pathway (Petersen *et al.,* 2011).

1.5.2 Bile acid-induced acute pancreatitis

As previously mentioned, migrating gallstones can obstruct the ampulla of Vater, the junction at which the common bile and pancreatic ducts unite. The acknowledgement of this site of blockage as a potential cause of AP dates back to the 20th century (Opie, 1901). In more recent years, gallstones have become a well-established and recognised cause of pancreatitis. Although gallstones are mainly asymptomatic, comprising cholesterol and bile salts, blockage of this junction can result in bile reflux into the biliopancreatic ductal system. This is termed the "common channel theory" of AP whereby a common channel is created behind the stone obstruction causing retrograde flow of bile into the pancreatic duct and pancreatic acinar cell injury (Armstrong and Taylor, 1986; Voronina *et al.,* 2002a; Pandol *et al.,* 2007; Vonlaufen *et al.,* 2008). Pancreatic ductal hypertension can also arise from

gallstone blockage of the pancreatic duct, preventing the outflow of pancreatic juice into the duodenum (Petersen and Sutton, 2006). Although this additional theory is thought to instigate acinar cell damage, there is more evidence in favour of the bile reflux theory as an initiator of AP (Perides *et al.,* 2010a).

In PACs, bile acids can be taken up by transporters such as the HCO_3-dependent organic anion transporting polypeptide-1 (OATP1), situated on the basolateral membrane. Moreover, the Na^+-dependent Na^+ taurocholate co-transporting polypeptide (NTCP), located on the apical membrane of the acinar cell accounts for approximately 25% of bile acid uptake (Kim *et al.,* 2002). In order to respond to bile in the lumen of the duct, the widely expressed G-protein-coupled cell surface, bile acid receptor, Gpbar1 is also positioned at the apex of the cell (Perides *et al.,* 2010b). The direct effect of bile acids such as taurolithocholic acid 3-sulfate (TLC-S) on isolated murine PACs was first reported in 2002 by Voronina and colleagues. Although TLC-S evoked oscillatory elevations in cytosolic Ca^{2+} at low concentrations, application of higher TLC-S concentrations (300 – 500 μM) induced sustained, cytosolic Ca^{2+} increases (Voronina *et al.,* 2002a). Higher concentrations of other bile salts, including sodium taurocholate and taurochenodeoxycholate, also triggered global, persistent increases in cytosolic Ca^{2+} *in vitro* (Kim *et al.,* 2002; Voronina *et al.,* 2002a). This data showed that the initial Ca^{2+} signal originated from intracellular Ca^{2+} release from both the ER and acidic intracellular stores through IP_3 and ryanodine receptors. The effect of low concentrations of bile acid on $[Ca^{2+}]_i$ has additionally been reported through SERCA pump inhibition with subsequent depletion of ER Ca^{2+} (Kim *et al.,* 2002; Gerasimenko *et al.,* 2006; Fischer *et al.,* 2007; Malo *et al.,* 2010). However, the persistent pathological Ca^{2+} elevations were derived from the extracellular environment through SOCE mechanisms. This was demonstrated during a maintained presence of bile acids and the removal of Ca^{2+} from the extracellular solution which resulted in intracellular Ca^{2+} levels rapidly returning to baseline. This highlighted the important role of Ca^{2+} influx in driving sustained cytosolic Ca^{2+} elevations induced by bile acids (Fig. 1.5) (Kim *et al.,* 2002). This pathological cytosolic Ca^{2+} overload is taken up by the mitochondria, inducing organellular dysfunction and ATP depletion which triggers cell death pathways (Pandol *et al.,* 2007).

1.5.3 Asparaginase-induced acute pancreatitis

Another cause of AP, as formerly mentioned, is L-asparaginase, namely asparaginase-associate pancreatitis. Although 5-year survival rates of more than 90% for childhood acute lymphoblastic leukaemia are owing to the intensification of chemotherapy treatments, increased levels of therapy-related toxicities have also ensued (Schmiegelow *et al.,* 2017). One of the most common reasons for discontinuing ASNase treatment in patients suffering with ALL is the development of AAP. This is unfortunate due to the essential part ASNase plays in successful multiagent chemotherapeutic regimes for childhood ALL (Raja *et al.,* 2012). There are three main sources of asparaginase used at present in the clinic, each with diverse pharmacodynamics, pharmacokinetic and immunogenic properties. The native L-asparaginase and the modified pegylated version, PEG-Asparaginase are both derived from *Escherichia coli* (*E. coli*). Whereas, Erwinase originates from *Erwinia chrysanthemi* (Muller and Boos, 1998; Duval *et al.,* 2002; Kurre *et al.,* 2002). By hydrolysing asparagine to aspartic acid and ammonia, L-asparaginase acts to diminish exogeneous sources of asparagine. As the majority of malignant lymphoblasts fail to produce the levels of asparagine necessary for lymphoblastic metabolism and growth, depletion of asparagine pools by L-asparaginase will result in cell death (Jaffe *et al.,* 1971; Muller and Boos, 1998; Duval *et al.,* 2002; Kurre *et al.,* 2002; Berg, 2011).

The mechanisms underlying the therapeutic effects of L-asparaginase on cancer cells in childhood ALL are, however, profoundly different to the actions by which asparaginase evokes acute pancreatitis (Broome, 1968). The latter of which have been largely unknown. Recent investigations, however, have revealed the mechanisms leading to AAP for the first time (Peng *et al.,* 2016; Peng *et al.,* 2018). ASNase primarily interacts with protease-activated receptor 2 (PAR2) to induce sustained elevations in cytosolic Ca^{2+} concentration in PACs, independent of asparagine (Peng *et al.,* 2016; Peng *et al.,* 2018). PARs are unique, G-protein-coupled seven transmembrane receptors and their activation results from an irreversible proteolytic mechanism. PAR2 is broadly expressed in human and animal tissues, including the pancreas and its activation is specifically carried out by trypsin and tryptase (Nystedt *et al.,* 1994; Molino *et al.,* 1997; Dery *et al.,* 1998). Although a role for PAR2 in AP pathology has previously been implicated, its precise function is debated in the field (Namkung *et al.,* 2004; Gorelick, 2007; Singh *et al.,* 2007; Laukkarinen *et al.,* 2008). Activation of

PAR2 results in PLC activation and the generation of IP_3 which leads to Ca^{2+} mobilisation. It is this signal transduction pathway that evokes $[Ca^{2+}]_i$ overload through excessive release of Ca^{2+} from internal Ca^{2+} stores, followed by SOCE which induces pancreatitis, similar to the actions of FAEEs and BAs (Soh *et al.,* 2010). This was confirmed by Peng and colleagues (2016) through the use of PAR2 inhibitors which prevented both ASNase-induced pathological $[Ca^{2+}]_i$ elevations and ASNase-evoked necrosis. Moreover, investigations have demonstrated that ASNase significantly effects both Ca^{2+} influx and extrusion. This is due to mitochondrial depolarisation and sustained elevations in mitochondrial Ca^{2+} levels which depletes ATP production and therefore inhibits PMCA pumps from removing Ca^{2+} from the cell (Peng *et al.,* 2016; Peng *et al.,* 2018). Several formulations of ASNase were used to confirm the mechanistic action of ASNase, including Asparaginase from both *E. coli* and *Erwinia chrysanthemi* as well as the drug ELSPAR and PEG-Asparaginase.

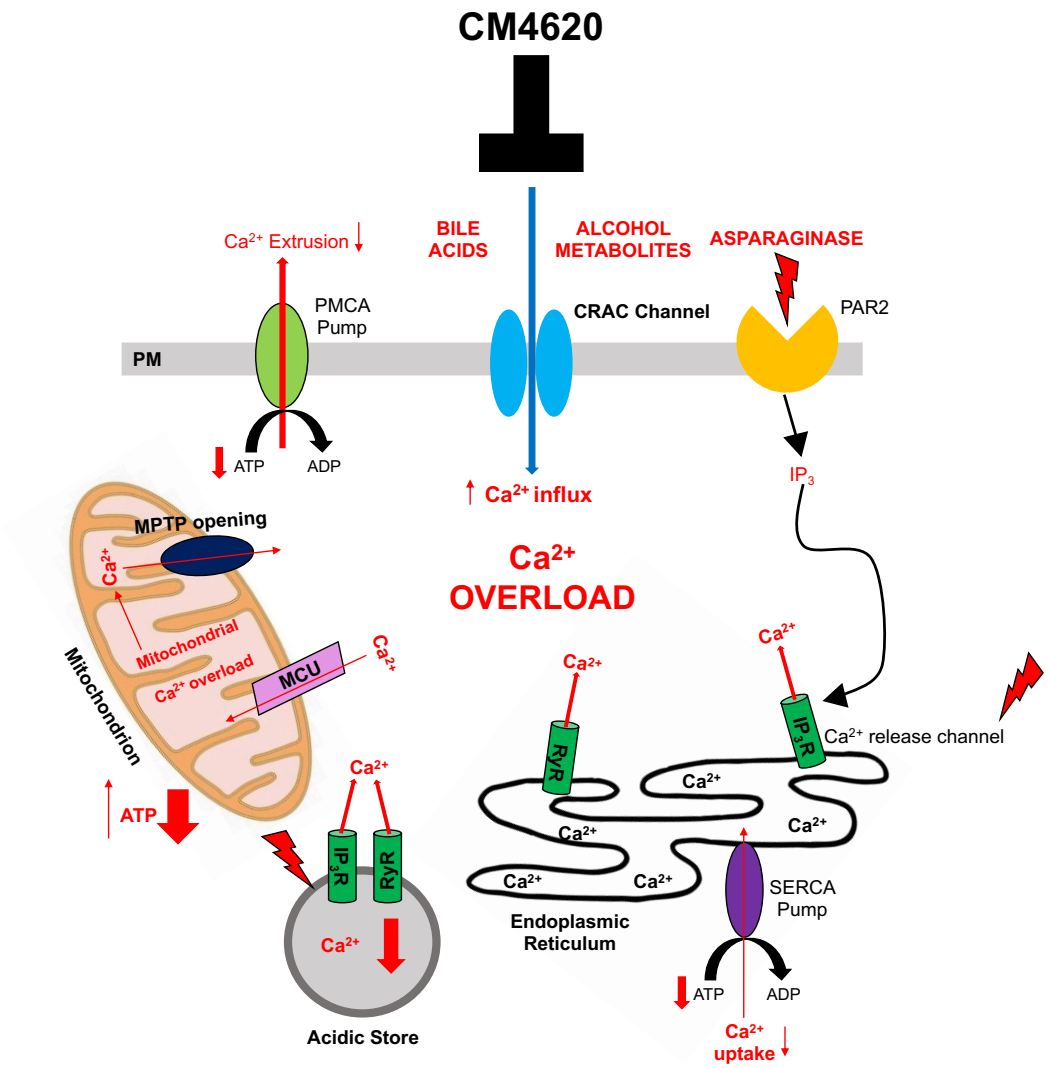

Figure 1.5. Pathological Ca^{2+} signalling in acute pancreatitis. Schematic diagram demonstrating the therapeutic potential of CM4620 on inhibiting CRAC (Ca^{2+} release-activated Ca^{2+}) channels in pancreatic acinar cells. CM4620 could inhibit sustained, global elevations in cytosolic Ca^{2+} concentrations which result from a variety of pathological agents. This would prevent further hallmarks of AP such as premature trypsin activation and necrosis (adapted from Gerasimenko and Gerasimenko, 2012). Abbreviations: ATP: adenosine triphosphate; Ca^{2+}: calcium; IP_3Rs: IP_3 receptor; MCU: mitochondrial Ca^{2+} uniporter; MPTP: mitochondrial permeability transition pore; PAR2: protease-activated receptor 2; PMCA: plasma membrane Ca^{2+} ATPase; RyR: ryanodine receptor; SERCA: sacro/endoplasmic reticulum Ca^{2+}-activated ATPase.

1.6 Therapeutic avenues for acute pancreatitis

There is currently no cure or specific therapy available for AP. Treatments are predominantly based on nutritional support, pain control and fluid resuscitation which do not combat the primary pathological event, a sustained $[Ca^{2+}]_i$ overload in PACs causing premature intracellular protease activation (Petersen and Sutton, 2006; Wu and Banks, 2013). However, due to significant improvements in our understanding of the pathological Ca^{2+} signalling events in AP, numerous therapeutic targets have come to fruition.

The principal target for preventing pancreatic injury during AP ought to be the initial site of pancreatic damage, namely, the pancreatic acinar cells. Inhibition of Ca^{2+} release from intracellular ER stores, enhancing Ca^{2+} extrusion, protection of mitochondrial events and inhibition of Ca^{2+} entry are all possible therapeutic avenues for AP (Petersen and Sutton, 2006).

1.6.1 Therapeutically targeting internal Ca^{2+} release

Massive Ca^{2+} release from both the ER and acidic stores occurs via IP_3R and RyR and plays a major role in the cytosolic Ca^{2+} overload that initiates AP disease progression. Some success of targeting this pathway therapeutically has been demonstrated. Pharmacological inhibition of IP_3Rs in PACs and knock outs of type 2 and 3 IP_3Rs in mice has been investigated (Gerasimenko *et al.,* 2009). Following pathological stimulation with POAEE, low levels of Ca^{2+} release and trypsinogen activation were shown in type 2 and 3 IP_3R knock outs. An even more significantly diminished intracellular trypsin activity was observed in cells from POAEE-induced double IP_3R knock outs. Additionally, antibodies against type 2 and 3 IP_3Rs markedly reduced POAEE-evoked Ca^{2+} release and trypsinogen activation (Gerasimenko *et al.,* 2009).

Calmodulin is an intracellular Ca^{2+} sensor known to protect against excessive Ca^{2+} release and trypsinogen activation by regulating numerous IP_3R mechanisms of Ca^{2+} entry (Michikawa *et al.,* 1999; Gerasimenko *et al.,* 2011; Petersen *et al.,* 2011). The therapeutic ability of calmodulin activator Ca^{2+}-like peptides 3 (CALP-3) has therefore been investigated. CALP-3, at a concentration of 100 μM, effectively eliminated the characteristic effects of ethanol on intact PACs, such as Ca^{2+} release and necrosis. CALP-3 did not affect physiological ACh and CCK-evoked oscillations (Gerasimenko *et al.,* 2011; Ferdek *et al.,* 2017). Recently, the development of a more potent, modified CALP-3 led to investigations showing its effectiveness at much lower concentrations, such as 0.1 μM, further reinforcing its therapeutic potential at protecting PACs against pathological Ca^{2+} damage (Gerasimenko *et al.,* 2014a).

High concentrations of caffeine have also been reported to inhibit IP_3R-mediated Ca^{2+} release via inhibition of PLC-mediated IP_3 production, *in vitro* (Toescu *et al.,*1992; Huang *et al.,* 2017). Caffeine prevented sustained rises in $[Ca^{2+}]_i$, mitochondrial membrane potential deficiency and necrosis in PACs. 25mg/kg caffeine was also administrated *in vivo* in mouse models of

AP where it markedly ameliorated pancreatic injury. Caerulin (a CCK analogue), TLC-S and ethanol and POA were used to induce AP in these mouse models (Huang *et al.,* 2017). Patients rarely receive treatment within 48 hours after the start of AP disease progression, thus the successful impact of delayed caffeine administration (24 hours) in preventing numerous pathological hallmarks of AP further strengthens its therapeutic value (Gerasimenko *et al.,* 2017). Although it has recently been shown that caffeine effectively inhibits cell death elicited by the amino acid L-arginine *in vitro,* necrosis responses to the basic amino acid L-ornithine were not significantly affected by caffeine and cell death caused by L-histidine was remarkably exacerbated by caffeine. In contrast to caerulin-, bile acid, fatty acid and ethanol-induced AP models, caffeine did not significantly protect against all the histopathological parameters in a L-arginine-induced murine model of AP (Zhang *et al.,* 2019). Furthermore, additional effects of caffeine include activation of RyR-mediated Ca^{2+} release in the heart sarcoplasmic reticulum with the possibility of severe cardiac arrhythmias (Lur *et al.,* 2011). Coupled with its relatively low affinity for the IP_3R, the use of caffeine as a potential AP treatment is limited (Wakui *et al.,* 1990).

The anti-apoptotic B-cell lymphoma-2 (Bcl-2) protein has also been shown to regulate Ca^{2+} release by binding to and influencing intracellular Ca^{2+} channels. Vervliet and colleagues demonstrated the ability of low concentrations of the Bcl-2-homology (BH) 4 domain of Bcl-2 to inhibit IP_3Rs and RyRs through direct interaction. The BH4 domains of Bcl-2 and Bcl-X_L also have the ability to inhibit, via RyR and IP_3R blockage, pathological Ca^{2+} overload in PACs evoked by TLC-S. This subsequently minimises the damaging effects of TLC-S-induced necrosis (Vervliet *et al.,* 2018). These studies demonstrated a novel use of the BH4 domains of Bcl-2 and Bcl-X_L as peptide tools in reducing RyR-evoked Ca^{2+} overload in AP pathology (Vervliet *et al.,* 2014; Vervliet *et al.,* 2016; Vervliet *et al.,* 2018). However, the shortage of specific IP_3R and RyR inhibitors limit their usefulness as inhibitors of Ca^{2+} release from internal stores for AP therapy (Gerasimenko *et al.,* 2017). As a modulator of intracellular Ca^{2+} homeostasis, the Bcl-2 protein not only inhibits intracellular Ca^{2+} release, but also regulates PMCA activity. In 2012, Ferdek and colleagues revealed that Bcl-2 can suppress PMCA-mediated Ca^{2+} extrusion. Bcl-2 knock out cells more efficiently extruded Ca^{2+} from the cytosol compared to control PACs thus providing protection against the damaging effects of excessive extracellular Ca^{2+} (Ferdek *et al.,* 2012). Inducing oxidative stress in PACs where Bcl-2 protein

expression is silenced, strongly promotes apoptotic pathways whilst protecting against excessive necrosis (Ferdek *et al.,* 2012).

Alternatively, blockage of NAADP-mediated Ca^{2+} release with, for example, the cell-permeable NAADP analogue and selective antagonist, Ned-19 has also been explored as a therapeutic avenue. At a high concentration of 100 μM, Ned-19 blocked binding to the NAADP thus inhibiting NAADP-mediated Ca^{2+} release (Rosen *et al.,* 2009; Gerasimenko *et al.,* 2015). The plant alkaloid, tetrandrine, has been shown to potently inhibit NAADP-stimulated Ca^{2+} release and TPC-dependent Ca^{2+} currents (Sakurai *et al.,* 2015). There has been increasing interest into the anti-inflammatory effects of Tetrandrine due to its ability to regulate inflammatory cell function and inhibit both inflammatory mediator release and free radical damage (Choi *et al.,* 2000; He *et al.,* 2011). Although numerous attempts at therapeutically targeting excessive internal Ca^{2+} release in PACs have been made, none of the aforementioned examples have reached clinical trials. Furthermore, IP_3Rs and RyRs are widely expressed and are vital for cellular functions such as secretion and proliferation. Therefore, blockade of Ca^{2+} overload via these receptors may detrimentally impact on other, important cell functions, so their safety as a therapy for AP is doubtful.

1.6.2 Therapeutically targeting mitochondrial dysfunction

A principle event in the initiation of AP induced by FAEE, bile acids and ASNase is mitochondrial dysfunction in which oxidative stress is exacerbated, hence it is considered as a significant target for drug development (Criddle *et al.,* 2006b; Booth *et al.,* 2011). Cyclophilin D is an important regulator of the MPTP which opens as a result of mitochondrial Ca^{2+} overload. Opening of the MPTP causes mitochondrial membrane depolarisation and ATP depletion thus preventing removal of Ca^{2+} from the cytosol through ATPase pumps (Halestrap and Richardson, 2015). In 2005, investigations showed that loss of cyclophilin D protects against damaging Ca^{2+} overload as well as the ensuing necrotic cell death thus improving cell fate (Baines *et al.,* 2005; Nakagawa *et al.,* 2005). Further findings demonstrated resistance of MPTP opening in cyclophilin D knock out mice which prevented the loss of mitochondrial membrane potential, inhibiting the subsequent acinar cell necrosis resulting from ATP depletion (Shalbueva *et al.,* 2013). Utilising a combination of ethanol and CCK to evoke AP in cyclophilin D knockout mice afforded considerable protection against the hallmarks of AP as reduced necrosis, trypsin and serum amylase levels and

increased ATP levels were observed (Shalbueva *et al.,* 2013). Therefore, cyclophilin D and MPTP blockade is clearly an important therapeutic target for preventing necrosis in diseases such as AP. Additionally, the administration of small molecule cyclophilin D molecules protected against mitochondrial membrane depolarisation and necrosis in murine and human PACs evoked by TLC-S.

As previously mentioned, ROS have been shown to play a part in the development of AP due to increases in oxidative status and the diminished antioxidant capacity shown in clinical studies and *in vivo* experiments (Bjelakovic *et al.,* 2012; Criddle *et al.,* 2006a). Although controversial within the literature, the targeting of antioxidants to mitochondria could be a possible therapeutic approach for AP as well as for other diseases in which mitochondrial dysfunction is a core feature. However, there is evidence that antioxidant therapy can promote cellular processes such as melanoma metastasis (Le Gal *et al.,* 2015). In PACs, application of the antioxidant N-acetylcysteine (NAC) inhibited the production of BA-evoked ROS which subsequently initiated necrosis in place of apoptotic cell death (Criddle *et al.,* 2006a; Booth *et al.,* 2011; Chvanov *et al.,* 2015). This highlighted a significant role for ROS in influencing acinar cell fate. More recently, Armstrong and colleagues (2019) investigated and compared the effects of antioxidant MitoQ on PAC bioenergetics, ATP generation and cell fate against decyltriphenylphosphonium bromide (DecylTPP), a non-antioxidant control and the general antioxidant, NAC. MitoQ accumulates on the inner mitochondrial membrane whereby mitochondrial membrane potential drives its uptake into the organelle (Asin-Cayuela *et al.,* 2004; Finichiu *et al.,* 2013). Seahorse XF24 analysis of respiratory function and plate-reader analysis of cellular ATP and necrosis levels was used to compare the effects of these three compounds. Sustained elevations in basal respiration and blockage of spare respiratory capacity resulted from the application of both MitoQ and NAC. These effects were marginal following the use of DecylTPP, further confirming the capability of these antioxidants. Moreover, MitoQ and DecylTPP significantly decreased mitochondrial ATP turnover capacity and cellular ATP concentrations. Compensatory increases in glycolysis and concentration-dependent elevations in PAC apoptosis and necrosis resulted from all three compounds. The authors therefore proposed that a negative feedback control of basal cellular metabolism is significantly influenced by ROS. The targeting of antioxidants to mitochondria causes both specific and non-specific effects on bioenergetics which significantly influences PAC health (Armstrong *et al.,* 2019).

ATP metabolism plays a major role in Ca^{2+} homeostasis and regulation in PACs (Hainóczky *et al.,* 1995; Petersen, 2003; Smyth *et al.,* 2008; Yadav and Lowenfels, 2013). Recent investigations by Peng and colleagues have shown that restoring ATP supply provides an impressively high degree of protection against pancreatic necrosis. The first, detailed studies into the role of glycolysis in AP *in vitro* and *in vivo* were subsequently carried out (Peng *et al.,* 2016; Peng *et al.,* 2018). Removal of extracellular glucose had a very minimal effect on ATP depletion, evoked by alcohol metabolites, bile acids or asparaginase, in isolated mouse PACs or clusters (Peng *et al.,* 2018). This indicated that these AP-inducing agents severely inhibit glucose metabolism. However, when substituting glucose with both pyruvate and galactose as a source of energy supply, ATP loss, aberrant Ca^{2+} signals, mitochondrial Ca^{2+} responses, mitochondrial depolarisation and any succeeding necrosis was significantly reduced or inhibited. As galactose is converted into glucose-6-phosphate independently of hekokinases (HKs), it is an alternative carbon energy source for glycolysis. Galactose is eventually metabolised to pyruvate via the glycolytic pathway and enters glycolysis by bypassing HK at a slower rate than glucose (Bustamante and Pedersen, 1977; Holden *et al.,* 2003). These results indicate that glucokinase/HK activity is inhibited during AP pathology. However, under these pathological conditions, the protective effects of galactose and pyruvate suggest that mitochondrial oxidative phosphorylation can function effectively thus producing sufficient levels of ATP for the cell (Vervliet *et al.,* 2016). Although pyruvate demonstrated a high degree of protection against pancreatic necrosis, galactose is more stable in solution, metabolised at a relatively slower rate and has been utilised in feeding and intravenous (IV) injection *in vivo* protocols (Berry *et al.,* 1995; An *et al.,* 2012; Sclafani and Ackroff, 2014). The safety of galactose administration in humans, even at high mM concentrations, has also been shown. At 100 mM, galactose is potently present in a variety of milk sources as the glucose-galactose disaccharide, lactose and is absorbed in the intestine as free galactose. Free galactose is also a component of breast milk at mM concentrations as well as existing in formula milk at concentrations of 2 - 4 mM (Cavalli *et al.,* 2006). In lactose-free milk, galactose is present at levels approaching 100 mM (Ohlsson *et al.,* 2018). The remarkable effect of galactose was therefore further explored in mouse models of AP, induced by asparaginase or a combination of ethanol and fatty acids. Galactose markedly diminished acinar necrosis, oedema and inflammatory infiltration to more control-like values in both alcohol-induced pancreatitis and in the novel animal model of asparaginase-induced AP (Peng *et al.,* 2018).

1.6.3 CRAC channel inhibitors

Although numerous therapeutic targets have been investigated, none of the aforementioned avenues have reached clinical trial stage. The recognition of SOCE as a potential therapeutic target for acute pancreatitis (AP) dates back to as early as 2000 (Raraty *et al.,* 2000). The pharmacological development of specific CRAC channel inhibitors for AP treatment has significantly expanded over recent years and is the principle focus of this study (Prakriya and Lewis, 2015). The substantial therapeutic appeal of CRAC channels is due to the dependence of intracellular protease activation on cytosolic Ca^{2+} overload which, preceding Ca^{2+} depletion of the ER, results from sustained, CRAC channel-mediated Ca^{2+} entry (Fig. 1.5) (Gerasimenko *et al.,* 2013). Targeting Ca^{2+} entry would also remove the need for pharmacological intervention of intracellular components such as the ER and mitochondria (Petersen, 2014). Furthermore, aberrant CRAC channel activity has been implicated in other human disorders, mentioned in section 1.4.3. This has resulted in academic institutions and pharmaceutical companies expressing an interest and collaborating in CRAC channel inhibitor development (Parekh, 2010; DiCapite *et al.,* 2011; Osherovich, 2013; Tian *et al.,* 2016).

Our knowledge of the molecular components of the CRAC channel has improved significantly, permitting the development of compounds targeting either STIM1 or the pore of the Orai channel, through inhibiting the pore itself or disrupting STIM-Orai communication (Tian *et al.,* 2016). Pyrazole compounds such as GSK-7975A (2,6-difluoro-N-1(1-(4-hydroxy-2-(trifluoromethyl)benzyl)-1H-pyrazol-3-yl)benzamide), produced by GlaxoSmithKline, have been particularly effective as Orai1 and Orai3-specific inhibitors (Derler *et al.,* 2013; Gerasimenko *et al.,* 2013). At low micromolar concentrations, the novel compound GSK-7975A was reported to completely inhibit CRAC-mediated Ca^{2+} influx in human lung mast cells, rat basophilic leukaemia (RBL-2H3) cells and mast and T-cells from human, rat, mouse and guinea pig preparations (Ashmole *et al.,* 2012; Derler *et al.,* 2013; Rice *et al.,* 2013). More importantly, in isolated murine PACs, GSK-7975A markedly prevented toxic POAEE-evoked $[Ca^{2+}]_i$ elevations, trypsin and protease activity and cellular necrosis. GSK-7975A also strikingly reduced both asparaginase-evoked Ca^{2+} influx and toxic levels of necrosis (Geraimenko *et al.,* 2013; Peng *et al.,* 2016).

1.6.4 Novel CRAC channel inhibitor, CM4620

Due to a lack of specificity and high toxicity, the majority of CRAC channel inhibitors have not reached clinical trials. Over the past decade, however, the biotechnology company CalciMedica has generated numerous selective and potent CRAC channel inhibitors, including CM2489, which was the first to be tested in humans and complete Phase I clinical trials for moderate-to-severe plaque psoriasis treatment (Jairaman and Parakirya, 2013). The compound CM_128 (also known as CM4620) successfully inhibited Ca^{2+} influx in human PACs at concentrations of 1 μM. In both mouse and human PACs, CM_128 was significantly more potent at inhibiting SOCE than GSK-7975A. Furthermore, CM_128 prevented acinar necrosis and all local and systemic hallmarks of AP exhibited in three alcohol metabolite or bile acid induced mouse models (Wen *et al.,* 2015).

CM4620, a novel small molecular entity of Orai1 inhibitors developed by CalciMedica is the focus of this study. CM4620 has completed Phase I clinical trials and was granted fast-track designation by the FDA (Food and Drug Administration), for the treatment of AP. Furthermore, results are due to be published on CalciMedica's CM4620-based Phase IIa clinical trial (NCT03709342) for treating moderate to severe AP (CalciMedica, 2019). This is the most advanced step, thus far, in therapeutic development for AP (Pevarello *et al.,* 2014). A recent study by Waldron and colleagues sought to examine the effectiveness of CM4620 in *in vivo* models of pancreatitis. The inflammatory pathways relating to SOCE in PACs, immune cells and the recently discovered resident cells situated in close proximity with acinar cells in the periacinar space, namely pancreatic stellate cells (PaSCs) were also investigated (Apte *et al.,* 2013; Waldron *et al.,* 2019). Intravenous infusion of CM4620 in *in vivo* rat models of pancreatitis significantly diminished pancreatic oedema, acinar cell vacuolisation, intrapancreatic trypsin activity and acinar cell necrosis. The expression of inflammatory cytokines in pancreas and lung tissues and cytokine generation in human peripheral blood mononuclear cells and rodent PaSCs were markedly decreased thus revealing a role for Orai1/STIM1 in the cellular inflammatory pathways involved in AP. However, the long-term application of this inhibitor is doubtful due to these profound effects on immune cells (Waldron *et al,* 2019).

Successful preliminary investigations on the effect of CRAC channel inhibitor, CM4620, on Ca^{2+} entry in mouse PACs influenced this thesis. These results are depicted in Figs. 1.6, 1.6.1 and 1.6.2. Freshly isolated

PACs were initially perfused with NaHEPES solution in the absence of external Ca^{2+}. ER Ca^{2+} stores were then depleted using the specific SERCA pump inhibitor, CPA, in the absence of external Ca^{2+}. This process activated SOCE, represented in Fig. 1.6 by a considerable peak of Ca^{2+} influx. After a stable $[Ca^{2+}]_i$ plateau was reached, external Ca^{2+} was removed, causing Ca^{2+} efflux from the cytosol through extrusion pathways within the plasma membrane. This standard protocol was subsequently adapted to introduce the CRAC channel inhibitor (Fig. 1.6.1). PACs were preincubated with 1 μM (Fig. 1.6.1A) and 10 μM CM4620 (Fig. 1.6.1B) for approximately 30 minutes, prior to administration of external Ca^{2+}. Higher concentrations of CM4620 progressively depressed the $[Ca^{2+}]_i$ plateau.
10 μM CM4620 very significantly inhibited the amplitude of $[Ca^{2+}]_i$ elevation due to Ca^{2+} entry, close to the initial control baseline, compared to untreated control cells (Fig. 1.6). 1 μM CM4620 also very markedly and significantly reduced the amplitude of Ca^{2+} influx (Fig. 1.6.2).

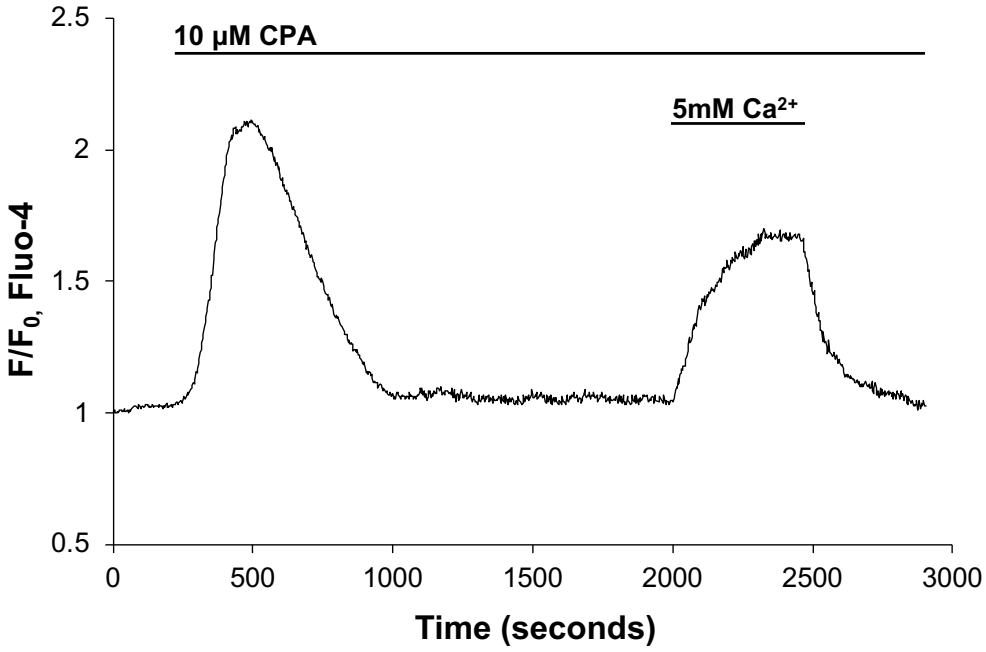

Figure 1.6. The standard store depletion protocol. Typical representative control trace in which the endoplasmic reticulum (ER) Ca^{2+} stores of PACs (*n* = 25) were emptied using the ER Ca^{2+} pump inhibitor, cyclopiazonic acid (CPA) (10 μM), in a Ca^{2+}-free solution. This resulted in a large rise in cytosolic Ca^{2+} (200 - 500 seconds) followed by a decline to baseline levels due to the absence of external Ca^{2+} (500 - 1000 s). The addition of 5 mM Ca^{2+} to the external solution subsequently caused a marked rise in cytosolic Ca^{2+} which eventually plateaued (2000 - 2500 s). At this point, external Ca^{2+} was removed causing cytosolic Ca^{2+} levels to return to baseline (2500 - 3000s).

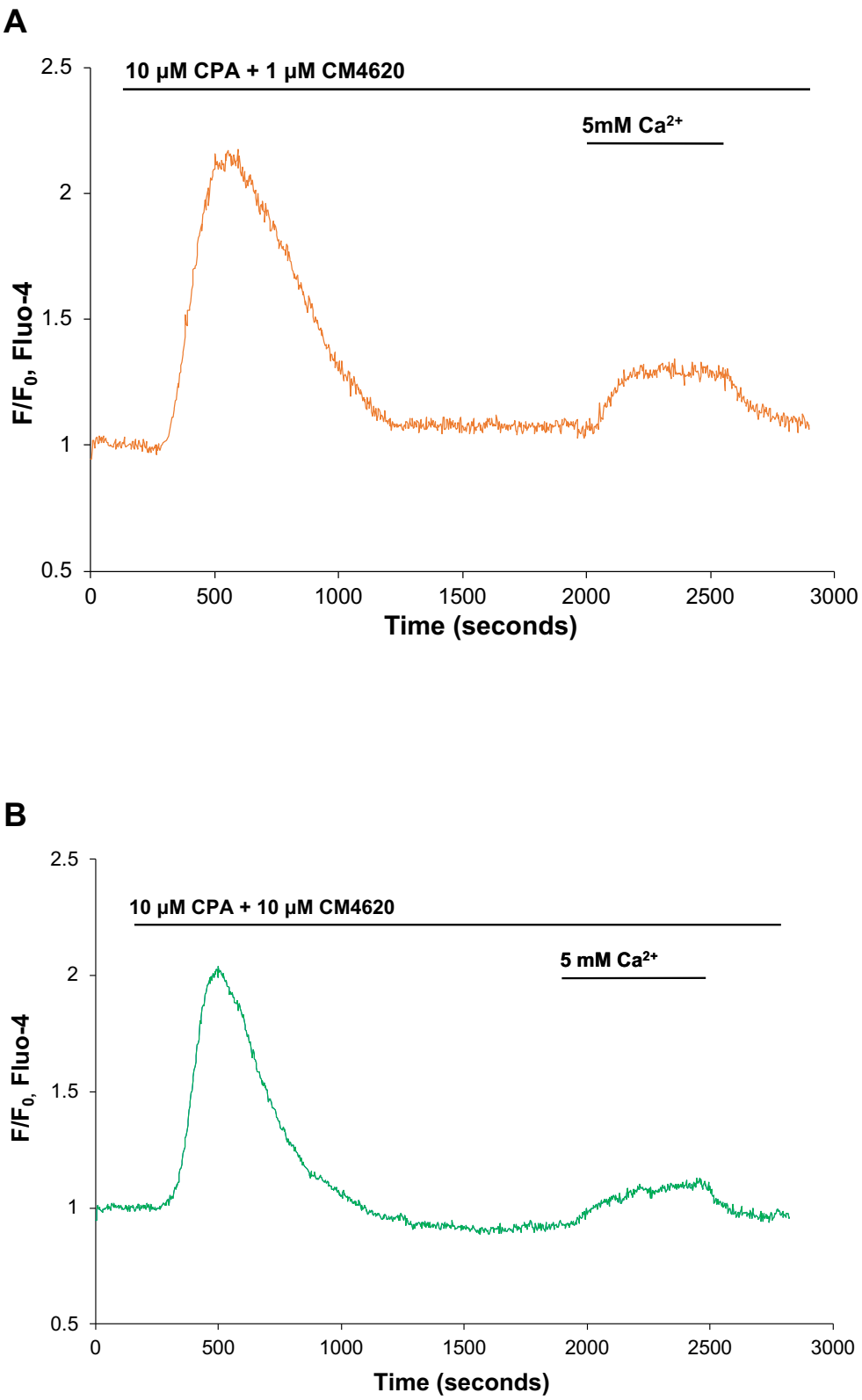

Figure 1.6.1. The inhibitory effect of pre-incubation of CM4620 on CRAC channel-mediated Ca^{2+} entry in PACs. Representative traces showing pre-incubation of Fluo-4 loaded cells with **(A)** 1 µM (orange trace) and **(B)** 10 µM (green trace) CM4620 before the re-administration of 5 mM external Ca^{2+} at 2000 seconds which caused a significant reduction in Ca^{2+} entry (23 cells/group), compared to control cells shown in Fig 1.6.

Mean $[Ca^{2+}]_i$ amplitude change due to Ca^{2+} influx ($\Delta F/F_0$)

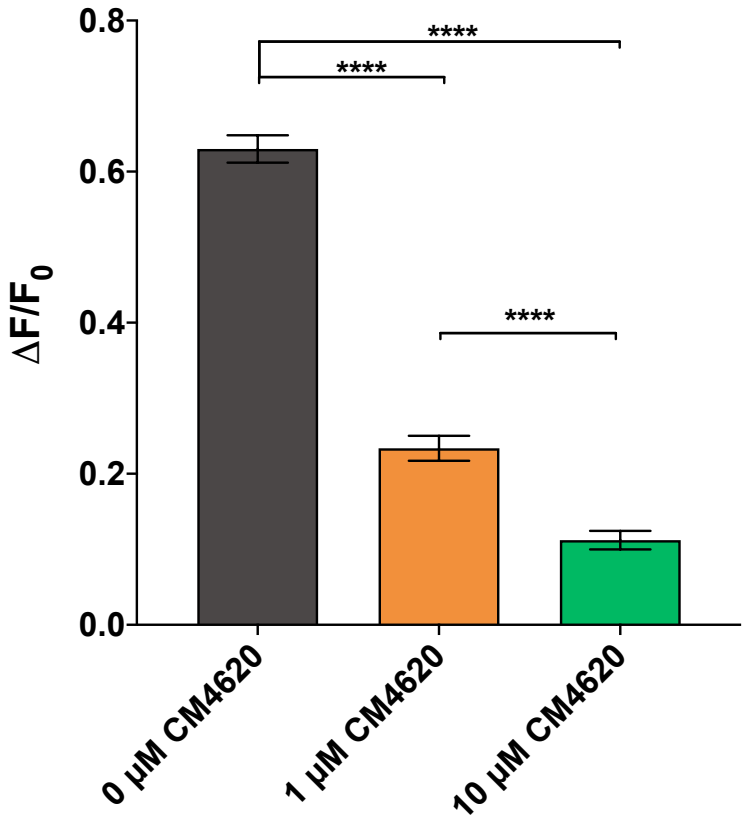

Figure 1.6.2. Effect of CM4620 on mean $[Ca^{2+}]_i$ amplitude change ($\Delta F/F_0$) as a result of Ca^{2+} entry in PACs. Quantitative analysis depicting a significant concentration-dependent difference ($P < 0.0001$) in averaged amplitudes of Ca^{2+} entry following pre-incubation with CM4620, compared with control cells is shown. *P* values were calculated using one-way ANOVA followed by a Tukey's post-hoc test to confirm differences between groups, ****, $P < 0.0001$. Data presented as mean ± SEM.

1.7 Aims and objectives of the study

The aim of this project is to continue to determine the effects of novel CRAC channel inhibitor, CM4620 on the pathogenesis of AP whilst investigating the potential therapeutic use of CM4620 in inhibiting AP pathology. This study has the following objectives:

[1] Measure potential effects of CM4620 on physiological Ca^{2+} signalling and, in particular, recovery of the Ca^{2+} responses in isolated PACs induced by physiological concentrations of ACh.

[2] Measure the effects of CM4620 on store-operated Ca^{2+} influx *in vitro* in mouse PACs.

[3] Measure the *in vitro* effects of CM4620, at low nanomolar concentrations, on cellular necrosis elicited by AP-inducing agents, such as bile acids, alcohol metabolites and asparaginase. The effectiveness of combining low concentrations of CM4620 with energy supplement galactose on cell death levels, evoked by AP-inducing agents will also be investigated.

[4] Measure the effects of nanomolar concentrations of CM4620 *in vivo* in mouse models of alcohol-induced pancreatitis.

CHAPTER 2: MATERIALS AND METHODS

CHAPTER 2: Materials and Methods

2.1 Materials and reagents

Acetylcholine (ACh) (cat. A6625-25G) was obtained from Sigma-Aldrich, Dorset, UK. It was prepared in water at a stock concentration of 10 mM, aliquoted and stored at -20°C.

Bile acid (BA) (cat. S9875-100G) was also purchased from Sigma-Aldrich and contained a mixture of the sodium salts of taurocholic, glycocholic, deoxycholic and cholic acids. It was stored at room temperature, prepared fresh at 0.06% concentration in NaHEPES and used immediately.

D-galactose (cat. G5388-100G), dimethyl sulfoxide (DMSO) (cat. D8418-100ML), ethanol (cat. 459836-100ML) and formaldehyde (37% stock solution) (cat. F1635-4L) were obtained from Sigma-Aldrich as well as palmitoleic acid (POA) (cat. P9417-100MG), which was prepared fresh in ethanol at a 30 mM stock concentration and used immediately at 30 µM.

Asparaginase (cat. AB73439) was purchased from Abcam, Cambridge, UK and prepared in NaHEPES buffer at a 5000 IU/ml stock concentration, aliquoted and frozen at -20°C. It was used at a 200 IU/ml final concentration.

Calcium chloride ($CaCl_2$) (cat. 21114-1L) was supplied by Fluka, Loughborough, UK. A 1 M stock solution was kept at room temperature.

CM4620 was supplied by CalciMedica, La Jolla, California. A 10 mM stock concentration of CM4620 in DMSO was prepared, aliquoted and stored at -20°C.

Cover glass 32 x 32 mm, thickness Number 1 and sterile phosphate-buffered saline (PBS) (cat. E504-100ML), stored at room temperature, were purchased from VWR International Leicestershire, UK.

Cyclopiazonic acid (CPA) (cat. 1235) was obtained from Tocris, Bristol, UK, prepared in DMSO at 20 mM stock concentration and stored at -20°C.

2.2 Preparation of solutions

2.2.1 Preparation of NaHEPES solution

NaHEPES buffer was prepared as follows: 140 mM sodium chloride (cat. S3014- 500G); 4.7 mM potassium chloride (cat. P9541-500G); 10 mM HEPES (4-(2-Hydroxyethyl)piperaxine-1-ethanesulfonic acid) (cat. H4034-100G); 1 mM magnesium chloride (obtained from 1 M stock solution, cat. M1028-10X1ML); 10 mM D(+)glucose (cat. G8270-100G). NaOH (Calbiochem, Nottingham, UK) was used to adjust pH to 7.2. 1 mM $CaCl_2$ was added to the NaHEPES solution for pancreatic acinar cell isolation and the majority of experimental work, when required (Gerasimenko *et al.,* 1996a). All above reagents were purchased from Sigma-Aldrich, unless otherwise stated.

2.2.2 Preparation of collagenase solution

Type V collagenase (cat. C9263-100MG), obtained from Sigma-Aldrich, was prepared in NaHEPES buffer (supplemented with 1 mM $CaCl_2$) to produce a 31.25 CDU ml^{-1} stock solution. The solution was divided into 1 ml aliquots and stored at -20°C.

2.2.3 Preparation of fluorescent dyes

Fluo-4-AM (cat. F14201) was purchased from Thermo Fisher Scientific, Paisley, UK. A 2 mM stock solution was prepared in DMSO, aliquoted, frozen at -20°C and protected from light.

Propidium iodide (PI) (cat. P3566), supplied by Thermo Fisher Scientific, was stored at 4°C at a 1 mg/ml stock concentration and protected from light.

2.3 Isolation of pancreatic acinar cells

All regulated procedures involving animals were performed in compliance with the UK Home Office regulations under the Animal (Scientific Procedures) Act, 1986. Training and oversight of procedures were conducted by competent Cardiff University employees and in accordance with national requirements. C57BL6/J male mice (6-8 weeks old, 23 ± 3 g in weight and shown in Fig. 2.1) were obtained from Charles River Laboratories

(Margate, UK). They were housed in Cardiff University's School of Biosciences animal unit with corn cob bedding and an enriched environment, which included nesting material and cardboard tunnels. Up to five mice were kept in each plastic cage (12 hour light cycle) and a standard rodent chow diet with free access to water was maintained before and throughout experiments. According to Schedule 1 of the UK Animal (Scientific Procedures) Act 1986, the mice were humanely killed by cervical dislocation (Gerasimenko *et al.,* 1996a).

Figure 2.1. Photograph of a wild type C57BL6/J mouse used in this study. Mice were purchased from Charles River Laboratories (Margate, UK) and used for pancreatic tissue isolation procedures (adapted from C57BL/6 Mouse Model Information Sheet, 2019).

The pancreas was rapidly dissected from a mouse and washed twice in NaHEPES buffer solution, supplemented with 1 mM $CaCl_2$. The tissue was subsequently injected with 1 ml collagenase (31.25 CDU ml^{-1}) and incubated in this solution, in a shaking water bath for 5-6 minutes at 37°C. This allowed partial digestion of the tissue. After incubation, the tissue was transferred into a 15 ml falcon tube and suspended in NaHEPES, to remove any remaining collagenase solution. Manual agitation of the tissue, by pipetting, was then performed to release single pancreatic acinar cells or small acinar clusters. The supernatant was collected and transferred to a fresh falcon tube with the addition of NaHEPES buffer. This step was repeated numerous times before the cells were centrifuged for one minute at 200xg. The supernatant was discarded and the cell pellet was re-suspended in fresh NaHEPES buffer solution and centrifuged a second time. The final cell pellet was suspended in 2 ml NaHEPES solution and used in experiments within 4 hours after isolation. All experiments were conducted at room temperature (Gerasimenko *et al.,* 1996a).

2.4 Cytosolic Ca^{2+} measurements

Freshly isolated, intact PACs were loaded with the AM form of the Ca^{2+} sensitive fluorescent probe, Fluo-4. A final concentration of 5 μM was used and cells were loaded for 45 minutes at room temperature. After incubation, the cells were centrifuged as described previously, re-suspended in fresh NaHEPES solution (supplemented with 1 mM Ca^{2+}) and used for measurements of cytosolic Ca^{2+}. The cells were adhered to glass coverslips and continuously perfused, in a flow chamber, with a NaHEPES-based extracellular solution (Gerasimenko *et al.,* 1996a). An inverted Olympus IX71 system (Tokyo, Japan: x 40 oil objective; excitation 470 nm; emission 515-560 nm; 100 ms exposure time, 1 image/second) was used for Fluo-4 measurements and to visualise cells. WinFluo software was used to collect and record data.

2.5 Store depletion protocol

Cells were continuously perfused with a Ca^{2+}-free NaHEPES solution for approximately five minutes, in order to prevent Ca^{2+} entry. PACs were then treated with CPA (10 μM), a specific SERCA pump inhibitor, to deplete ER stores of Ca^{2+} in the absence of external Ca^{2+}. ER store depletion resulted in SOCE channel activation, however, absence of external Ca^{2+} prevented further Ca^{2+} entry from occurring. Therefore, 5 mM Ca^{2+} was re-admitted to the extracellular solution, facilitating Ca^{2+} entry to the cytosol and enabling this phase of the response to be analysed. Extracellular Ca^{2+} was removed once a $[Ca^{2+}]_i$ plateau was reached. The subsequent phase of Ca^{2+} extrusion across the plasma membrane was also further analysed and enabled the return of cytosolic Ca^{2+} to baseline levels.

2.5.1 Store depletion with pre-incubation of CRAC channel inhibitor, CM4620

To investigate the effect of CM4620 on SOCE into freshly isolated PACs, a similar protocol (as described previously in Section 2.5) was used for ER Ca^{2+} store depletion, but with the addition of both CM4620 (10 μM) and CPA (10 μM) at 200s. Therefore, during CPA-induced depletion of ER Ca^{2+} stores, PACs were incubated with CM4620 for approximately 30 minutes, again in the absence of external Ca^{2+}. Extracellular Ca^{2+} (5 mM) was then re-admitted to solution, in the presence of CM4620 (10 μM), to enable Ca^{2+} entry. Once

maximal Ca^{2+} entry and the subsequent cytosolic Ca^{2+} plateau phase was established, extracellular Ca^{2+} was again removed from the solution, as previously described. The presence of CM4620 was continued until baseline cytosolic Ca^{2+} levels were reached. This protocol was further replicated to investigate the effect of lower CRAC channel inhibitor concentrations. Cells were instead pre-incubated with 1 μM CM4620, together with CPA (10 μM).

2.6 Cellular necrosis assay

PACs were freshly isolated as previously described in Section 2.3. The final cell suspension was equally divided into 1 ml aliquots in order to investigate different experimental conditions. Up to 4 conditions were measured during each experiment: (1) negative control in the form of untreated cells; (2) positive control in the form of a necrosis-inducing reagent; (3) primary protective agent and necrosis-inducing agent; (4) combination of primary and secondary protective agents and necrosis-inducing agent. These conditions are summarised in Table 2.1. Pre-incubation of cells with various concentrations of primary protective agent CM4620 (10 μM, 1 μM, 100 nM, 50 nM, 10 nM, 1 nM, 200 pM) and the secondary protective agent, galactose (1 mM), were conducted for 30 and 20 minutes respectively. The subsequent treatment of cells with either BA, POA or asparaginase, to induce necrosis, lasted two hours. Each incubation was staggered at different time intervals, enabling sufficient time for imaging. At the end of the two-hour incubation period, cells were stained with PI (1 μg/ml final concentration) for 10 minutes and visualised on a Lecia confocal microscope TCS SPE (Leica Microsystems, Milton Keynes, UK), with a 40x oil objective. Positive PI staining (excitation 532 nm, emission: 585-705 nm), represented by intense red nuclei staining due to plasma membrane rupture, allowed for the detection of necrotic cells. 20 to 25 images, per condition, were taken and the total number of cells was calculated by counting the number of necrotic (PI positive staining) and viable (PI negative staining) cells. At least three independent experiments (N = 3) for each condition were performed (>100 cells per condition). This enabled the average percentage of necrotic cells of the total number of cells ± SEM to be calculated and presented as a bar chart (Gerasimenko *et al.,* 2013).

Table 2.1. Conditions measured during each cellular necrosis experiment.

Condition measured	Treatment of cells
Negative control (1)	Cells untreated. No application of necrosis-inducing agents or protective agents.
Positive control (2)	Cells incubated for 2 hours with a necrosis-inducing agent, such as bile acid, palmitoleic acid or asparaginase.
Primary protective agent (3)	Cells incubated with a preventative CRAC channel inhibitor, CM4620 (30 minute pre-incubation), as well as a necrosis-inducing reagent.
Primary and secondary protective agents (4)	Cells pre-incubated with a combination of two protective agents, i.e. CM4620 and galactose (for 30 and 20 minutes respectively), followed by a necrosis-inducing agent.

2.7 *In vivo* model of acute pancreatitis induced by fatty acid ethyl ester

All animal procedures were ethically reviewed and performed according to the Animals Scientific Procedures Act (1986), under the UK Home Office (Dr Oleg Gerasimenko, PPL: PDFF54638; PIL: I925AC360). Adult C57BL6/J male mice (20-25 g) were housed as previously described in Section 2.3, in groups of 2-3 mice per cage. The mice received two hourly intraperitoneal (IP) injections of POA (150 mg/kg) combined with ethanol (1.35 g/kg) to induce alcohol/fatty acid AP (FAEE-AP). In order to reduce potential damage to peritoneal organs at the injection site, 200 μl sterile phosphate-buffered saline (PBS) was immediately injected before the ethanol/POA injection. Control mice received two hourly IP injections of PBS alone. 24 hours prior to FAEE-AP induction, analgesia was given by oral administration of 2.5 μg/ml buprenorphine hydrochloride. Animals were randomly assigned to three groups for evaluation: (1) PBS (n = 2); (2) POA and ethanol combination, inducing FAEE-AP (n = 2); (3) FAEE-AP + 0.1 mg/kg CM4620 (n = 3). In the treatment group, mice were co-administered IP injections of 0.1 mg/kg CM4620 (dissolved in PBS) with ethanol/POA injections, at 1-hour intervals. Animals were sacrificed 24 hours after the first injection and pancreas tissues were extracted for histological analysis, to assess the severity of FAEE-AP. The experimental protocol for the *in vivo* model of FAEE-AP was repeated three times.

2.8 Histology and evaluation of AP severity

Pancreatic tissues were fixed in 4% formaldehyde, 24 hours before processing. Fixed pancreatic tissues were then embedded in paraffin and stained with haematoxylin and eosin (H&E) (4 μm thickness). 15 or more random fields (magnification, x200) per slide were assessed for oedema, inflammatory cell infiltration and acinar necrosis by two independent investigators in a blinded manner, as previously described (Wildi *et al.,* 2007; Van Laetham *et al.,* 1996). The histopathological scoring system (scale, 0-3) is summarised in Table 2.2., as described by Van Laetham and colleagues (1996). The sum of individual scores for pancreatitis severity for ≥6 mice/group was presented as a bar chart with mean ± SEM for each parameter.

Table 2.2. Scoring criteria utilised for histological evaluation of acute pancreatitis severity (modified from Wildi *et al.,* 2007 and Van Laetham *et al.,* 1996).

Parameter	Score	Indication
Oedema	0	Absent
	1	Focally increased between lobules
	2	Diffusely increased
	3	Acini disrupted and separated
Inflammatory cell infiltrate	0	Absent
	1	In ducts (around ductal margins)
	2	In the parenchyma (< 50% of the lobules)
	3	In the parenchyma (> 50% of the lobules)
Pancreatic acinar cell necrosis	0	Absent
	1	Periductal necrosis (< 5%)*
	2	Focal necrosis (5-20%)
	3	Diffuse parenchymal necrosis (20-50%)

*Approximate percentage of cells involved per field examined

2.9 Statistical Analysis

For quantitative analysis of Ca^{2+} responses, all fluorescence values were normalised and plotted as F/F_0 where F is the recorded fluorescence and F_0 is the baseline fluorescence of each trace. In order to correct experiments performed over a long duration, linear correction of focus drift was used. For $[Ca^{2+}]_i$ measurements of ACh-elicited responses in the presence and

absence of CM4620, areas under individual traces were calculated. The formula: $\Sigma(F/F_0 - F_1) \times \Delta t$, was used, where Δt is the time interval. Obtained values were then averaged and presented as bar charts.

For every recorded $[Ca^{2+}]_i$ trace for SOCE-based experiments, both phases of Ca^{2+} intrusion and extrusion were analysed and compared between control and PACs pre-incubated with CM4620. Changes in Ca^{2+} entry were determined by calculating the difference of the $F:F_0$ ratio at the peak of Ca^{2+} influx and at the baseline (after store depletion). The amplitude changes in F/F_0 ($\Delta F/F_0$) obtained for control PACs and cells treated with 10 μM and 1 μM CM4620 were then averaged and presented as bar charts. Calculations of the initial rate of Ca^{2+} influx and efflux were also evaluated as time values ($t_{1/2}$) corresponding to the half-maximal point of Ca^{2+} influx and efflux, respectively. The data for control and cells treated with 10 μM and 1 μM CM4620 were presented as bar charts with average $t_{1/2}$ influx and efflux.

Results are presented as mean ± SEM, where *N* represents the number of individual experiments and *n* corresponds to the number of single acinar cells. GraphPad Prism 5 and Excel 2019 were used to produce graphs, charts and calculations. Statistical significance and p-values were calculated using a two-tailed Student's t-test or a one-way ANOVA for data from more than two conditions, with the threshold set at 0.05 and asterisks representing the range (*$P < 0.05$, **$P < 0.01$, ***$P < 0.001$, ****$P < 0.0001$).

CHAPTER 3:

RESULTS - The effect of pharmacological inhibition of CRAC channels on physiological $[Ca^{2+}]_i$ responses in pancreatic acinar cells

CHAPTER 3: The effect of pharmacological inhibition of CRAC channels on physiological $[Ca^{2+}]_i$ responses in pancreatic acinar cells

3.1 CM4620 efficacy in response to physiological and pathological responses elicited by ACh in pancreatic acinar cells

The secretagogue ACh plays an important role both physiologically and pathologically in PACs, as mentioned previously. Small doses of ACh induce normal, cytosolic Ca^{2+} spiking which is fundamental for PAC secretory functions. The effect of CM4620-mediated CRAC inhibition on normal cytosolic Ca^{2+} spiking, evoked by ACh was therefore investigated. PACs were freshly isolated from the pancreas of a wild type C57BL6 mouse, as described before, and loaded with Fluo-4, AM. For untreated, control PACs (n = 19), NaHEPES solution, supplemented with 1 mM Ca^{2+} was first applied to cells for 200s before the application of ACh (20 nM and 1 μM). As seen in Fig. 3.1A, as expected, a small concentration of ACh (20 nM applied at 200s) stimulated transient cytosolic Ca^{2+} responses, or Ca^{2+} oscillations in control cells. These responses originated and subsequently declined to baseline levels. Whereas, stimulation with maximal secretagogue concentration (1 μM at 1200s) evoked one large, global cytosolic Ca^{2+} spike, lasting for around 100s before returning to baseline levels (Fig. 3.1A).

Following pre-treatment of cells with 1 μM CM4620 for 30 minutes (n = 31), the repetitive, local $[Ca^{2+}]_i$ spikes induced by 20 nM ACh were not entirely inhibited by CM4620 (Fig. 3.1B, 200 – 1000s). Quantitative analysis of experiments of the types shown in Fig. 3.1 was carried out by comparing the effect of pre-treatment with CM4620 (1 μM) on $[Ca^{2+}]_i$ elevations above the baseline (area under the curve) recorded during application of 20 nM ACh (Fig. 3.2) and 1 μM ACh (Fig. 3.3). The effect of CM4620-mediated CRAC blockade on normal $[Ca^{2+}]_i$ spiking elicited by 20 nM ACh, although markedly reduced, was only entirely inhibited in 25.8% cells (3.2A, orange trace). Average $[Ca^{2+}]_i$ elevations evoked by 20 nM ACh were significantly decreased (**, $P < 0.01$) from 95.15 ± 14.42 a.u. in control cells (grey trace and column in 3.2A and B) to 51.38 ± 6.29 a.u. in cells pre-incubated with 1 μM CM4620 (orange trace and column in 3.2A and B). Although the averaged maximal amplitudes of the elevations in cytosolic Ca^{2+} were significantly lower in cells pre-treated with CM4620 (1.38 ± 0.069) compared to control cells (1.93 ± 0.15) following administration of 20 nM ACh, the

responses were not entirely prevented (Fig. 3.2A and C). The degree of reduction observed here is likely due to partial depletion of the ER during a lengthy period of incubation with CM4620. A more marked reduction (***, $P < 0.001$) in average areas under $[Ca^{2+}]_i$ changes, induced by supramaximal concentrations of ACh (1 μM), was observed in cells pre-treated with 1 μM CM4620 (orange column, 247.1 ± 17.78 au) compared to control cells (grey column 351.8 ± 24.5 au) (Fig. 3.1B, 1200-00s and Fig. 3.3B). CM4620 was significantly effective at blocking the SOCE triggered by ACh. Interestingly, cells pre-incubated with CM4620 recovered to baseline levels at a significantly faster rate (97.7 seconds ± 6.68, *** $P < 0.001$) compared to untreated cells cells (141.6 ± 7.67), following maximal stimulation with 1 μM ACh (Fig. 3.3C).

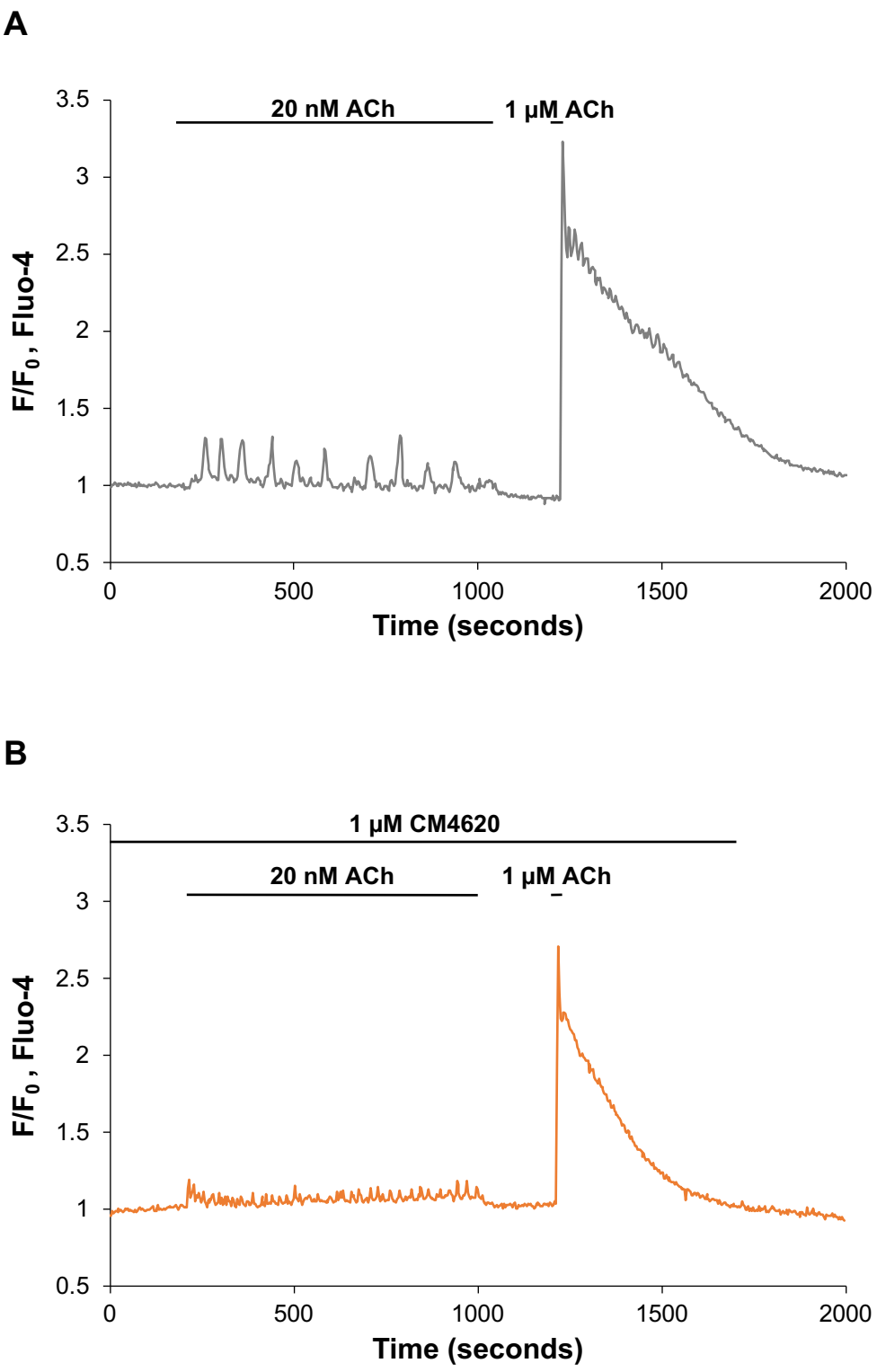

Figure 3.1. Representative trace of the effect of CM4620 on $[Ca^{2+}]_i$ spike generation evoked by acetylcholine (ACh) in mouse pancreatic acinar cells. (A). In untreated, control acinar cells, application of lower concentrations (20 nM at 200s) of ACh initiated small, transient and fairly repetitive oscillations in $[Ca^{2+}]_i$ which declined to baseline levels between spikes. Stimulation with 1 µM ACh (1200s) induced a sharp, global increase in cytosolic Ca^{2+} concentration which eventually returned to baseline levels (n = 19, grey trace). **(B).** Pre-treatment with 1 µM CM4620 for 30 minutes only marginally reduces Ca^{2+} oscillations induced by a low concentration (20 nM at 200s) of ACh (n = 31, orange trace) compared with control. 1 µM CM4620 inhibits the phase of $[Ca^{2+}]_i$ elevation evoked by a high concentration of ACh (1 µM at 1200s).

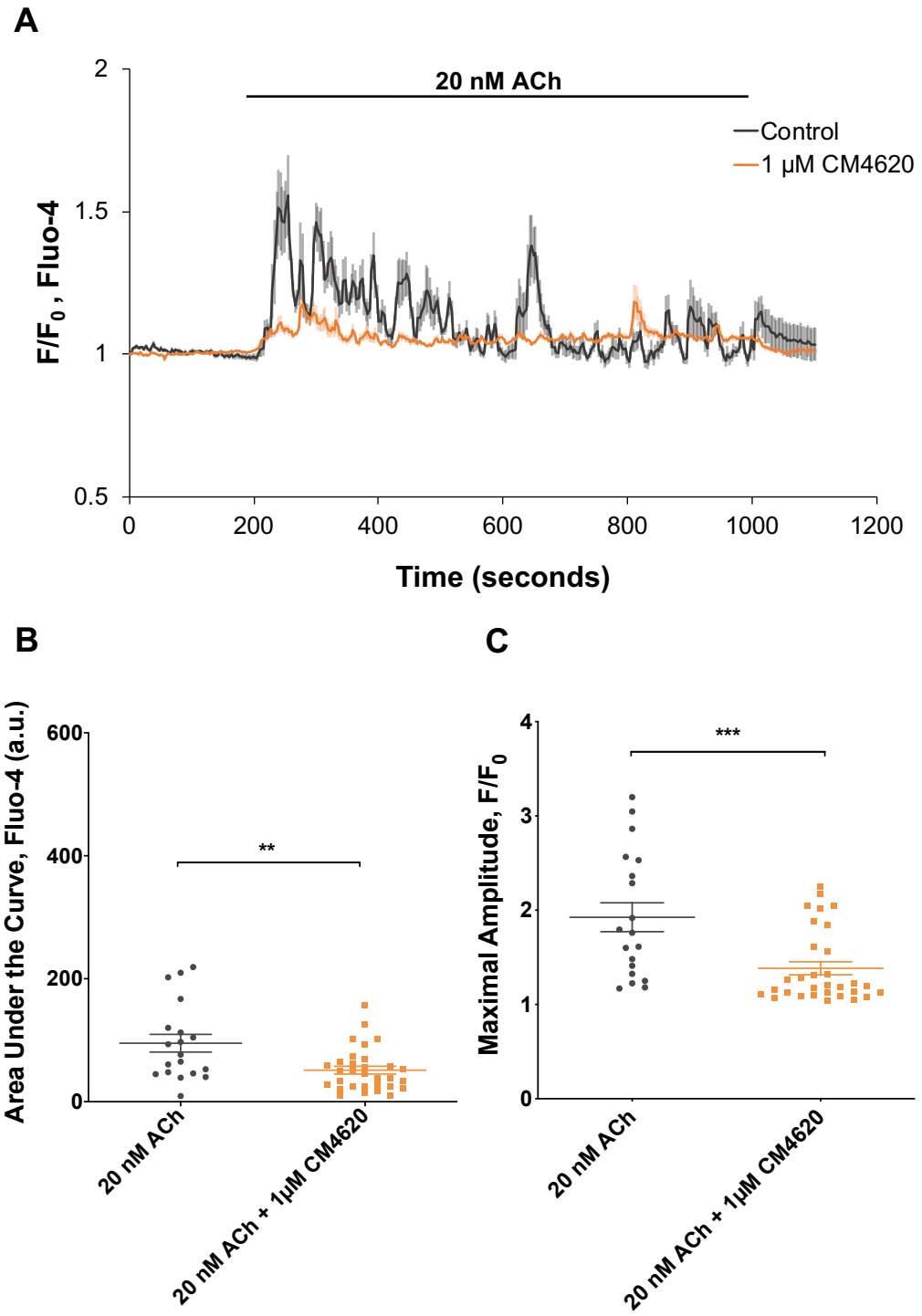

Figure 3.2. Quantitative analysis of experiments measuring the effects of inhibiting CRAC channels on changes in cytosolic Ca^{2+} concentration, induced by 20 nM ACh. (A). Averaging $[Ca^{2+}]_i$ elevations induced by 20 nM ACh recorded over a duration of 800s (200 – 1000s), resulted in a marked reduction in Ca^{2+} oscillations in cells pre-incubated with 1 μM CM4620 (for 30 minutes) (orange trace, n = 31) compared to untreated, control cells (grey trace, n= 19). $[Ca^{2+}]_i$ responses induced by 20 nM ACh were completely inhibited in 25.81% cells pre-treated with CM4620. **(B).** Comparison of the integrated $[Ca^{2+}]_i$ rises above the baseline (area under the curve) evoked by 20 nM ACh in experiments shown in A. Averaged areas under $[Ca^{2+}]_i$ responses in the presence of 1 μM CM4620 were slightly, but significantly lower (orange bar, 51.38 ± 6.29 au, ** $P < 0.01$) than in control (grey bar, 95.15 ± 14.42 au). **(C).** Comparison of the maximal amplitudes of the increases in $[Ca^{2+}]_i$ shown in A. Averaged maximal amplitudes of the elevations in $[Ca^{2+}]_i$ were significantly lower in cells pre-incubated with 1 μM CM4620 (1.38 ± 0.069, *** $P < 0.001$) compared to control (1.93 ± 0.15). Data represent mean values ± SEM, P values were calculated using a two-tailed Student's t-test.. Experiments were performed in standard buffer containing 1 mM $CaCl_2$.

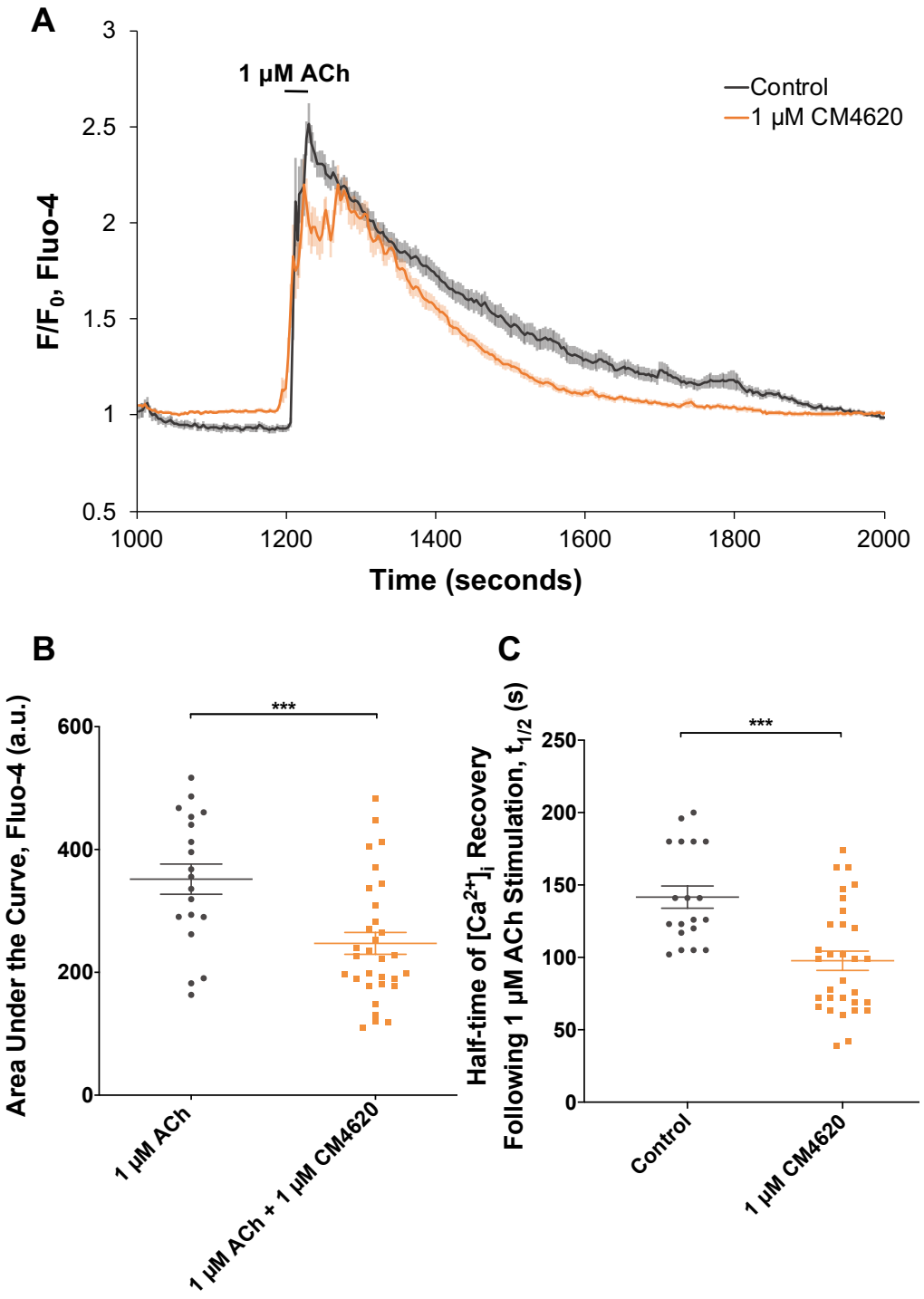

Figure 3.3. Quantitative analysis of experiments measuring the effects of high concentrations of ACh (1 μM) on cytosolic Ca^{2+} responses, following pre-incubation of cells with 1 μM CM4620. (A). Average traces of $[Ca^{2+}]_i$ responses evoked by a high ACh concentration (1 μM) recorded over a duration of 800s (1200 – 2000s). In this case, blockade of CRAC channels with 1 μM CM4620 (orange trace, n = 31) evoked a large initial rise in $[Ca^{2+}]_i$, similar to control cells (grey trace, n = 19), but significantly reduced the sustained plateau phase. $[Ca^{2+}]_i$ returned to the pre-stimulation baseline level. **(B).** Comparison of the average areas under $[Ca^{2+}]_i$ changes induced by a high concentration of ACh (1 μM applied at 1200s) in the traces shown in A. Grey bar represents untreated control cells (351.8 ± 24.5 au), whereas the orange bar represents cells incubated with 1 μM CM4620 for 30 minutes (247.1 ± 17.78). The mean values ± SEM of the responses in the presence of CM4620 were significantly lower (***, $P < 0.001$) than in control. **(C).** Comparison of the half-times of cytosolic Ca^{2+} recovery following maximal stimulation with 1 μM ACh shown in A. Cells pre-treated with CM4620 recovered to baseline levels at a significantly faster rate (97.7 seconds ± 6.68, *** $P < 0.001$) than control cells (141.6 seconds ± 7.67). Data represent mean values ± SEM, P values were calculated using a two-tailed Student's t-test.

3.2 CM4620 does not affect resting $[Ca^{2+}]_i$ responses in PACs

In order for CM4620 to be considered an effective therapeutic for AP, its effect on resting $[Ca^{2+}]_i$ concentrations should be minimal. Therefore, 1 μM CM4620 was applied to freshly isolated PACs for a duration of 800 seconds in standard buffer, supplemented with both 1 mM $CaCl_2$ and 1 μM CM4620 (n = 17, orange trace). As depicted by the representative traces in Fig. 3.4A, Ca^{2+} concentration (recorded by changes in Fluo-4) remained relatively stable with no substantial $[Ca^{2+}]_i$ spikes observed, following CM4620 treatment at 200s (orange trace). This was similar to the corresponding baseline recording (grey trace, Fig. 3.4B). The average trace of Ca^{2+} concentration following CM4620 treatment (n = 17, orange trace) compared to the average underlying baseline recording (n = 5, grey trace), portrayed as a control, is shown in Fig. 3.5. This data further depicts the stable responses when cells are at rest. When compared to the data shown in Section 3.1 (Figs. 3.2 and 3.3) where Ca^{2+} responses are significantly inhibited by CM4620 following ACh stimulation, these results suggest CM4620 does not block all Ca^{2+} influx. Therefore, only evoked cells show some modest differences.

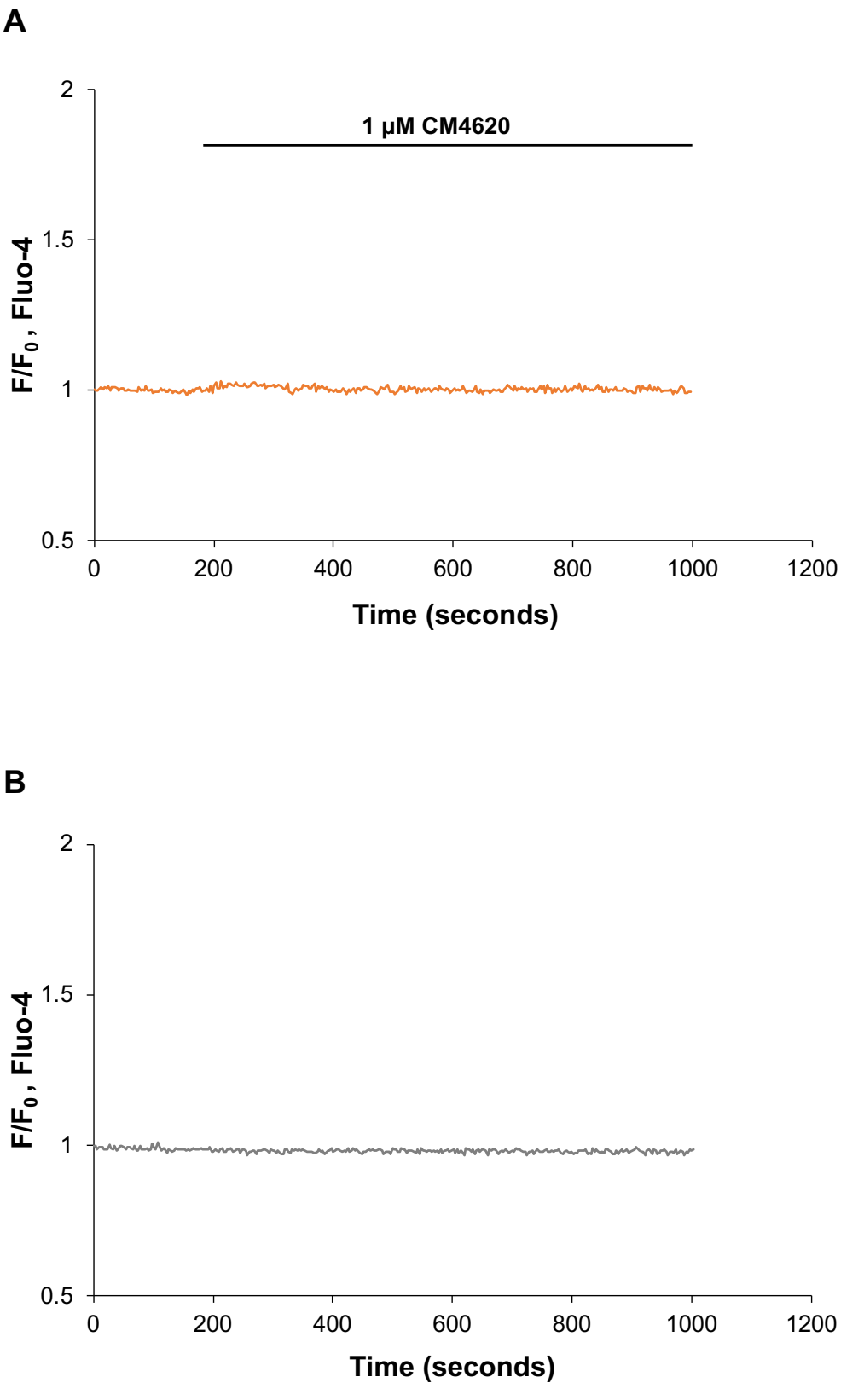

Figure 3.4. The effect of CM4620 application on resting cytosolic Ca^{2+} concentration in acinar cells is minimal. (A). Representative trace of 1 µM CM4620 applied, alone, to freshly isolated pancreatic acinar cells for 800 seconds (orange trace). **(B).** Representative trace of underlying baseline recording portrayed as a control (grey trace). Experiments were performed for a total of 1000 seconds in standard buffer supplemented with 1 mM $CaCl_2$.

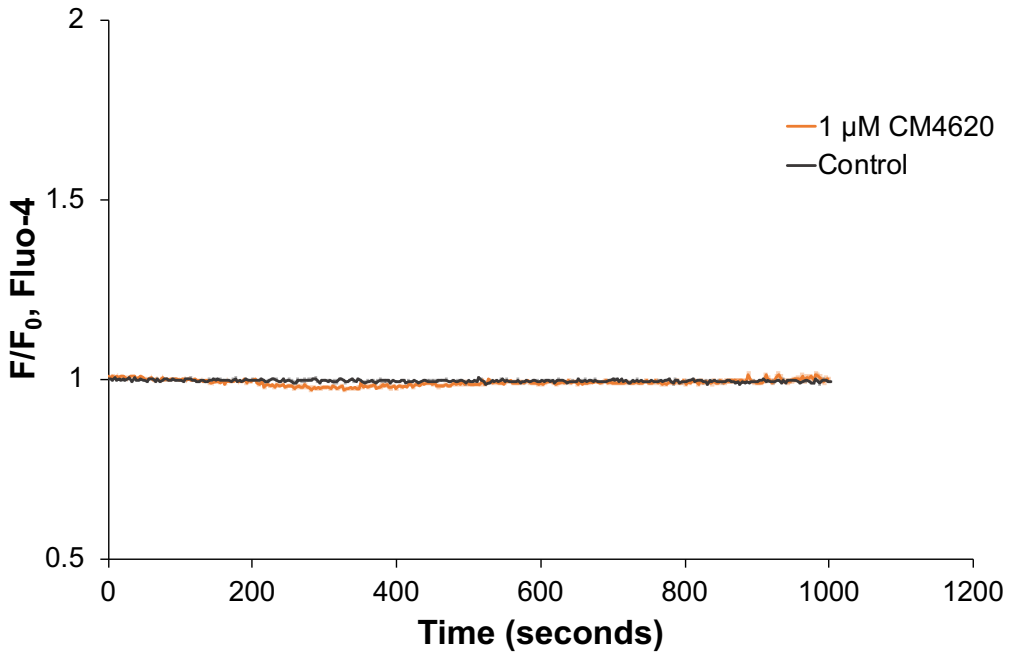

Figure 3.5. Resting cytosolic Ca^{2+} concentration in acinar cells is stable following treatment of CM4620. Averaging $[Ca^{2+}]_i$ responses induced by 1 μM CM4620 at 200s, recorded over a duration of 800s (200 – 1000s, n = 17). Levels of $[Ca^{2+}]_i$ remained relatively stable and no substantial elevations or declines in cytosolic Ca^{2+} concentration were observed. Experiments were performed for a total of 1000 seconds in standard buffer supplemented with 1 mM $CaCl_2$.

CHAPTER 4:
RESULTS - Pharmacological inhibition of store-operated Ca^{2+} influx in murine pancreatic acinar cells

CHAPTER 4: Pharmacological inhibition of store-operated Ca^{2+} influx in murine pancreatic acinar cells

4.1 Pharmacological inhibition of store-operated Ca^{2+} influx, with CM4620, affects signalling in pancreatic acinar cells

The effect of CRAC channel inhibitor, CM4620, on Ca^{2+} entry in mouse PACs was previously investigated and is represented by preliminary data shown in Fig. 1.6, 1.6.1 and 1.6.2, in section 1.6.4. The average traces depicted in Fig. 4.1 focus on the important phase of Ca^{2+} influx from 2000s onwards (Fig. 4.1B). 10 μM CM4620 very significantly inhibited the amplitude of $[Ca^{2+}]_i$ elevation due to Ca^{2+} entry, close to the initial control baseline, by around 84% ($P < 0.0001$, $n = 23$), compared to untreated control cells ($n = 25$). 1 μM CM4620 also very markedly and significantly reduced the amplitude of Ca^{2+} influx by 65% ($P < 0.0001$, $n = 23$). The significant inhibitory effect of pre-incubation of PACs with CM4620 on SOCE occurred in a concentration-dependent manner and is quantitatively summarised in Fig. 4.1.1 as mean changes in $[Ca^{2+}]_i$ amplitude due to Ca^{2+} influx. This figure was previously presented in section 1.6.4 as preliminary data.

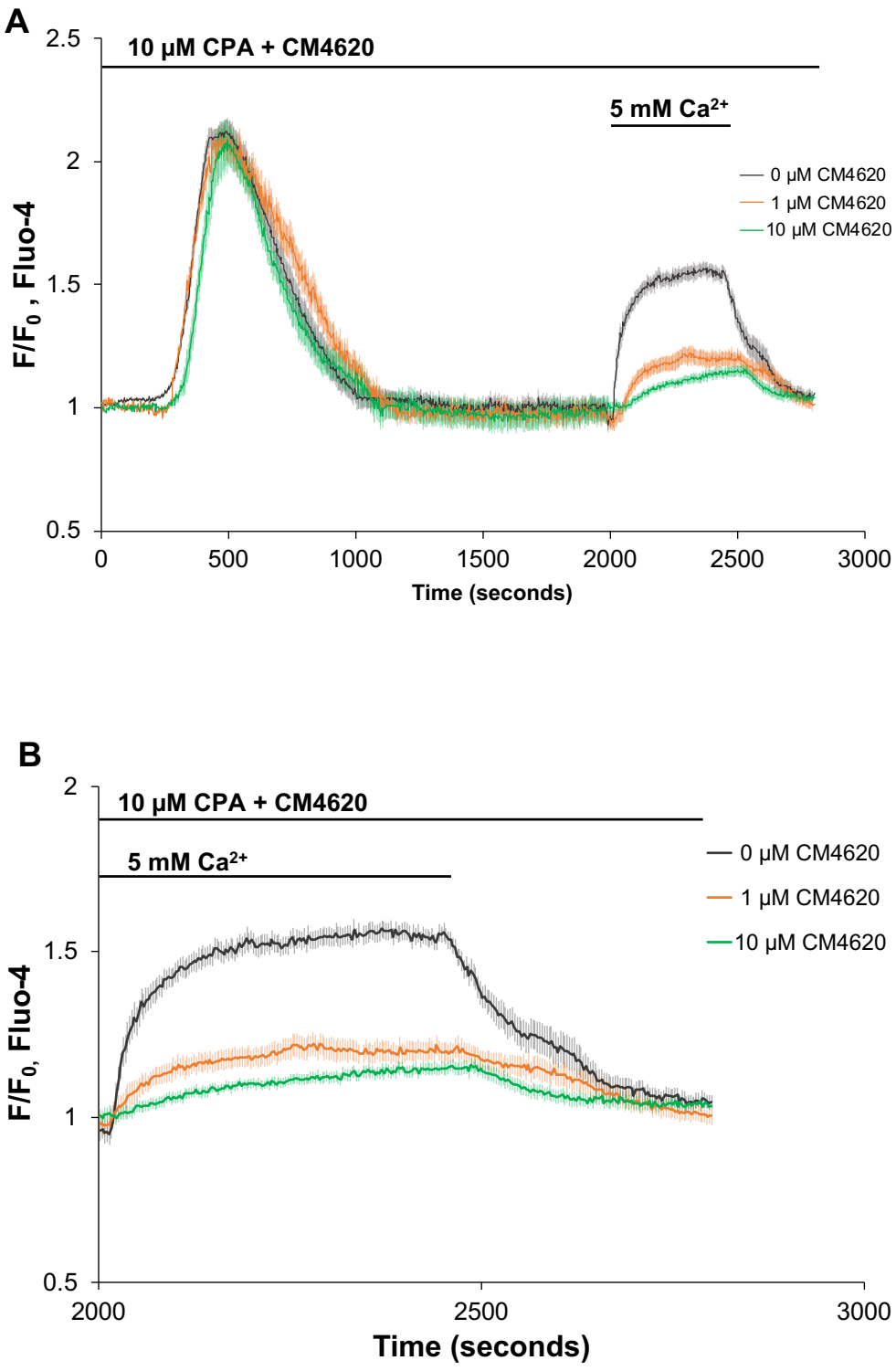

Figure 4.1. Effect of CM4620 on mean $[Ca^{2+}]_i$ changes as a result of Ca^{2+} entry in PACs. (A) Average $[Ca^{2+}]_i$ responses from experiments shown also in Fig. 1.6. and 1.6.1, section 1.6.4. 200s – 1000s demonstrates CPA-induced $[Ca^{2+}]_i$ elevation. Compared to isolated control acinar cells (dark grey trace, *n* = 25), pre-incubating cells with both 10 µM (green trace, *n* = 23) and 1 µM CM4620 (orange trace, *n* = 23) throughout the store depletion protocol clearly reduces the extent of Ca^{2+} entry (2000s onwards). **(B)** Average $[Ca^{2+}]_i$ responses shown from 2000s onwards in (A). Compared to isolated untreated PACs, pre-incubating cells with both 10 µM and 1 µM CM4620 clearly reduces the extent of Ca^{2+} entry.

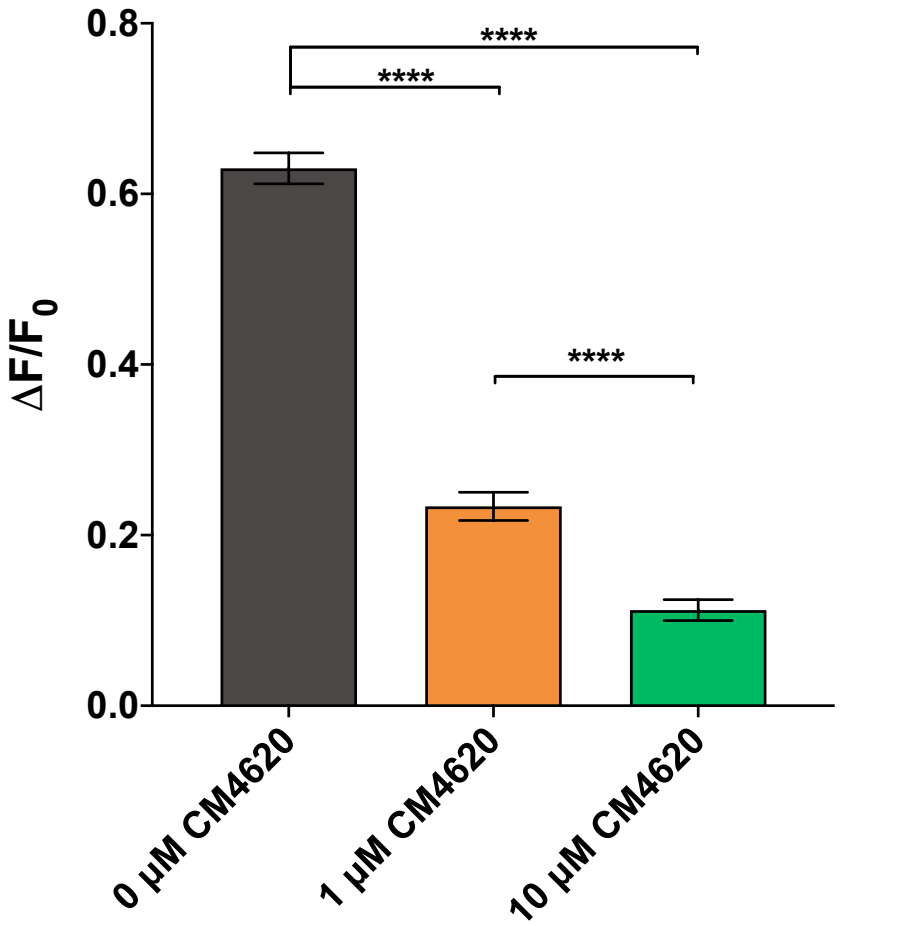

Figure 4.1.1. Effect of CM4620 on mean $[Ca^{2+}]_I$ amplitude change ($\Delta F/F_0$) as a result of Ca^{2+} entry in PACs. Quantitative analysis of experiments shown in section 1.6.4 as well as from 2000s onwards in Fig. 4.1A and B. Significant concentration-dependent differences ($P < 0.0001$) in averaged amplitudes of Ca^{2+} entry following pre-incubation with both 10 μM (green bar, $n = 23$) and 1 μM CM4620 (orange bar, $n = 23$), compared with control cells (dark grey bar, $n = 25$), is shown. This figure is also previously displayed in Fig. 1.6.2. *P* values were calculated using one-way ANOVA followed by a Tukey's post-hoc test to confirm differences between groups, ****, $P < 0.0001$. Bars presented as mean ± SEM.

Although the main focus of these investigations was the effect of CM4620 on SOCE (presented in Fig. 4.1B and Fig. 4.1.1), the effect of CM4620 on CPA-induced calcium elevations was also recorded. The CRAC channel inhibitor did not significantly influence ($P > 0.05$) CPA-evoked Ca^{2+} release from intracellular stores (200 – 1000s, Fig. 4.1A), hence the first 2000 seconds are removed from Fig. 4.1B. This is quantitively presented in Fig. 4.1.2. which shows no changes in mean CPA-induced $[Ca^{2+}]_i$ amplitude responses after CM460 pre-incubation.

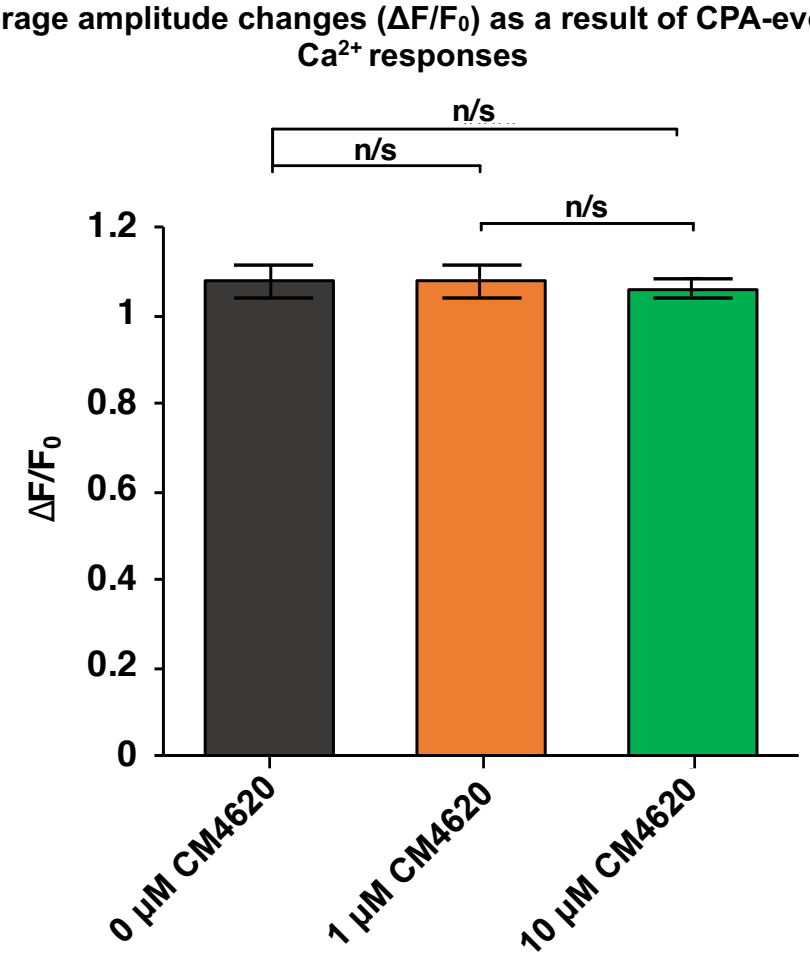

Figure 4.1.2. Effect of CM4620 on mean $[Ca^{2+}]_i$ amplitude change ($\Delta F/F_0$) as a result of CPA-induced Ca^{2+} responses in PACs. Quantitative analysis of CPA-induced $[Ca^{2+}]_i$ elevations, shown in Fig. 4.1A, from 200 - 1000 seconds. Compared to untreated control cells, 1 µM and 10 µM CM4620 did not significantly influence averaged changes in amplitudes of the CPA-evoked $[Ca^{2+}]_i$ increase. *P* values were calculated using one-way ANOVA followed by a Tukey's post-hoc test to confirm differences between groups, n/s, $P > 0.05$. Bars presented as mean ± SEM.

4.2 CM4620 enhances Ca^{2+} influx and extrusion across the plasma membrane

Figs. 4.2 and 4.3 show the relationship between CM4620 and changes in both the rate of rise and decline, depicted as half-times of $[Ca^{2+}]_i$ responses, due to Ca^{2+} influx and efflux respectively, following CPA-induced Ca^{2+} release from ER stores. This analysis is based on the phase of SOCE shown in Figure 4.1A (2000s onwards) and emphasised in Fig. 4.1B.

Pre-incubation of PACs with 1 μM CM4620 markedly slowed the initial rate of $[Ca^{2+}]_i$ elevation due to Ca^{2+} entry ($P < 0.0001$, $n = 23$), compared to untreated, uninhibited cells. This is depicted in Fig. 4.2 by longer half-times of the response. 10 μM CM4620 also further decelerated the rate of rise of $[Ca^{2+}]_i$ ($P < 0.0001$, $n = 23$), compared to untreated cells ($n = 25$) (Fig. 4.2). The half-time of Ca^{2+} entry was approximately five times longer in cells pre-treated with 10 μM CM4620, compared to control.

The extrusion of Ca^{2+} via plasma membrane pumps (described in section 1.3.2) is represented in Fig. 4.3 by the decrease in $[Ca^{2+}]_i$ upon the removal of 5 mM external Ca^{2+}. The effect of CM4620 is summarised by the half-time of $[Ca^{2+}]_i$ recovery. Pre-incubation of PACs with 1 μM and 10 μM CM4620 did not significantly affect the rate of $[Ca^{2+}]_i$ decline (half-time of the decrease) due to Ca^{2+} efflux ($P > 0.05$, $n = 23$), compared to untreated cells ($n = 25$) (Fig. 4.3).

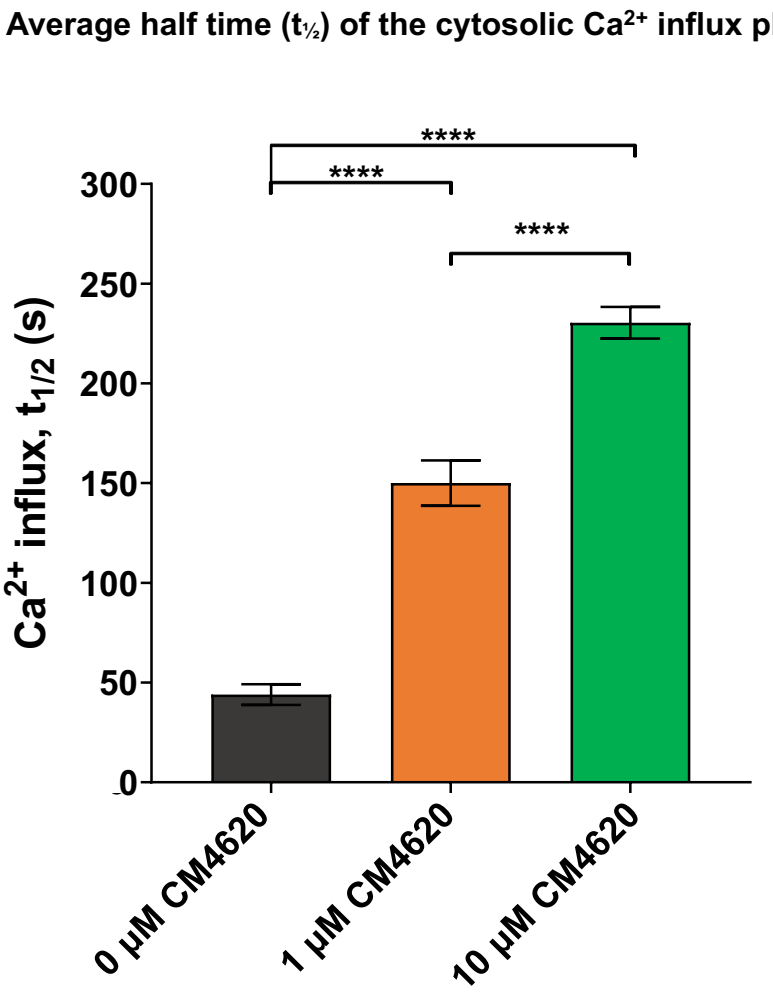

Figure 4.2. CM4620 decelerates Ca^{2+} entry in isolated murine PACs. Following CPA-induced Ca^{2+} release from ER stores, the external solution was supplemented with 5 mM Ca^{2+} to compare the rate of rise of $[Ca^{2+}]_i$ due to Ca^{2+} entry ($t_{1/2}$, seconds). Uninhibited, control cell (dark grey, n = 25) $[Ca^{2+}]_i$ responses during the Ca^{2+} influx process were relatively quick. Whereas, in the presence of 1 µM CM4620 (orange, n = 23) the half time ($t_{1/2}$) of Ca^{2+} influx was increased, representing slower $[Ca^{2+}]_i$ responses following admission of external Ca^{2+} (P < 0.0001). This effect was concentration-dependent, with 10 µM (green, n = 23) CM4620 (23 cells/group) further decelerating $[Ca^{2+}]_i$ responses. P values were calculated using one-way ANOVA followed by a Tukey's post-hoc test to confirm differences between groups, ****, P < 0.0001. Bars presented as mean ± SEM.

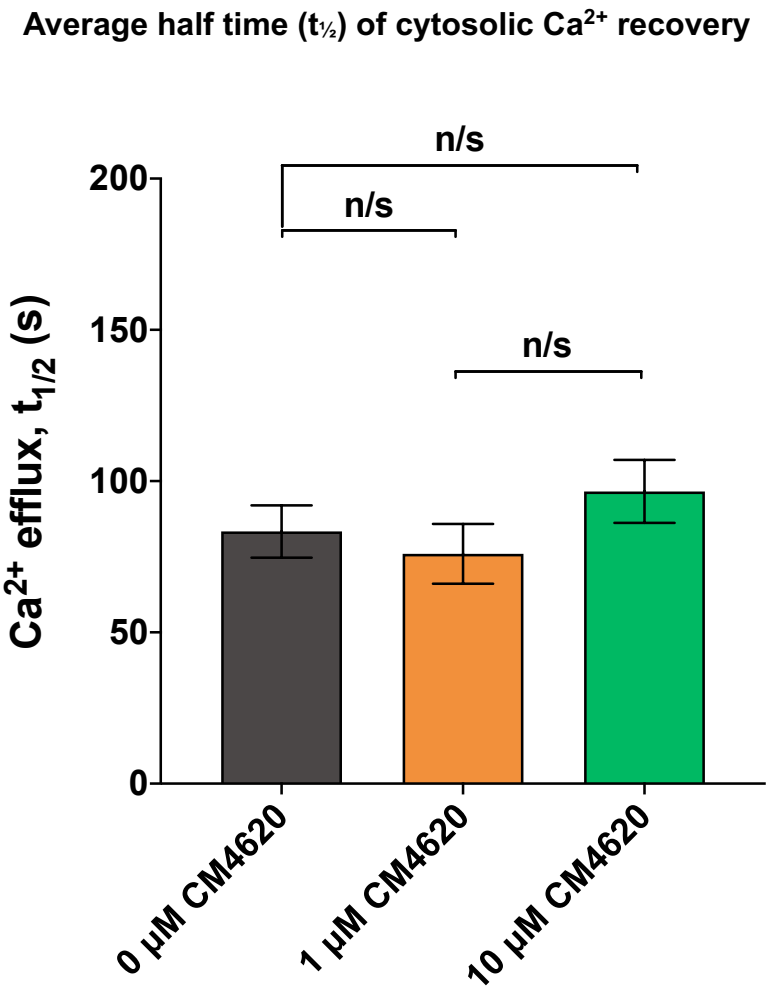

Figure 4.3. CM4620 does not affect extrusion in isolated murine PACs. After removal of external Ca^{2+}, the half-time of the Ca^{2+} efflux phase was unaffected with CM4620 pre-incubation ($P > 0.05$), compared to control. *P* values were calculated using one-way ANOVA followed by a Tukey's post-hoc test to confirm differences between groups, N/s, $P > 0.05$. Bars presented as mean ± SEM.

CHAPTER 5:
RESULTS - The protective role of CM4620 against necrosis in pancreatic acinar cells

CHAPTER 5: The protective role of CM4620 against necrosis in pancreatic acinar cells

5.1 CM4620-mediated CRAC channel inhibition protects against bile-induced necrosis

It is essential for CRAC channel inhibitors to effectively prevent Ca^{2+}-mediated acinar cell necrosis, in order to be considered a beneficial therapeutic for AP. Following successful investigations depicted by the data in Chapter 3 and 4, the present study was devised to continue researching the protective effects of the novel CRAC channel inhibitor, CM4620. The effect of CM4620 on activation of the necrotic cell death pathway in isolated mouse PACs, using various agents, such as BA, POA and ASNase was of particular interest. Although novel CRAC channel inhibitor, CM4620, is the first AP therapy to reach Phase III clinical trials, the long-term application of this inhibitor is doubtful due its profound effect on immune cells (Waldron *et al.,* 2019). Therefore, this study investigated the effects of low, sub-micromolar concentrations of CM4620 on BA-, POA- and ASNase-induced necrosis. This will facilitate the transition to researching the effects of CM4620 in *in vivo* experimental mouse models of AP whilst reducing the chances of potential side effects of CRAC channel inhibition. Furthermore, due to recent discoveries of the remarkable protective properties of galactose against necrosis, the effect of galactose in combination with CM4620 on bile-induced cell death was investigated. (Peng *et al.,* 2018).

CM4620 provided remarkable protection against BA-induced necrosis, as shown in Fig. 5.1 which depicts the effect of a CM4620-based cellular necrosis assay carried out in accordance with the protocol described in section 2.6. PACs were incubated for two hours with a BA mixture (0.06 g/ml sodium choleate) to evoke necrosis, representative of the most common cause of AP, gallstone biliary disease. In control cells, low levels of necrosis result from the process of PAC isolation as cells are alive and healthy (Fig. 5.1, grey column). As expected, the results in Fig. 5.1 show a significant increase in the percentage of BA-induced necrotic cells, compared to untreated control cells ($P < 0.0001$). An average increase of 15.77% was recorded, from an average of 4.11 ± 0.21% necrosis in control cells to 19.88 ± 0.52% in PACs treated with BA. The level of necrosis elicited by BA treatment was significantly diminished when PACs were pre-incubated with

CM4620 alone (green columns), for 30 minutes before the lengthy BA incubation, at 50 nM, and 100 nM ($P < 0.0001$) (Fig. 5.1). This significant decrease in necrosis levels was also found in preliminary data (not shown) with 1 μM and 10 μM CM4620 ($P < 0.0001$). Although levels of necrosis were reduced, the effect of pre-treating cells with a concentration of 10 nM CM4620 before their 2-hour exposure to BA was not significant ($P > 0.05$). The percentage of necrotic cells was diminished but not completely inhibited following treatment with 100 nM and 50 nM CM4620 (11.33 ± 0.18% and 13.66 ± 0.47%, respectively). However, pre-incubating PACs with 1 μM and 10 μM CM4620 (preliminary data, not shown) generated necrosis levels that were only marginally higher from the control with no significant difference ($P > 0.05$) reported between 10 μM CM4620 and untreated PACs.

5.2 CM4620 in combination with galactose significantly protects against bile-induced necrosis

The degree of necrosis elicited by BA treatment was more significantly diminished when cells were pre-treated with energy supplement, galactose (20 minutes) in combination with all three nanomolar concentrations of CM4620 (100 nM, 50 nM and 10 nM, orange columns), compared to CM4620 alone (green columns) (Fig. 5.1). These values were decreased to almost the same level as the controls. It is clear that CM4620 can effectively protect PACs against BA-induced necrosis in a concentration-dependent manner, at 10 nM, 50 nM and 100 nM. But this protection is more effective when galactose is applied in combination with 10 nM ($P < 0.0001$), 50 nM ($P < 0.01$) and 100 nM ($P < 0.05$) CM4620.

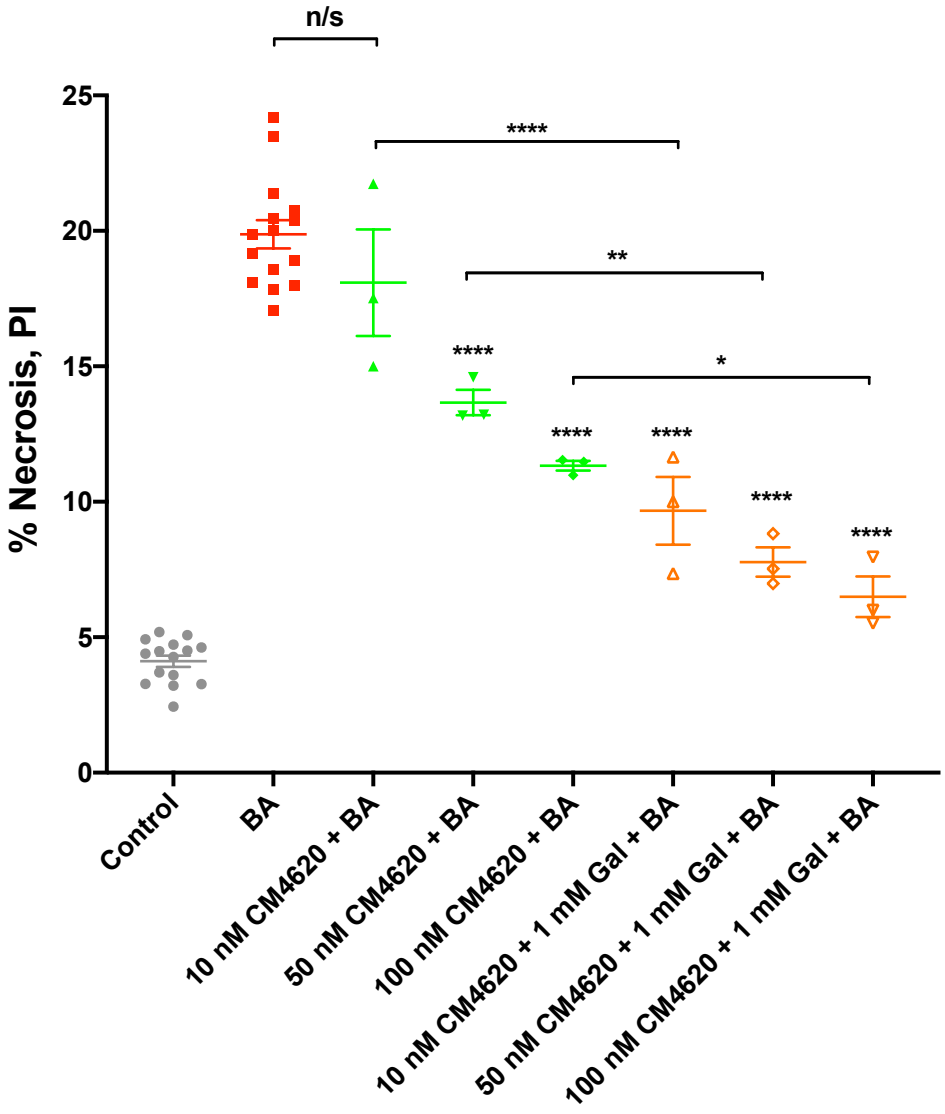

Figure 5.1. CM4620 and galactose provide substantial protection against bile-induced necrosis in PACs. Bile-induced (0.06 g/ml sodium choleate) necrosis is markedly reduced by adding 100 nM CM4620 (green column, 11.33% ± 0.18%, $P < 0.0001$) and even further reduced to nearly control level by adding 1 mM galactose (orange column, 6.49% ± 0.75%, $P < 0.0001$), in comparison to BA alone (19.88% ± 0.52%). Similar results depicted with 50 nM CM4620 (green column, 13.66% ± 0.47). Bile-evoked necrosis is not as effectively reduced by treating cells with 10 nM (18.09 ± 2.0%, $P > 0.05$). A combination of CM4620 (10 nM) and 1 mM galactose does markedly diminish cell death induced by BA (9.67% ± 1.25%, $P < 0.0001$). At least 3 series experiments/group with more than 150 cells in each sample. Data presented as mean ± SEM. *P* values were calculated using one-way ANOVA followed by a Tukey's post-hoc test to confirm differences between groups. n/s, $P > 0.05$; *, $P < 0.05$; **, $P < 0.01$; ****, $P < 0.0001$.

5.3 CM4620-mediated CRAC channel inhibition protects against alcohol metabolite-induced necrosis

The protective ability of low concentrations of CM4620 alone and in combination with galactose, against necrosis induced by BA (Figure 5.1) prompted an investigation into the effect of this CRAC channel inhibitor on POA-induced pathology. PACs were pre-treated with low concentrations of CM4620, such as 50 nM, 1 nM and 200 pM for 30 minutes. In the second treatment group, PACs were pre-incubated with both CM4620 and 1 mM galactose (for 20 minutes). Both treatment groups were then exposed to the alcohol metabolite, palmitoleic acid (30 μM), for 2 hours to elicit necrosis. The collective results of the experiments are shown in Fig. 5.2.

In comparison to the average necrosis level of untreated control cells (4.67 ± 0.38%, grey column), treatment with POA substantially decreases the number of live cells, causing an increase in necrosis (18.47 ± 0.27%, red column) (Fig. 5.2). The overall protective capability of CM4620 pre-incubation, alone (green columns), against POA-induced necrosis was more pronounced compared to BA-evoked necrosis, for all concentrations used (Fig. 5.2). Pre-treatment of PACs with 50 nM (green column) significantly reduces levels of necrosis (4.43% ± 0.22%) compared to POA alone ($P < 0.0001$). Furthermore, these values were only marginally higher than control cells wherein no significant difference between 50 nM CM4620 and untreated cells was found ($P > 0.05$). This demonstrates a more profound protective therapeutic capacity compared to results from BA-induced necrosis and CM4620 treatment. The effectiveness of 1 nM and 200 pM CM4620 alone on reducing levels of necrosis (10.15% ± 0.66%, $P < 0.0001$, and 11.05% ± 0.97%, $P < 0.0001$, respectively), compared with POA treatment is also shown. In contrast to the effects shown in Fig. 5.1., applying 50 nM with 1 mM galactose had no significant effect on POA-evoked necrosis levels (4.27% ± 0.5%, $P > 0.05$) compared to CM4620 alone. However, POA-evoked necrosis levels were still more potently reduced with 50 nM CM4620-galactose combination treatment (orange column) compared to this concentration of CM4620 applied alone.

At even lower concentrations, the degree of necrosis elicited by POA treatment was dramatically and significantly diminished with a combination of 1 nM CM4620 and galactose (5.99% ± 0.62%, $P < 0.001$) together with 200 pM CM4620 and galactose (7.89% ± 0.44%, $P < 0.01$), compared to

CM4620 alone (Fig. 5.2). This combination of treatments almost entirely inhibited POA-evoked necrosis. No significant difference was found when comparing the necrosis levels of 1 nM CM4620 in combination with galactose and control cells ($P > 0.05$). The results shown in Fig. 5.2 show that CM4620 can successfully protect PACs against necrosis, evoked by POA, at 50 nM, 1 nM and 200 pM concentrations. The addition of galactose with 50 nM CM4620 yields very similar levels of protection against necrosis to CM4620 alone (n/s, $P > 0.05$). Whereas the combination of 1 nM and 200 pM CM4620 with galactose provides a more significant reduction in POA-induced necrosis compared with the application of CM4620 individually. Overall, all concentrations of CM4620 alone and in combination with galactose markedly reduced levels of necrosis in comparison to POA applied solely to cells ($P < 0.0001$).

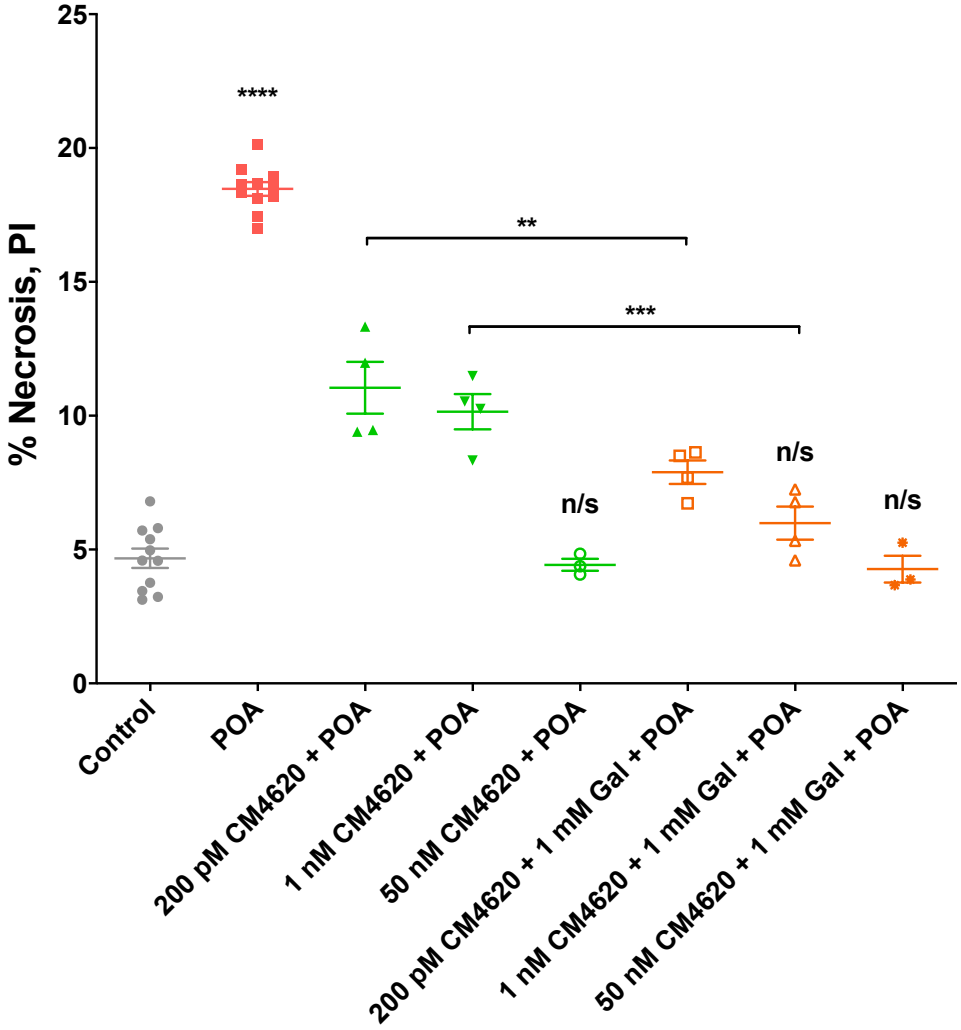

Figure 5.2. CM4620 and galactose provide substantial protection against alcohol metabolite-induced necrosis in PACs. Palmitoleic acid (POA)-evoked (30 μM) necrosis is significantly reduced by adding 50 nM (4.43% ± 0.22%, $P < 0.0001$), 1 nM (10.15% ± 0.66%, $P < 0.0001$) and 200 pM (11.05% ± 0.97%, $P < 0.0001$) CM4620 alone (green columns). No significant difference was shown between 50 nM CM4620 alone and 50 nM CM4620 in combination with 1 mM galactose ($P > 0.05$). Adding galactose with both 1 nM and 200 pM CM4620 was significantly effective in reducing POA-induced necrosis levels in cells, compared to CM4620 alone ($P < 0.001$ and $P < 0.01$, respectively). At least 3 series experiments/group with more than 150 cells in each sample. Data presented as mean ± SEM. *P* values were calculated using one-way ANOVA followed by a Tukey's post-hoc test to confirm differences between groups, n/s, $P > 0.05$; **, $P < 0.01$; ***, $P < 0.001$; ****, $P < 0.0001$.

5.4 CM4620-mediated CRAC channel inhibition protects against asparaginase-induced necrosis

The protective effects of various Ca^{2+} entry channel inhibitors, including GSK-7975A and CM_128, against alcohol- and bile acid-related pancreatic pathology have been well documented (Gerasimenko *et al.,* 2013; Voronina *et al.,* 2015; Wen *et al.,* 2015). However, investigations into the effectiveness of CRAC channel blockade on asparaginase-evoked necrosis is limited (Peng *et al.,* 2016). This study therefore tested the result of CRAC inhibition (CM4620, 200 pM) on asparaginase-induced necrosis levels. As seen in Fig 5.3, levels of ASNase-induced necrosis were reduced following treatment of PACs with 200 pM CM4620 alone (green column, $P < 0.05$) and 200 pM CM4620 in addition to 1 mM galactose (orange column, $P < 0.001$) compared to asparaginase (14.53 $\pm$ 0.68%, red column). Although pre-incubating cells with picomolar concentrations (200 pM) of CM4620 significantly diminished the level of ASNase-evoked necrosis (11.29 $\pm$ 0.49%), combining this CRAC channel inhibitor with galactose was more effective at protecting cells against necrosis (8.85 $\pm$ 0.38%, $P < 0.05$) (Fig. 5.3).

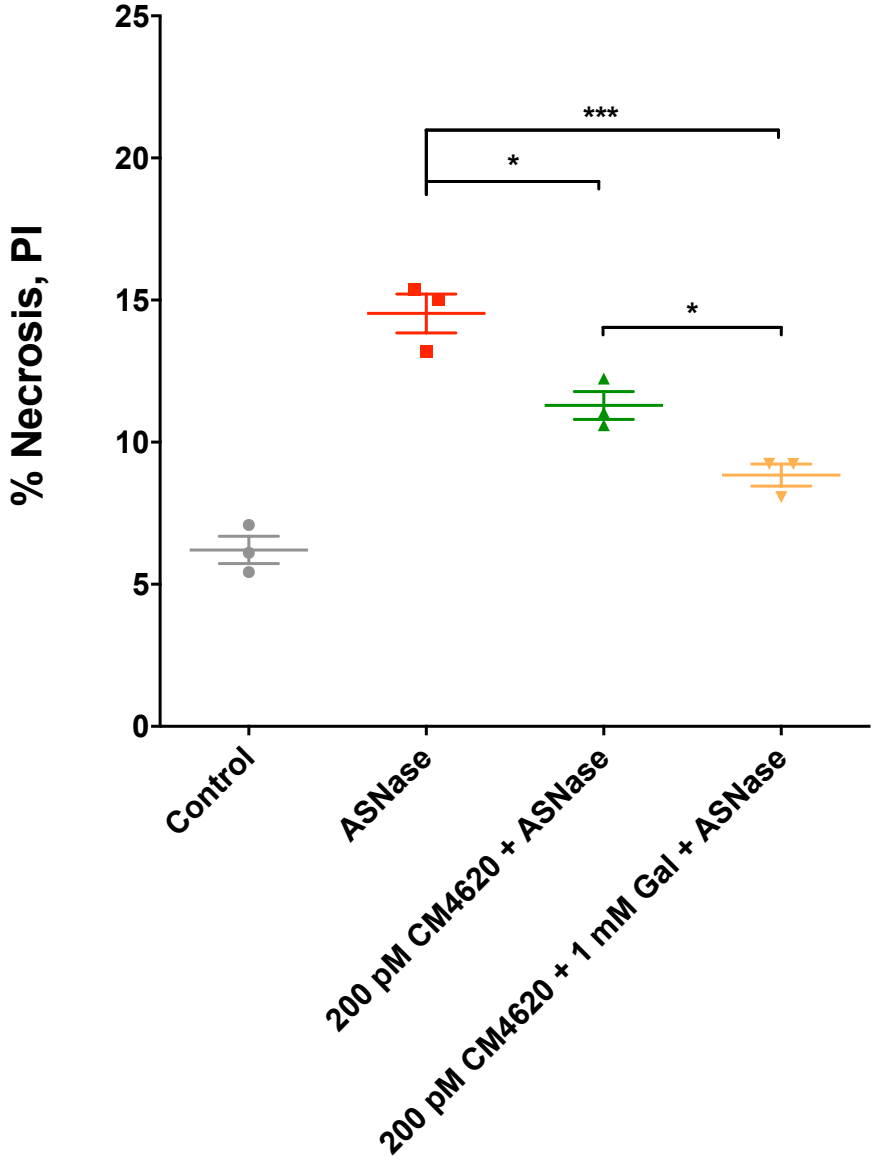

Figure 5.3. Asparaginase-induced necrosis is markedly decreased following CM4620 and galactose pre-treatment in PACs. Using substantially low concentrations of CM4620 (200 pM) still reduces the extent of necrosis (11.29% ± 0.49%, $P < 0.05$) compared to AP-inducing agent, asparaginase (ASNase). Using a galactose-CM4620 combination approach in this case reduces ASNase-evoked necrosis further (8.85% ± 0.38%, $P < 0.001$). At least 3 series experiments/group with more than 150 cells in each sample. Data presented as mean ± SEM. *P* values were calculated using one-way ANOVA followed by a Tukey's post-hoc test to confirm differences between groups, *, $P < 0.05$; ***, $P < 0.001$.

Representative images of PACs derived from the different experimental conditions measured in this study and their corresponding levels of PI staining, are presented in Fig. 5.4. When acinar cells were pre-incubated with CM4620 and a combination of CM4620 and galactose, the degree of cellular necrosis (PI positive staining), evoked by POA in this case, but also seen in BA- and ASNase-induced cells was significantly reduced to untreated, control cell levels. This reinforces the protective ability of CM4620 against this key hallmark of AP.

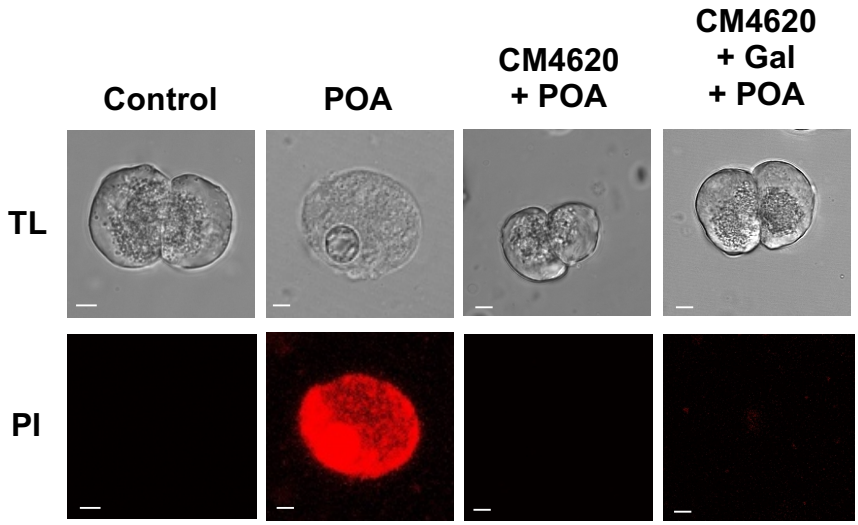

Figure 5.4. Representative images of PI uptake in PACs from control, treatment and POA groups. Transmitted light (TL) images (above) and propidium iodide (PI)-stained fluorescence images (below) (scale bar: 5 μm) show the effect of POA on PI uptake into the cell, representing the extent of necrosis. Cells evoked by POA, as well as by BAs and ASNase, had the highest uptake of PI whereas the two treatment groups (CM4620 alone and CM4620 and galactose) showed less PI uptake. The level of necrosis in control cells was low with minimal PI uptake into the cell.

CHAPTER 6:

RESULTS - The effects of nanomolar concentrations of CM4620 in *in vivo* mouse models of alcohol-induced pancreatitis

CHAPTER 6: The effects of nanomolar concentrations of CM4620 in *in vivo* mouse models of alcohol-induced pancreatitis

The previous chapters (Chapters 4 and 5) have demonstrated the remarkable inhibitory capability of CM4620 on CPA-induced SOCE as well as its ability to protect against activation of BA-, POA- and ASNase-induced necrotic cell death pathways at low, nanomolar concentrations *in vitro.* In the majority of cases, combining CM4620 with galactose more effectively reduced levels of necrosis. The study described in this chapter sought to determine the role of low CM4620 concentrations in an experimental mouse model of AP *in vivo*.

To evaluate the protective effects of CM4620 on disease severity *in vivo,* murine models of FAEE-AP were utilised in order to clinically represent alcohol-induced AP. Two intraperitoneal injections of sterile PBS (200 μl) were administered to control mice hourly. FAEE-AP was induced in mice through injections of POA (150 mg/kg) combined with ethanol (1.35 g/kg). Histological slides obtained from FAEE-AP mice (red columns) demonstrated pancreatic damage with extensive inflammation, necrosis and acinar cell oedema thus significantly increasing the total pathohistological score compared to control murine models ($P < 0.0001$) (Figs. 6.1 and 6.2). The co-administration of CM4620 (0.1 mg/kg) and ethanol/POA at 1-hour intervals significantly reduced all pancreatic parameters (Fig. 6.1, green columns), generating an overall average histological score of 1.85 ± 0.18%, which was significantly lower than the average total score for FAEE-AP (4.12 ± 0.08%, $P < 0.0001$).

A

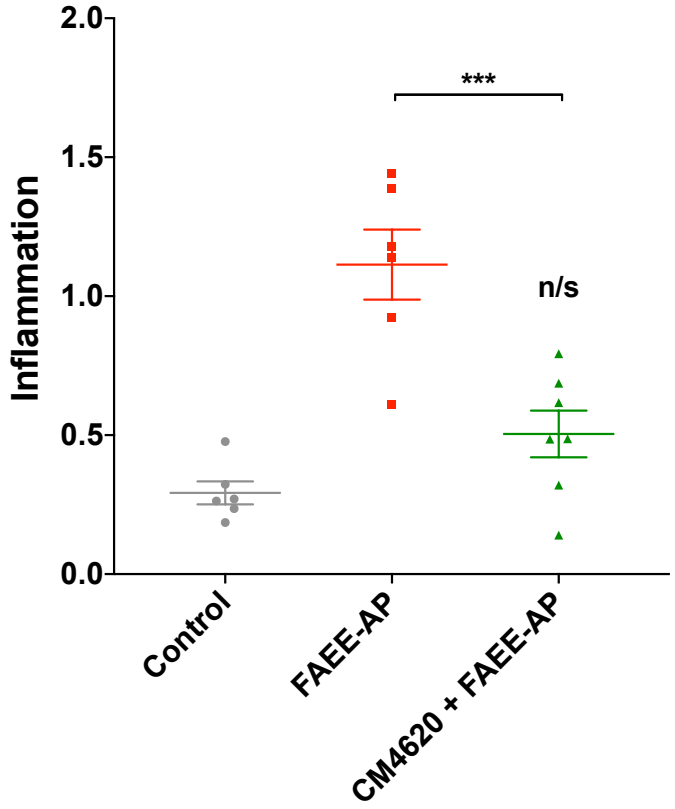
Inflammation
2.0
1.5
1.0
0.5
0.0
***
n/s
Control
FAEE-AP
CM4620 + FAEE-AP

B

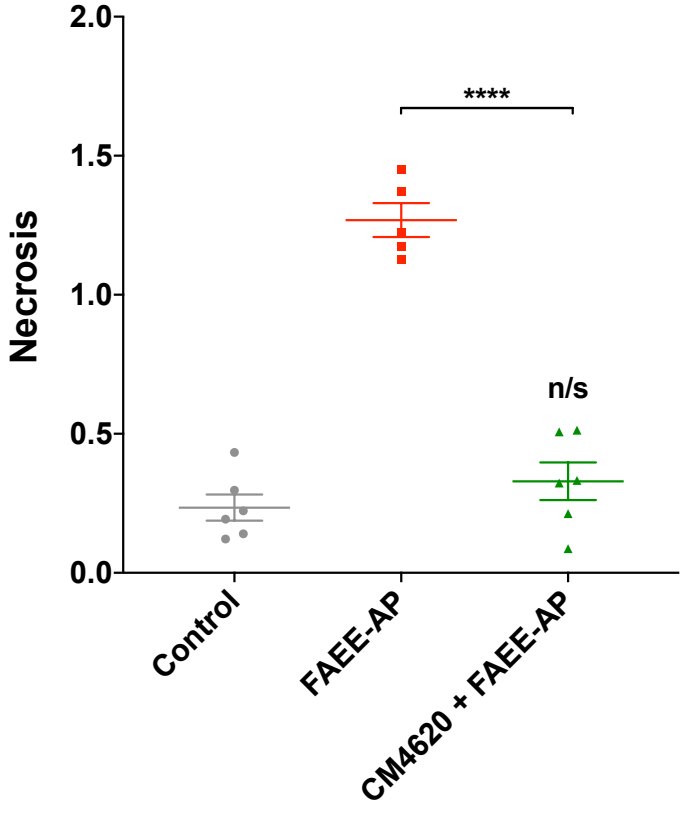
Necrosis
2.0
1.5
1.0
0.5
0.0
****
n/s
Control
FAEE-AP
CM4620 + FAEE-AP

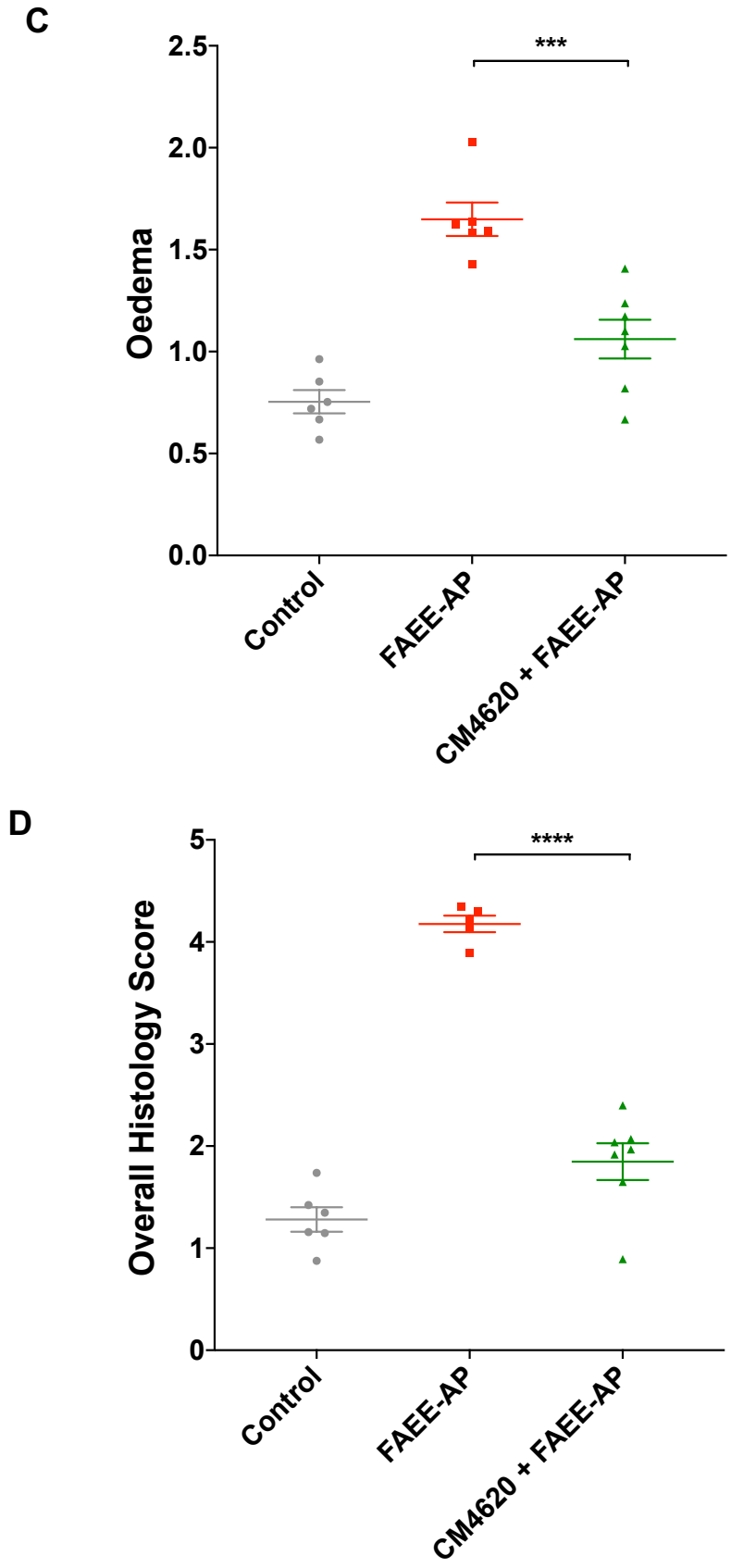

Figure 6.1. CM4620 markedly diminishes pancreatic histopathology in alcohol/fatty acid (FAEE)-induced AP *in vivo* models. The FAEE-AP model (red columns) induced significant increases in inflammation **(A)**, necrosis **(B)**, oedema **(C)** and total histology score **(D)** compared to control (grey columns). Administration of 0.1 mg/kg CM4620 via intraperitoneal injections markedly protected against all pathological changes evoked by POA and ethanol (FAEE- AP) *in vivo* (green columns, $P < 0.001$). Data shown as mean ± SEM, ≥6 mice/group. n/s, $P > 0.05$; ***, $P < 0.001$; ****, $P < 0.0001$, one-way ANOVA followed by Tukey's post-hoc test.

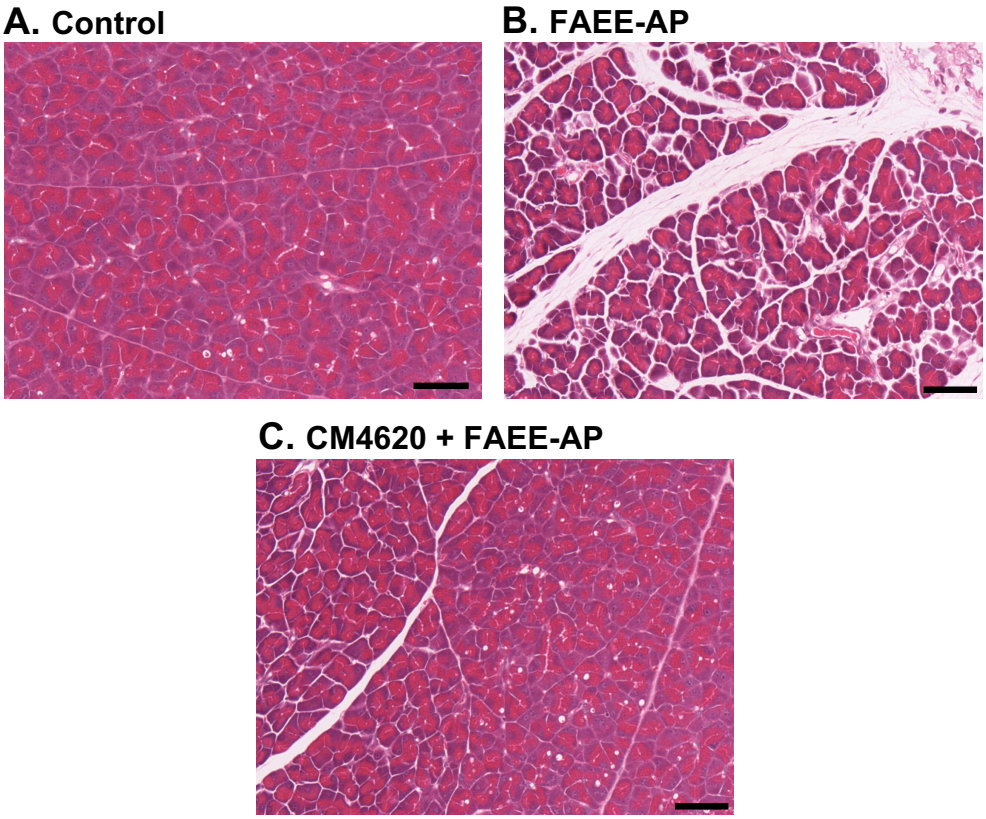

Figure 6.2. Representative images of haematoxylin-eosin (H&E)-stained pancreatic acinar tissue sections. Micrograph images demonstrate **(A)** normal pancreatic histology (as a result of saline injection), **(B)** typical histopathology induced by FAEE-AP alone and typical histopathology from FAEE-AP with **(C)** administration of CM4620 (0.1 mg/kg). Magnification x200, Scale bar: 50 µm. Micrograph taken on an Olympus BX41 brightfield microscope.

CHAPTER 7: DISCUSSION

CHAPTER 7: Discussion

The aim of this thesis was to determine the effects of novel CRAC channel inhibitor, CM4620 on the pathogenesis of AP, a life-threatening disorder with no specific therapy or cure. This project investigated the potential therapeutic use of CM4620 in inhibiting cytosolic Ca^{2+} overload and whether low concentrations of this inhibitor could protect against necrosis thus targeting the primary triggers in acute pancreatitis pathology. Current treatments in the clinic for AP are largely supportive and include pain management and fluid balance (Wu and Banks, 2013). The vast majority of drugs that have reached clinical trials for AP have not been successful in preventing disease morbidity and mortality (Kambhampati *et al.,* 2014; Singh *et al.,* 2015). The failure of clinical development for a variety of pancreatitis therapeutics, such as protease inhibitors, immunomodulators, anti-secretory or anti-inflammatory agents and antioxidants, is likely due to their targeting of the disease in its latter stages. When attempting to halt disease progression at this stage, the principal hallmarks of AP, including protease activation, pancreatic necrosis and inflammation have unfortunately already transpired.

Improving the design of clinical trials whereby therapeutic agents target the primary pathological event, namely the intracellular protease activation evoked and maintained by excessive Ca^{2+} signalling in pancreatic acinar cells, will be more beneficial in generating the first rational and effective AP treatment (Ward *et al.,* 1995; Petersen and Sutton, 2006; Gerasimenko *et al.,* 2014a; Lankisch *et al.,* 2015). It is very well established in the literature that toxic elevations in cytosolic Ca^{2+} initially result from internal Ca^{2+} store release. However, the subsequent phase of CRAC-mediated Ca^{2+} entry plays a critical role in acinar cell damage as it drives the sustained phase of Ca^{2+} elevation resulting in intracellular Ca^{2+} overload, intracellular proenzyme activation thus triggering the development of AP (Raraty *et al.,* 2000; Petersen and Sutton, 2006; Petersen *et al.,* 2009). CRAC channels have therefore become a popular focus of investigation in recent years as potential therapeutic targets for pancreatitis as well as other human diseases (Parekh, 2010; Prakriya and Lewis, 2015).

7.1 The effectiveness of CM4620 as a specific CRAC channel inhibitor in PACs

The current data describing a novel molecular entity developed by CalciMedica, CM4620, provides fresh evidence for the importance of store-operated Ca^{2+} entry via CRAC channels and their role in triggering the pathological Ca^{2+} signalling in PACs which drives cellular necrosis, causing AP. In particular, these results also strengthen previous evidence suggesting a potential role for CRAC blockade in AP therapy (Gerasimenko *et al.,* 2013; Voronina *et al.,* 2015; Wen *et al.,* 2015; Waldron *et al.,* 2019).

The initial studies reported in Chapter 3 tested CM4620 efficacy in response to the classic acinar cell secretagogue ACh which evokes both physiological and pathological responses in PACs. Low, nanomolar and supramaximal concentrations of ACh were administered to Fluo-4-loaded murine PACs in the presence or absence of CM4620. The SOCE elicited by supramaximal concentrations of ACh was significantly reduced in cells pre-treated with CM4620. CM4620 also markedly reduced the rate of recovery to baseline in response to these high secretagogue concentrations. This has been previously investigated by Gerasimenko and colleagues (2013) with another CRAC channel inhibitor, GSK7975A (developed by GlaxoSmithKline). Similarly, GSK7975A reduced the late elevated $[Ca^{2+}]_i$ plateau phase in response to stimulation with a high concentration of ACh. However, GSK7975A had minor effects on the normal, physiological Ca^{2+} oscillations induced by ACh or CCK (Geraimenko *et al.,* 2013). Moreover, this study showed that directly applying CM4620 to freshly isolated PACs did not generate any substantial changes in $[Ca^{2+}]_i$. The results depicted in this thesis suggest that when cells are at rest (Fig. 3.4 and 3.5), there are no difference in resting Ca^{2+} levels. But if a cell is evoked with ACh, responses are markedly inhibited by CM4620. This suggests that CM4620 does not inhibit all Ca^{2+} influx thus only evoked cells demonstrate some modest differences.

7.1.1 CM4620 significantly reduces toxic elevations of cytosolic Ca^{2+}

In order to be considered an ideal therapeutic for AP, it is vital for a CRAC channel inhibitor to effectively inhibit Ca^{2+} influx, thus preventing toxic cytosolic Ca^{2+} overload and reducing levels of cellular necrosis that typically ensue. Preliminary results investigated the effect of pre-incubating mouse

PACs with CM4620 (1 μM and 10 μM). These high concentrations very significantly inhibited CPA-induced SOCE, measured using fluorescent Ca^{2+} imaging. Administration of CM4620 at high concentrations (10 μM) results in an 84% reduction in the amplitude of CRAC-mediated Ca^{2+} influx (Fig. 1.6.1 and Fig. 1.6.2), compared with control cells in the presence of 5 mM external Ca^{2+}. The inhibitory effect of CM4620 on SOCE amplitude after decreasing the concentration from 10 μM to 1 μM is similarly efficient (65%) (Fig. 1.6.1 and Fig. 1.6.2).

Although CM4620 does not completely block SOCE, these results are comparable to the percentage of SOCE inhibition generated by another CRAC channel inhibitor, GSK-7975A. The marked inhibition of toxic elevations in $[Ca^{2+}]_i$ by GSK-7975A has been previously reported by numerous authors (Gerasimenko *et al.,* 2013; Voronina *et al.,* 2015; Wen *et al.,* 2015). Wen and colleagues also investigated the effectiveness of CRAC channel inhibitor CM_128 (also known as CM4620) *in vitro* in murine and human PACs (Wen *et al.,* 2015). CM_128 inhibited thapsigargin-evoked SOCE entry in human and mouse acinar cells more effectively than GSK-7975A at 1 μM. A recent study further confirmed that CM4620 attenuates SOCE in murine acinar cells (Waldron *et al.,* 2019).

This thesis is in direct correlation with and further confirms the results presented by these authors, providing fresh evidence for the remarkable effect of CRAC channel blockade and specifically the ability of CM4620 to inhibit CPA-induced SOCE. Pre-treatment of cells with 1 μM and 10 μM CM4620 also slows the initial rate of SOCE, compared to control PACs (Fig. 4.2), further validating the protective abilities of CM4620 as a CRAC channel inhibitor. Although the effectiveness of CRAC channel inhibition is mainly reported by the extent of Ca^{2+} influx, which contributes to overall toxic $[Ca^{2+}]_i$ elevations in AP, changes in Ca^{2+} efflux were also analysed in this study. As expected, pre-treatment of cells with 1 μM and 10 μM CM4620 did not significantly affect the times taken to reach half maximal Ca^{2+} efflux, compared to control cells (Fig. 4.3).

7.1.2 CM4620, at low nanomolar concentrations, protects against cellular necrosis elicited by bile acids, alcohol metabolites and asparaginase

The extent of cellular necrosis is one principal determinant of AP severity in both *in vitro* and *in vivo* experimental models (Kaiser *et al.,* 1995; Gukovskaya and Pandol, 2004; Criddle *et al.,* 2007). Therefore, reductions in the level of necrosis in PACs by CRAC channel inhibitors is an extremely valuable indication of their translational potential to the clinic. As a successful inhibitor of damaging elevations in cytosolic Ca^{2+}, the next objective of this project was to test the protective effects of CM4620 on activation of the necrotic cell death pathway, evoked by toxic stimuli in murine pancreatic acini *in vitro* (Chapter 5). This was also investigated following successful preliminary findings using high concentrations (10 μM and 1 μM) of CM4620. These concentrations significantly diminished the extent of necrosis, relatively close to control levels when induced with sodium choleate – a mixture of various bile salts that mimic clinical biliary AP. As CM4620 is currently in clinical trials, it is paramount that we consider the risks as well as the benefits of inhibiting CRAC channel activity. In 2017, Ahuja and colleagues demonstrated the presence of intestinal bacterial outgrowth and dysbiosis in mouse pancreatic acini following genetic deletion of Orai1. This ultimately led to significant mortality within 3 weeks (Ahuja *et al.,* 2017). Although this case involved complete and permanent genetic deletion of Orai1, the potential long-term effects of CRAC channel inhibitors on the immune system should be considered. The principle aim of this study, therefore, was to explore whether substantially reducing the concentration of CM4620 still effectively protects PACs against damaging levels of AP-evoked necrosis. Therapeutically, lower concentrations would minimise any potential side-effects resulting from CRAC channel inhibition.

At much lower concentrations than reported previously (Wen *et al.,* 2015; Waldron *et al.,* 2019), 100 nM and 50 nM of CM4620 markedly reduced the extent of bile-induced necrosis to levels of 11.33% and 13.66%, respectively compared to BA alone. However, this was still significantly higher than levels of necrosis in untreated cells. The effect of applying galactose as a form of ATP supplementation has recently shown remarkable protective effects against pancreatitis-induced necrosis (Peng *et al.,* 2018). In this study, the addition of galactose to CM4620 (100 nM, 50 nM and 10 nM) significantly ($P < 0.0001$) reduced the percentage of bile-induced necrosis to near control

levels (Fig. 5.1). Combining 100 nM CM4620 with galactose had the most significant effect in protecting against BA-evoked necrosis.

When using the alcohol metabolite, POA, to induce necrosis in PACs, CM4620 at novel concentrations of 50 nM, 1 nM and 200 pM, in combination with galactose (1 mM) had the most significant effect in reducing necrosis levels (Fig. 5.2). Again, these were almost equal to or minimally higher than control levels. All concentrations of CM4620 applied in combination with galactose were most effective at protecting cells against necrosis induced by POA. Additionally, in some cases, the protective effect of CM4620 (50 nM) alone was not significantly different from combining CM4620 and galactose against POA-evoked cell death.

Utilising concentrations of CM4620 as low as 200 pM significantly diminished levels of asparaginase-induced necrosis (Fig. 5.3). Galactose provided further protection when combined with 200 pM CM4620. These findings are particularly encouraging as only one other CRAC channel inhibitor, GSK-7975A at high concentrations of 10 μM, has been shown to protect against asparaginase-induced necrosis, to date (Peng *et al.,* 2016). This further confirms the effectiveness of CM4620, *in vitro*, as a therapeutic inhibitor of AP-related necrosis as well as showing a novel benefit of utilising picomolar concentrations of CM4620 and the potential benefit of combining this CRAC channel inhibitor with galactose.

This data confirms and reinforces the potential preventative capacity of CM4620 against necrosis evoked by all the principal AP-inducing agents. In the majority of cases, galactose can further improve this effect. It would be desirable to further expand this conclusion by comparing the combination treatment against galactose alone as a protective therapy against AP-induced necrosis. The effects of galactose alone on pancreatic necrosis have previously been investigated and published (Peng *et al.,* 2018). The novel findings presented in this thesis are particularly promising as some CRAC channel inhibitors, such as 2-APB, have been reported to actually cause cellular necrosis (Gerasimenko *et al.,* 2013). Reductions in necrosis by CM4620 could, however, result from processes other than Ca^{2+} entry. Therefore, it is worthwhile noting that PACs ought to be exposed to 2-APB, which will evoke cell death and inhibit CRAC channels, before confirming the protective effect of CM4620 against cellular necrosis (Gerasimenko *et al.,* 2013). Furthermore, the process of counting the number of necrotic and

viable cells should be double-blinded to avoid inherent experimenter bias. Similarly, GSK-7975A and CM_128 inhibited activation of the necrotic cell death pathway induced by aforementioned mediators of AP, in mouse and human PACs (Gerasimenko *et al.,* 2013; Voronina *et al.,* 2015; Wen *et al.,* 2015; Waldron *et al.,* 2019). However, the lowest concentration of CRAC channel inhibitors used by these authors was 1 μM, reinforcing the novelty and magnitude of the protective ability of CM4620. Overall, the ability of CM4620 to inhibit CRAC-mediated Ca^{2+} entry (induced by intracellular store depletion) and necrosis (evoked by bile, alcohol metabolites and asparaginase) was an initial step towards *in vivo* mouse model investigations to confirm the effectiveness of low, nanomolar concentrations of CM4620 as a CRAC channel inhibitor.

7.2 CM4620 administration reduces pancreatitis responses in alcohol-induced mouse acute pancreatitis

In vivo investigations, shown in Chapter 6, of alcohol-induced AP involved administering CM4620 at a dosage equivalent to 50 nM *in vitro* (0.1 mg/kg) which is lower than reported previously (28 mg/kg, Wen *et al.,* 2015; 20 mg/kg, Waldron *et al.,* 2019). The effect of 0.1 mg/kg CM4620 significantly improved pathohistological scores (measuring inflammation, necrosis and oedema). The findings presented in this study provide the first insight into the remarkable potency of CM4620 and are in agreement with other authors. Wen and colleagues (2015) administered GSK-7975A and CM_128 at various doses and time points to three experimental mouse models of clinical AP and reported amelioration of all local and systemic parameters of AP such as oedema, necrosis and inflammation. This comprehensive *in vivo* evaluation implied the potential translation of CRAC channel inhibition, as a novel therapeutic strategy, to clinical trials (Wen *et al.,* 2015). Last year, Waldron and colleagues also reported protective effects of CM4620 in another *in vivo* mouse model (Waldron *et al.,* 2019). The results presented in this thesis therefore further reinforce the therapeutic potential of CM4620 as a viable treatment for clinical AP, a devastating disease which currently lacks a specific cure. The novelty of utilising lower concentrations of CM4620 is particularly important in preventing any potential long-term immune side effects of CRAC channel blockade.

7.3 Clinical implications of CM4620

CRAC channels have been functionally associated in the pathogenesis of a variety of diseases, other than AP. New data on breast cancer cell lines by Yang and colleagues (2009) revealed SOCE, facilitated by Orai1 and STIM1, plays a vital role in tumour migration *in vitro* and metastasis *in vivo.* The authors concluded that CRAC channel inhibitors could be utilised in preventing the formation of malignant secondary tumours in breast cancer cells (Yang *et al.,* 2009). Braun and colleagues (2009) demonstrated that the CRAC channel is a significant mediator of ischemic cardiovascular and cerebrovascular events. Their research showed high expression of Orai1 in human and mouse platelets. Furthermore, platelets in Orai1-deficient mice exhibited defective SOCE which caused resistance to pulmonary thromboembolism, arterial thrombosis and ischemic brain infarction (Braun *et al.,* 2009). It's also been implied that CRAC channel inhibitors could successfully manage airway inflammation and bronchoconstriction in asthma. Oral administration of the CRAC channel inhibitor BTP2 prevented asthmatic bronchoconstriction and eosinophil infiltration in sensitised guinea pigs (Yoshino *et al.,* 2007). Expression of Orai1 and STIM1 in human airway muscle has been reported thus strengthening the therapeutic potential of CRAC channel inhibitors as anti-asthma drugs (Peel *et al*., 2008). Use of CRAC channel inhibitor GSK-7975A in other *in vitro* and *in vivo* models of disease, including thrombotic events causing stroke and asthma, has also been described (Ashmole *et al.,* 2012; van Kruchten *et al.,* 2012). These findings, coupled with the effects of CM4620 observed in this study, indicate a wide variety of potentially valuable therapeutic approaches for CRAC channel inhibition.

Although CRAC channels are ubiquitous cellular constituents, it was originally thought that these channels were predominantly situated in the immune system. Specific CRAC channel inhibitors have thus been produced to target immunological disorders by numerous companies, including CalciMedica (Parekh, 2010; DiCapite *et al.,* 2011). CM4620 may have an additional advantageous therapeutic effect on the inflammatory process contributing towards AP pathobiology. It has been reported that CRAC channel inhibitors prevent SOCE in numerous immune cells and responses, such as mast and T-cells as well as neutrophil migration and activation, which exacerbates AP in its early stages (Bergmeier *et al.,* 2013). CRAC channel blockade could inhibit distinctive immune responses,

protecting against pancreatic inflammation thus limiting the severity of AP and associated mortality (Gea-Sorli and Closa, 2010; Akinosoglou and Gogos, 2014). Indeed, a marked reduction in the severity of experimental pancreatitis as a result of immune response prevention has been observed (Gukovskaya *et al.,* 2002). In 2019, Waldron and colleagues demonstrated that CM4620 decreases cytokine production as well as myeloperoxidase activity and cytokine expression in pancreas and lung tissues. These findings support the idea of Orai1/STIM1 channel participation in the inflammatory responses during AP (Waldron *et al.,* 2019). It should be noted, however, that Vaeth and colleagues (2015) recently reported that phagocytosis and cytokine generation by macrophages is functionally dependent on cytosolic Ca^{2+} signals but not necessarily SOCE. While SOCE blockade in innate immune cells, through Orai1/STIM1 knockouts, impairs neutrophil and macrophage function, some aspects of their functionality are not completely prevented hence immune responses can still be instigated (Vaeth *et al.,* 2015). Although T cells appear to be predominantly inhibited by CRAC channel blockers, they occur in smaller numbers in the inflamed pancreas (Demols *et al.,* 2000; Akinosoglou and Gogos, 2014). While further confirmation on the distribution of CRAC channels in immune and pancreatic cells and their sensitivity to inhibitors is required, the role of these channels in Ca^{2+} entry is less pronounced in electrically excitable cells. Such cells, including cardiac myocytes, neurones and skeletal myocytes, possess and are dependent on other ion channels (for example, non-selective cation channels) to provide Ca^{2+} influx (Stiber *et al.,* 2008; Moccia *et al.,* 2015). Additionally, even though non-excitable cells (for example hepatocytes) mainly rely on CRAC-mediated Ca^{2+} entry for vital cellular processes like exocytosis, Gerasimenko and colleagues (2013) observed minimal effects of GSK-7975A on hepatocytes *in vitro.* These observations together with the minor effects of CRAC channels on excitable cell functionality reinforce the validity of targeting CRAC-mediated SOCE for AP therapy.

7.4 Limitations

This study utilised fluorescent microscopy measurements of intracellular Ca^{2+} concentration to investigate CRAC channel inactivation in PACs. Alternatively, electrophysiology techniques have been employed by several authors when measuring alterations in CRAC channel conductance, following channel inactivation, in various cell lines and in the presence of external Ca^{2+} (Hoth and Penner, 1993; Fierro and Parekh, 1999; Litjens *et*

al., 2004). Application of such techniques, for example whole cell patch clamp, allow measurements of current through specific ion channels, in isolation from other factors and ion channel fluxes. Although CRAC channels are the main mediators of SOCE in PACs, non-selective cation channels such as TRPC3 also contribute to Ca^{2+} influx, but to a lesser extent. Moreover, CPA-evoked store depletion could activate TRPC3, due to its speculated STIM1 binding capabilities, as well as CRAC channels (Lee *et al.,* 2014). Recorded $[Ca^{2+}]_i$ elevations, as reported in this study, would thus arise from both TRPC and CRAC-mediated Ca^{2+} entry. Assessing Ca^{2+} entry through each channel, with fluorescent Ca^{2+} indicators, is only viable when using their corresponding inhibitors. The lack of and poorly understood specificity and potency of novel CRAC channel blockers can therefore prove problematic when analysing their inhibitory effect on Ca^{2+} entry, using Ca^{2+}-sensitive fluorescent probes such as Fluo-4. On the other hand, the distinctive biophysical fingerprints of CRAC and TRPC3 channel currents allow them to be distinguished during electrophysiological studies (Cheng *et al.,* 2013; Prakriya and Lewis, 2015). In addition, concurrent measurements of channel conductance, with whole cell patch clamp, and intracellular Ca^{2+} changes, with fluorescent indicators and microscopy, have been successfully utilised in PACs to provide real time recordings of channel currents and spatiotemporal features of Ca^{2+} signalling (Voronina *et al.,* 2002b). Using electrophysiology would further reveal the impact of CM4620 on CRAC channel Ca^{2+} influx.

Furthermore, non-ratiometric measurements presented in this report of fluorescence signals, with Ca^{2+} indicator Fluo-4, were not converted to absolute $[Ca^{2+}]_i$ concentrations. This can be achieved with additional calibration methods to further improve our understanding of CRAC channel inhibition in murine PACs. Such methods can be employed to Fluo-4 non-ratiometric recordings using the following equation: $[Ca^{2+}]_i = K_d\ [(F - F_{min}) / (F_{max} - F)]$ (Grynkiewicz *et al.,* 1985; Bootman *et al.,* 2013). At the end of experiments, the Ca^{2+} depleted state (F_{min}) and Ca^{2+} saturated state (F_{max}) should be established. This protocol has been previously described and involves treating Fluo-4 loaded PACs with the Ca^{2+} ionophore, ionomycin (20 μM), and 2 mM EGTA (ethylene glycol tetraacetic acid), a Ca^{2+} chelator used to deplete Ca^{2+} from the cytoplasm, in a Ca^{2+}- free buffer. This enables the determination of F_{min}. Subsequently, ionomycin was added to the cells in a buffer with 2 mM $CaCl_2$ to saturate the fluorescent indicator and to determine F_{max} which is reached once a plateau is observed (Sherwood *et al.,* 2007; McCombs and Palmer, 2008). Moreover, F is the fluorescence

ratio value whereas K_d represents the dissociation constant of Ca^{2+} binding site (~350 nM for Fluo-4; Gerasimenko *et al.,* 2006).

Interference of global Ca^{2+} influx measurements by fluorescent microscopy can results from Ca^{2+} efflux pathways across the plasma membrane, ER membrane and into the mitochondria. In this report, interference in the Ca^{2+} signal would predominantly arise from PMCA activation as CPA, a SERCA pump inhibitor, was utilised during CRAC channel activity recordings. To prevent this interference, previous investigators have used Ba^{2+} ions, instead of Ca^{2+}, in the extracellular solution as Ba^{2+} readily passes through CRAC channels but cannot be extruded across the plasma membrane by Ca^{2+} ATPases (Kwan and Putney, 1990; Bakowski and Parekh, 2007; Zeiger *et al.,* 2011). In this study, the effect of CRAC channel inhibitor, CM4620, on Ca^{2+} influx could have been more accurately measured by substituting Ca^{2+} ions for Ba^{2+} ions.

Evidence of the effect of CM4620 on toxic $[Ca^{2+}]_i$ elevations in PACs exposed to all AP-inducing agents utilised in this current study is required. Demonstrating inhibition of BA- alcohol- and asparaginase-evoked $[Ca^{2+}]_i$ elevations with CM4620 will reinforce its protective effects against cellular necrosis presented here. As mentioned previously, it would be desirable to measure galactose alone as a protective treatment against AP-induced necrosis. Although investigations by Peng and colleagues (2018) have shown that galactose alone significantly protects against pancreatic necrosis, it would be interesting to directly compare galactose alone treatments against the effects of CM4620 and the CM4620-galactose combination. Furthermore, when considering the clinical application of CM4620, the necrosis findings presented in this study are limited as the AP-inducing agents are added together with the CRAC inhibitor and galactose. In a clinical setting, CM4620 and a combination of CM4620 with galactose would be utilised as a treatment after AP has been induced in patients. Lastly, it would be important to investigate the capability of low nanomolar concentrations of CM4620, again depicted in the necrosis assays of this study, on inhibiting SOCE.

7.5 Future considerations

The CRAC channel is considered a viable drug target for AP therapy as it is the main channel for Ca^{2+} entry in acinar cells, a process which extensively facilitates aberrant intracellular Ca^{2+} signalling during AP thus contributing

towards hallmarks of the disease (Lur *et al.,* 2009; Gerasimenko *et al.,* 2013). Several potential areas of interest for the future can be determined from this study to reinforce the therapeutic potential of targeting CRAC channels and more specifically, the benefits of using lower concentrations of CM4620.

Firstly, it would be interesting and necessary to investigate the effects of various CM4620 concentrations on Ca^{2+} influx when treated in an acute manner. This would involve application of CM4620 following re-admission of external Ca^{2+} after CPA treatment, once a plateau is established. It is crucial for an effective AP intervention to have the ability to diminish Ca^{2+} entry when administered in the presence of a sustained $[Ca^{2+}]_i$ elevation. The relatively long preincubation (30 minutes) of CM4620 reported in this study could prove problematic and result in slow time courses in $[Ca^{2+}]_i$ decline. This may, however, signify periods of Ca^{2+} extrusion via the PMCA and remains to be determined. The effect of CM4620 on pathological mitochondrial Ca^{2+} responses as well as intracellular ATP levels, induced by AP-inducing agents, should also be investigated. The possible restoration of these mitochondrial Ca^{2+} and ATP levels to near control by CM4620 would be appealing. Galactose has previously protected against ATP loss and has restored mitochondrial potential and Ca^{2+} levels to near control levels (Peng *et al.,* 2016; Peng *et al.,* 2018).

The potential studies described in *in vitro* models would strengthen the findings presented here on murine acinar cell responses. Further investigations into the effects of CM5620 in *in vivo* experimental models of AP should be carried out. Ideally, multiple rodent models should be utilised with varying forms of AP disease induction, such as ductal injections of TLCS or intravenous administration of asparaginase which are widely used as representatives of acute biliary pancreatitis and asparaginase-associated pancreatitis, respectively (Laukkarinen *et al.,* 2007; Lerch and Gorelick, 2013; Wen *et al.,* 2015). It would also be interesting to utilise other murine models by using, for example, high doses of basic amino acids (most often L-arginine) which are widely used in animal models of AP (Zhang *et al.,* 2019).CM4620 should successfully ameliorate all hallmarks of AP exhibited by these models to be considered an ideal therapeutic for AP. CM4620 could also be tested in combination with galactose. Galactose is relatively stable in solution, slowly metabolised and has successfully been administered by both intraperitoneal injections and feeding (drink) in AP mouse models (Peng *et al.,* 2018). Comprehensive, preclinical justification

for CM4620 CRAC channel blockade in early stage AP therapy can be reinforced by testing different time points of CM4620 administration in experimental models, following disease induction. This will ascertain the impact of early vs late drug administration on preventing pancreatic acinar injury and necrosis which is an important issue in clinical trials testing drugs for AP intervention (Wen *et al.,* 2015). In clinical practice, the time frame in which AP patients present to hospital following the onset of symptoms and require treatment varies from hours to days. Rapidly administering the treatment following disease onset thus reducing the extent of pancreatic necrosis, injury and subsequent inflammation is thought to be fundamental in maximising therapeutic benefits (Wen *et al.,* 2015).

7.6 Concluding remarks

The findings presented in this report confirm the hypothesis that CRAC channel blocker, CM4620, effectively inhibits both store-operated Ca^{2+} entry, induced by ER store depletion. This is of great importance as reductions in cytosolic Ca^{2+} would eliminate the premature activation of digestive enzymes and the subsequent autodigestion and cell death characteristics of AP. The novel results in this thesis demonstrate that low, nanomolar concentrations of CM4620 can prevent activation of the necrotic cell death pathway evoked by principal AP-inducing agents, including asparaginase, bile acids and alcohol metabolites *in vitro* in PACs. In the vast majority of cases, this protective effect is further improved when CM4620 is combined with galactose. Low doses of CM4620 were highly effective in reducing all disease parameters in representative *in vivo* animal models of alcoholic acute pancreatitis, one of the most common forms of the disease.

These results reinforce the viability of CRAC-mediated Ca^{2+} influx as a potential therapeutic target and suggest that CM4620 in addition to, or in combination with galactose could be a useful tool, therapeutically. Administering low concentrations of CM4620 could also reduce the chance of side-effects resulting from CRAC channel inhibition. It is hopeful that CRAC channel blockade could be translated into clinical usage against the life-threatening condition of acute pancreatitis, to which there currently is no specific cure.

References

References

Ahmed Ali, U., Issa, Y., Hagenaars, J.C., Bakker, O.J., van Goor, H., Nieuwenhuijs, V.B., Bollen, T.L., *et al.* (2016). Risk of recurrent pancreatitis and progression to chronic pancreatitis after a first episode of acute pancreatitis. *Clinical Gastroenterology and Hepatology* **14:**738-46.

Ahuja, M., Schwartz, D.M., Tandon, M., Son, A., Zeng, M., Swaim, W., Eckhaus, M., *et al.* (2017). Orai1-mediated antimicrobial secretionfrom pancreatic acini shapes the gut microbiome andregulates gut innate immunity. *Cell Metabolism* **25:**635-646.

Akinosoglou, K. and Gogos, C. (2014). Immune-modulating therapy in acute pancreatitis: Fact or fiction. *World Journal of Gastroenterology* **1:**107-11.

Alvarez, O.A. and Zimmerman, G. (2000). Pegaspargase-induced pancreatitis. *Medical and Pediatric Oncology* **34:**200-205.

Ambudkar, I.S. (2012). Polarization of calcium signaling and fluid secretion in salivary gland cells. *Current Medicinal Chemistry* **19:**5774-81.

An, F., Yang, G., Tian, J. and Wang, S. (2012). Antioxidant effects of the orientin and vitexin in Trollius chinensis Bunge in D-galactose-aged mice. *Neural Regeneration Research* **7**(33):2565-2575.

Apte, M.V., Pirola, R.C., Wilson, J.S. (2010). Mechanisms of alcoholic pancreatitis. *Journal of Gastroenterology and Hepatology* **12:**1816-26.

Apte, M.V., Wilson, J.S., Lugea, A. and Pandol, S.J. (2013). A starring role for stellate cells in the pancreatic cancer microenvironment. *Gastroenterology* **144**:1210-1219.

Armstrong, C.P. and Taylor, T.V. (1986). Pancreatic-duct reflux and acute gallstone pancreatitis. *Annals of Surgery* **204**:59-64.

Ashby, M.C. and Tepikin, A.V. (2002). Polarized calcium and calmodulin signaling in secretory epithelia. *Physiological Reviews* **82:**701-34.

Ashmole, I., Duffy, S.M., Leyland, M.L., Morrison, V.S., Begg, M. and Bradding, P. (2012). CRACM/Orai ion channel expression and function in human lung mast cells. *Journal of Allergy and Clinical Immunology* **129:**1628-1635.

Asin-Cayuela, J., Manas, A.R., James, A.M., Smith, R.A. and Murphy, M.P. (2004). Fine-tuning the hydrophobicity of a mitochondria-targeted antioxidant. *FEBS* **571**:9-16.

Badalov, N., Baradarian, R., Iswara, K., Li, J., Steinberg, W. and Tenner, S. (2007). Drug-induced acute pancreatitis: an evidence-based review. *Clinical Gastroenterology and Hepatology* **5:**648-661.

Baba, Y., Hayashi, K., Fujii, Y., Mizushima, A., Watarai, H., Wakamori, M., Numaga, T., *et al.* (2006). Coupling of STIM1 to store-operated Ca2 entry through its constitutive and inducible movement in the endoplasmic reticulum. *Proceedings of the National Academy of Sciences USA* **103:**16704-16709.

Baines, C.P., Kaiser, R.A., Purcell, N.H., Blair, N.S., Osinska, H. and Hambleton, M.A., Brunskill, E.W., *et al.* (2005). Loss of cyclophilin D reveals a critical role for mitochondrial permeability transition in cell death. *Nature* **434**(7033):658-62.

Bakowski, D. and Parekh, A.B. (2007). Voltage-dependent Ba2+ permeation through storeoperated CRAC channels: Implications for channel selectivity. *Cell Calcium* **42:**333-339.

Bano, D., Young, K.W., Guerin, C.J., Lefeuvre, R., Rothwell, N.J., Naldini, L., Rizzuto, R. *et al.* (2005). Cleavage of the plasma membrane Na+/Ca2+ exchanger in excitotoxicity. *Cell* **120:**275-285.

Berberián, G., Podjarny, A., DiPolo, R. and Beaugé, L. (2012). Metabolic regulation of the squid nerve Na^{+}/Ca^{2+} exchanger: recent kinetic, biochemical and structural developments. *Progress in Biophysics and Molecular Biology* **108**(1-2):47-63.

Bergmeier, W., Weidinger, C. and Zee, I. (2013). Emerging roles of store-operated Ca^{2+} entry through STIM and ORAI proteins in immunity, hemostasis and cancer. *Channels* **7:**379-391.

Berridge, M.J., Bootman, M.D. and Roderick, H.L. (2003). Calcium signalling: dynamics, homeostasis and remodelling. *Nature Reviews Molecular Cell Biology* **4:**517-529.

Berridge, M.J., Lipp, P. and Bootman, M.D. (2000). The versatility and universality of calcium signalling. *Nature Reviews Molecular Cell Biology* **1:**11-21

Berridge, M.J. (2011). Calcium signalling and Alzheimer's disease. *Neurochemical Research* **36**(7):1149-56.

Berry, G.T., Nissim, I., Lin, Z., Mazur, A.T., Gibson, J.B. and Segal, S. (1995). Endogenous synthesis of galactose in normal men and patients with hereditary galactosaemia. *Lancet* **346**(8982):1073-1074.

Bjelakovic, G., Nikolova, D., Gluud, L.L., Simonetti, R.G. and Gluud, C. (2012). Antioxidant supplements for prevention of mortality in healthy participants and patients with various diseases. Cochrane Database of Systematic Reviews CD007176.

Blaustein, M.P. and Lederer, W.J. (1999). Sodium/calcium exchange: its physiological implications. *Physiological Reviews* **79**(3):763-854.

Booth, D.M., Murphy, J.A., Mukherjee, R., Awais, M., Neoptolemos, J.P., Gerasimenko, O.V., Tepikin, A.V., *et al.* (2011). Reactive oxygen species induced by bile acid induce apoptosis and protect against necrosis in pancreatic acinar cells. *Gastroenterology* **140**(7):2116- 25.

Bootman, M.D., Rietdorf, K., Collins, T., Walker, S. and Sanderson, M. (2013). Ca2+-sensitive fluorescent dyes and intracellular Ca2+ imaging. *Cold Spring Harbor Protocols* **2:**83-89.

Boquist, K., Eliasson, L., Ammala, C., Renstrom, E. and Rorsman, P. (1995). Colocalization of L-type Ca2+ channels and insulin containing secretory granules and its significance for the initiation of exocytosis in mouse pancreatic β-cells. *European Molecular Biology Organisation Journal* **14:**50-57.

Braun, A., Varga-Szabo, D., Kleinschnitz, C., Pleines, I., Bender, M., Austinat, M., Bosl, M., *et al.* (2009). Orai1 (CRACM1) is the platelet SOC channel and essential for pathological thrombus formation. *Blood* **113:**9.

Brini M. and Carafoli, E. (2011). The Plasma Membrane Ca2+ ATPase and the Plasma Membrane Sodium Calcium Exchanger Cooperate in the Regulation of Cell Calcium. *Cold Spring Harbor Perspectives in Biology* **3:**a004168.

Broome, J.D. (1968). Studies on the mechanism of tumor inhibition by L-asparaginase. Effects of the enzyme on asparagine levels in the blood, normal tissues, and 6C3HED lymphomas of mice: differences in asparagine formation and utilization in asparaginase-sensitive and -resistant lymphoma cells. *Journal of Experimental Medicine* **127:**1055-1072.

Bultynck, G. and Parys, J.B. (2018). Ca2+ signalling and cell death: Focus on Ca2+-transport systems and their implication in cell death and survival. *Cell Calcium* **69:**1-3.

Bustamante, E. and Pedersen, P.L. (1977). High aerobic glycolysis of rat hepatoma cells in culture: role of mitochondrial hexokinase. *Proceedings of the National Academy of Sciences USA* **7**:3735-9.

CalciMedica Inc. (2019). CM46*20 Injectable Emulsion Versus Supportive Care in Patients with Acute Pancreatitis and SIRS* [Online]. Available at: https://clinicaltrials.gov/ct2/show/NCT03401190 [Accessed: 10 August 2019].
Calcraft, P.J., Ruas, M., Pan, Z., Cheng, X., Arredouani, A., Hao, X., Tang, J., *et al.* (2009). NAADP mobilizes calcium from acidic organelles through two-pore channels. *Nature* **459:**596-600.

Cancela, J.M., Gerasimenko, O.V., Gerasimenko, J.V., Tepikin, A.V. and Petersen, O.H. (2000). Two different but converging messenger pathways to intracellular Ca2+ release: the roles of NAADP, cADPR and IP3. *European Molecular Biology Organisation Journal* **19:**2549-2557.

Carafoli, E. (1994). Biogenesis: plasma membrane calcium ATPase: 15 years of work on the purified enzyme. *Federation of American Societies for Experimental Biology Journal* **8:**993-1002.

Cartwright, E.J., Mohamed, T., Oceandy, D. and Neyses, I. (2011). Calcium signalling dysfunction in heart disease. *Biofactors* **37:**175-81.

Case RM. (1978). Synthesis, intracellular transport and discharge of exportable proteins in the pancreatic acinar cell and other cells. *Biological Reviews of the Cambridge Philosophical Society* **53**(2): 211-354.

Cawley, T.A. (1788). A singular case of diabetes, consisting entirely in the quantity of urine with an enquiry into the different theories of that disease. *London Medical Journal* **9:**286-1788.

Cerny, J., Feng, Y., Yu, A., Miyake, K., Borgonovo, B., Klumperman, J., Meldolesi, J., *et al*. (2004). The small chemical vacuolin-1 inhibits Ca2+-dependent lysosomal exocytosis but not cell resealing. *EMBO Reports* 5:883-888.

Chakrabarti, R. and Chakrabarti, R. (2006). Calcium signaling in non-excitable cells: Ca2+ release and influx are independent events linked to two plasma membrane Ca2+ entry channels. *Journal of Cellular Biochemistry* **15**(6):1503-16.

Chandra, R. and Liddle, R.A. (2009). Neural and hormonal regulation of pancreatic secretion. *Current Opinion in Gastroenterology* **25:**441-6.

Cheng, K.T., Ong, H.L., Liu, X. and Ambudkar, I.S. (2013). Contribution and regulation of TRPC channels in store-operated Ca2+ entry. *Current Topics in Membranes* **71:**149-79.

Choi, H.S., Kim, H.S., Min, K.R., Kim, Y., Lim, H.K., Chang, Y.K. and Chung, M.W. (2000). Anti-inflammatory effects of fangchinoline and tetrandrine. Journal of Ethnopharmacology **69(**2):173-9.

Choi, S., Maleth, J., Jha, A., Lee, K.P., Kim, M.S., So, I., Ahuja, M., *et al.* (2014). The TRPCs-Orai interaction. *Handbook of Experimental Pharmacology* **223:**1035-1054.

Christensen, K.A., Myers, J.T. and Swanson, J.A. (2002). pH-dependent regulation of lysosomal calcium in macrophages. *Journal of Cell Science* **115:**599-607.

Chvanov, M., De Faveri, F., Moore, D., Sherwood, M.W., Awais, M., Voronina, S., Sutton, R. *et al.* (2018). Intracellular rupture, exocytosis and actin interaction of endocytic vacuoles in pancreatic acinar cells: initiating events in acute pancreatitis. *Journal of Physiology* **596:**2547-2564.

Chvanov, M., Huang, W., Jin, T., Wen, L., Armstrong, J., Elliot, V., Alston, B., *et al.* (2015). Novel lipophilic probe for detecting near-membrane reactive oxygen species responses and its application for studies of pancreatic acinar cells: Effects of pyocyanin and l-ornithine. *Antioxidant Redox Signalling* **22:**451–464.

Clapham, D.E. (2003). TRP channels as cellular sensors. *Nature* **426:**517-524.

Clemens, D.L., Schneider, K.J., Arkfeld, C.K., Grode, J.R., Wells, M.A. and Singh, S. (2016). Alcoholic pancreatitis: New insights into the pathogenesis and treatment. *World Journal of Gastrointestinal Pathophysiology* **7:**48-58.

Collins, S.R. and Meyer, T. (2011). Evolutionary origins of STIM1 and STIM2 within ancient Ca2 signaling systems. *Trends in Cell Biology* **21:**202–211.

Coté, G.A., Yadav, D., Slivka, A., Hawes, R.H., Anderson, M.A., Burton, F.R., Brand, R.E., *et al.* (2011). Alcohol and smoking as risk factors in an epidemiology study of patients with chronic pancreatitis. *Clinical Gastroenterology and Hepatology* **9:**266-273.

Covington, E.D., Wu, M.M., Lewis, R.S. (2010). Essential role for the CRAC activation domain in store-dependent oligomerization of STIM1. *Molecular Biology of the Cell* **21:**1897-1907.

Criddle, D.N. (2015). The role of fat and alcohol in acute pancreatitis: A dangerous liaison. *Pancreatology* **15:**S6-12.

Criddle, D.N., Gerasimenko, J.V., Baumgartner, H.K., Jaffar, M., Voronina, S., Sutton, R., Petersen, O.H., *et al.* (2007). Calcium signalling and pancreatic cell death: apoptosis or necrosis? *Cell Death and Differentiation* **14:**1285-94.

Criddle, D.N., Gillies, S., Baumgartner-Wilson, H.K., Jaffar, M., Chinje, E.C., Passmore, S., Chvanov, M., *et al.* (2006a)., Menadione-induced reactive oxygen species generation via redox cycling promotes apoptosis of murine pancreatic acinar cells. Journal of Biological Chemistry **281**:40485-40492.

Criddle, D.N., Murphy, J., Fistetto, G., Barrow, S., Tepikin, A.V., Neoptolemos, J.P., Sutton, R., *et al.* (2006b). Fatty acid ethyl esters cause pancreatic calcium toxicity via inositol trisphosphate receptors and loss of ATP synthesis. *Gastroenterology* **130**(3): 781-793.

Criddle, D.N., Raraty, M.G.T., Neoptolemos, J.P., Tepikin, A.V., Petersen, O.H. and Sutton, R. (2004). Ethanol toxicity in pancreatic acinar cells: mediation by nonoxidative fatty acid metabolites. *Proceedings of the National Academy of Sciences USA* **101**(29):10738-43.

C57BL/6 Mouse Model Information Sheet. (2019). [ebook] p.1. Available at: https://www.criver.com/sites/default/files/resources/C57BL6MouseModelInformationSheet.pdf [Accessed 30 Apr. 2019].

DeHaven, W.I., Jones, B.F., Petranka, J.G., Smyth, J.T., Tomita, T., Bird, G.S., Putney, J.W. (2009). TRPC channels function independently of STIM1 and Orai1. *Journal of Physiol*ogy **587:**2275-2298.

Demols, A., Le Moine, O., Desalle, F., Quertinmont, E., Van Laethem, J.L. and Devière, J. (2000). CD4(+)T cells play an important role in acute experimental pancreatitis in mice. *Gastroenterology* **118:**582-590.

Derler, I., Schindl, R., Fritsch, R., Heftberger, P., Riedl, M.C., Begg, M., House, D., *et al.* (2013). The action of selective CRAC channel blockers is affected by the Orai pore geometry. *Cell Calcium* **53:**139151.

Dery, O., Corvera, C.U., Steinhoff, M. and Bunnett, N.W. (1998). Proteinase-activated receptors: novel mechanisms of signaling by serine proteases. *American Journal of Physiology* **274:**C1429-C1452.

De Stefani, D., Raffaello, A., Teardo, E., Szabò, I. and Rizzuto, R. (2011). A 40 kDa protein of the inner membrane is the mitochondrial calcium uniporter. *Nature* **476**(7360):336-40.

De Faveri, F., Chvanov, M., Voronina, S., Moore, D., Pollock, L., Haynes, L., Awais, M., *et al.* (2019). LAP-like non-canonical autophagy and evolution of endocytic vacuoles in pancreatic acinar cells. *Autophagy* 1554-8627.

DiCapite, J.L., Bates, G.J. and Parekh, A.B. (2011). Mast cell CRAC channel as a novel therapeutic target in allergy. *Current Opinion in Allergy and Clinical Immunology* **11:**33-8.

Diczfalusy, M.A., Bjorkhem, I., Einarsson, C., Hillebrant, C.G. and Alexson, S.E. (2001). Characterization of enzymes involved in formation of ethyl esters of long-chain fatty acids in humans. The *Journal of Lipid Research* **42**(7):1025-1032.

Dingsdale, H., Voronina, S., Haynes, L., Tepikin, A. and Lur, G. (2012). Cellular geography of IP3 receptors, STIM and Orai: a lesson from secretory epithelial cells. *Biochemical Society Transactions* **40:**108-11.

Drake, R.L., Vogl, A.W. and Mitchell, A.W.M. (2014). Gray's Anatomy for Students. 3rd ed. Philadelphia: Elsevier, pp. 738-742.

Duval, M., Suciu, S., Ferster, A., Rialland, X., Nelken, B., Lutz, P., Benoit, Y., *et al.* (2002). Comparison of Escherichia coli-asparaginase with Erwinia-asparaginase in the treatment of childhood lymphoid malignancies: results of a randomized European Organisation for Research and Treatment of Cancer-Children's Leukemia Group phase 3 trial. *Blood* **99:**2734-2739.

Ellis, H. (2013). Anatomy of the pancreas and the spleen. *Surgery* **31:**263-266.

Fahrner, M., Derler, I., Jardin, I. and Romanin, C. (2013). The STIM1/Orai signalling machinery. *Channels* **7:**330-343.

Ferdek, P.E., Gerasimenko, J.V., Peng, S., Tepikin, A.V., Petersen, O.H. and Gerasimenko, O.V. (2012). A novel role for Bcl-2 in regulation of cellular calcium extrusion. *Current Biology* **22**(13):1241-6.

Ferdek, P.E., Jakubowska, M.A., Nicolaou, P., Gerasimenko, J.V., Gerasimenko, O.V. and Petersen, O.H. (2017). BH3 mimetic-elicited Ca2+ signals in pancreatic acinar cells are dependent on Bax and can be reduced by Ca2+-like peptides. *Cell Death and Dis*ease **8:**e2640.

Feske, S., Gwack, Y., Prakriya, M., Srikanth, S., Puppel, S.H., Tanasa, B., Hogan, P.G., *et al.* (2006). A mutation in Orai1 causes immune deficiency by abrogating CRAC channel function. *Nature* **441**(7090):179-85.

Fierro, L. and Parekh, A.B. (1999). Fast calcium-dependent inactivation of calcium release-activated calcium current (CRAC) in RBL-1 cells. *The Journal of Membrane Biology* **168:**9-17.

Finichiu, P.G., James, A.M., Larsen, L., Smith, R.A. and Murphy, M.P. (2013). Mitochondrial accumulation of a lipophilic cation conjugated to an ionisable group depends on membrane potential, ph gradient and pk(a): Implications for the design of mitochondrial probes and therapies. *Journal of Bioenergetics and Biomembranes* **45:**165-173.

Fischer, L., Gukovskaya, A.S., Penninger, J.M., Mareninova, O.H., Friess, H., Gukoovsky, I. and Pandol, S.J. (2007). Phosphatidylinositol 3-kinase facilitates bile acid-induced Ca(2+) responses in pancreatic acinar cells. *American Journal of Physiology-Gastrointestinal and Liver Physiology* **292:**G875–-886.

Flores-Calderon, J., Exiga-Gonzalez, E., MoranVillota, S., Martin-Trejo, J. and Yamamoto-Nagano, A. (2009). Acute pancreatitis in children with acute lymphoblastic leukemia treated with L-asparaginase. *Journal of Pediatric Hematology/Oncology* **31:**790-793

Foskett, J.K., White, C., Cheung, K.H. and Mak, D.O. (2007). Inositol trisphosphate receptor Ca2+ release channels. *Physiological Reviews* **87:**593-658.

Futatsugi, A., Nakamura, T., Yamada, M.K., Ebisui, E., Nakamura, K., Uchida, K., Kitaguchi, T., *et al.* (2005). IP3 receptor types 2 and 3 mediate exocrine secretion underlying energy metabolism. *Science* **309:**2232-4.

Garside, V.C., Kowalik, A.S., Johnson, C.L., DiRenzo, D., Konieczny, S.F., Pin, C.L. (2010). MIST1 regulates the pancreatic acinar cell expression of Atp2c2, the gene encoding secretory pathway calcium ATPase 2. *Experimental Cell Research* **316:**2859-2870.

Gea-Sorlí, S. and Closa, D. (2010). Role of macrophages in the progression of acute pancreatitis. *World Journal of Gastrointestinal Pharmacology and Therapeutics* **1:**107-11.

Gerasimenko, O.V. and Gerasimenko, J.V. (2012). Mitochondrial function and malfunction in the pathophysiology of pancreatitis. *European Journal of Physiology* **464:**89-99.

Gerasimenko, J.V., Charlesworth, R.M., Sherwood, M.W., Ferdek, P.E., Mikoshiba, K. and Parrington, J., Petersen, O.H., *et al.* (2015). Both RyRs and TPCs are required for NAADP-induced intracellular Ca^{2+} release. *Cell Calcium* **58**(3):237-45.

Gerasimenko, J.V., Gerasimenko, O.V. and Petersen, O.H. (2014a). The role of Ca2+ in the pathophysiology of pancreatitis. *Journal of Physiology* **592**(Pt 2):269-80.

Gerasimenko, J.V., Gerasimenko, O.V., Petersen, O.H. and Tepikin, A.V. (1996a). Short pulses of acetylcholine stimulation induce cytosolic Ca2+ signals that are excluded from the nuclear region in pancreatic acinar cells. *European Journal of Physiology* **432:**1055-1061.

Gerasimenko, J.V., Lur, G., Sherwood, M.W., Ebisui, E., Tepikin, A.V., Mikoshiba, K., Gerasimenko, O.V., Petersen, O.H. (2009). Pancreatic protease activation by alcohol metabolite depends on Ca2+ release via acid store IP3 receptors. *Proceedings of the National Academy of Sciences USA***106:**10758-10763.

Gerasimenko, J.V., Peng, S. and Gerasimenko, O.V. (2014b). Role of acidic stores in secretory epithelia. *Cell Calcium* **55:**346-354.

Gerasimenko, J.V., Peng, S., Tsugorka, T. and Gerasimenko, O.V. (2017). Ca2+ signalling underlying pancreatitis. *Cell Calcium* **70:**95-101.

Gerasimenko, O.V., Gerasimenko, J.V., Belan, P.V. and Petersen, O.H. (1996b). Inositol trisphosphate and cyclic ADP-ribose-mediated release of Ca2+ from single isolated pancreatic zymogen granules. *Cell* **84**:473-480.

Gerasimenko, O.V., Gerasimenko, J.V., Rizzuto, R.R., Treiman, M., Tepikin, A.V. and Petersen, O.H. (2002). The distribution of the endoplasmic reticulum in living pancreatic acinar cells. *Cell Calcium* **32:**261-268.

Gerasimenko, J.V., Gryshchenko, O.V. and Ferdek, P.E., Stapleton, E., Hébert, T.O., Bychkova, S., Peng, S., *et al.* (2013). Ca2+ release-activated Ca2+ channel blockade as a potential tool in antipancreatitis therapy. *Proceedings of the National Academy of Sciences USA* **110:**13186-13191.

Gerasimenko, J.V., Maruyama, Y., Yano, K., Dolman, N.J., Tepikin, A.V., Petersen, O.H. and Gerasimenko, O.V. (2003). NAADP mobilizes Ca2+ from a thapsigargin-sensitive store in the nuclear envelope by activating ryanodine receptors. *Journal of Cell Biology* **163:**271-282.

Gerasimenko, J.V., Peng, S., Tsugorka, T. and Gerasimenko, O.V. (2018). Ca^{2+} signalling underlying pancreatitis. *Cell Calcium* **70:**95-101.

Gerasimenko, J.V., Sherwood, M.W., Tepikin, A.V., Petersen, O.H. and Gerasimenko, O.V. (2006). NAADP, cADPR and IP3 all release Ca2+ from the endoplasmic reticulum and an acidic store in the secretory granule area. *Journal of Cell Science* **119:**226-238.

Gorelick, F. (2007). Pancreatic protease-activated receptors: friend and foe. *Gut* **56**(7):901-2.

Grondin, G. and Beaudoin, A.R. (1996). Immunocytochemical and cytochemical demonstration of a novel selective lysosomal pathway (SLP) of secretion in the exocrine pancreas. *Journal of Histochemistry and Cytochemistry* **44:**357-368.

Gross, S., Guzman, G., Wissenbach, U., Philipp, S., Zhu, M., Bruns, D. and Cavalie, A. (2009). TRPC5 is a Ca2-activated channel functionally coupled to Ca2-selective ion channels. *Journal of Biological Chemistry* **284:**34423-34432.

Gross, S.A., Wissenbach, U., Philipp, S.E., Freichel, M., Cavalie, A. and Flockerzi, V. (2007). Murine ORAI2 splice variants form functional Ca2+ release-activated Ca2+ (CRAC) channels. *The Journal of Biological Chemistry.* **282:**19375-84.

Grynkiewicz, G., Poenie, M., Tsien, R.Y. (1985). A new generation of Ca2+ indicators with greatly improved fluorescence properties. *The Journal of Biological Chemistry* **260:**3440-50.

Guerini, D., Coletto, L. and Carafoli, E. (2005). Exporting calcium from cells. *Cell Calcium* **38:**281-289.

Gukovskaya, A.S. and Gukovsky, I. (2011). Which way to die: the regulations of acinar cell death in pancreatitis by mitochondria, Ca^{2+}, and reactive oxygen species. *Gastroenterology* **140**:1876-80.

Gukovskaya, A.S. and Pandol, S.J. (2004). Cell death pathways in pancreatitis and pancreatic cancer. *Pancreatology* **4:**567-86.

Gukovskaya, A.S., Mouria, M., Gukovsky, I., Reyes, C.N., Kasho, V.N., Faller, L.D. and Pandol, S.J. (2002). Ethanol metabolism and transcription factor activation in pancreatic acinar cells in rats. *Gastroenterology* **122**(1):106-118.

Gukovskaya, A.S., Vaquero, E. and Zaninovic, V. (2002). Neutrophils and NADPH oxidase mediate intrapancreatic trypsin activation in murine experimental acute pancreatitis. *Gastroenterology* **122:**974984.

Gukovsky, I., Pandol, S.J. and Gukovskaya, A.S. (2011). Organellar dysfunction in the pathogenesis of pancreatitis. *Antioxidants and Redox Signaling* **15**(10):2699-2710.

Forsmark, C.E., Vege, S.S. and Wilcox, C.M. (2016). Acute pancreatitis. *The New England Journal of Medicine* **375:**1972-1981.

Haber, P.S., Apte, M.V., Applegate, T.L., Norton, I.D., Korsten, M.A., Pirola, R.C. and Wilson, J.S. (1998). Metabolism of ethanol by rat pancreatic acinar cells. *Journal of Laboratory and Clinical Medicine* **132:**294-302.

Haber, P.S., Apte, M.V., Moran, C., Applegate, T.L., Pirola, R.C., Korsten, M.A., McCaughan, G.W., *et al.* (2004). Non-oxidative metabolism of ethanol by rat pancreatic acini. *Pancreatology* **4:**82-89.

Hajnóczky, G., Robb-Gaspers, L.D., Seitz, M.B. and Thomas, A.P. (1995). Decoding of cytosolic calcium oscillations in the mitochondria. *Cell* **82**(3):415-24.

Hakamata, Y., Nakai, J., Takeshima, H. and Imoto, K. (1992). Primary structure and distribution of a novel ryanodine receptor/calcium release channel from rabbit brain. *The Federation of European Biochemical Societies* **312:**229-35.

Halestrap, A.P. and Richardson, A.P. (2015). The mitochondrial permeability transition: a current perspective on its identity and role in ischaemia/reperfusion injury. *Journal of Molecular and Cellular Cardiology* **78:**129-41.

Hamada, S., Masamune, A., Kikuta, K., Hirota, M., Tsuji, I. and Shimosegawa, T. (2014). Nationwide epidemiological survey of acute pancreatitis in Japan. *Pancreas* **43:**1244-1248.

Hamamoto, T., Yamada, S. and Hirayama, C. (1990). Nonoxidative metabolism of ethanol in the pancreas; implication in alcoholic pancreatic damage. *Biochemical Pharmacology* **39:**241-245.

He, F.Q., Qiu, B.Y., Li, T.K., Xie, Q., Cui, D.J., Huang, X.L., Gan, H.T. (2011). Tetrandrine suppresses amyloid-β-induced inflammatory cytokines by inhibiting NF-κB pathway in murine BV2 microglial cells. *International Immunopharmacology* **11**(9):1220-5.

Hirano, T., Saluja, A., Ramarao, P., Lerch, M.M., Saluja, M. and Steer, M. L. (1991). Apical secretion of lysosomal enzymes in rabbit pancreas occurs via a secretagogue regulated pathway and is increased after pancreatic duct obstruction. *Journal of Clinical Investigations* **87:**865-869.

Holden, H.M., Rayment, I. and Thoden, J.B. (2003). Structure and function of enzymes of the Leloir pathway for galactose metabolism. *Journal of Biological Chemistry* **278:**43885-8.

Hospital Admitted Patient Care Activity. (2018). *2017-18 – NHS Digital* [Online]. Available at: https://digital.nhs.uk/data-and information/publications/statistical/hospital-admitted-patient-care-activity/2017-18 [Accessed: 1 May 2019].

Hoth, M. and Penner, R. (1992). Depletion of intracellular calcium stores activates a calcium current in mast cells. *Nature* **355:**353-356.

Hoth, M. and Penner, R. (1993). Calcium release-activated calcium current in rat mast cells. *Journal of Physiology* **465**:359-86.

Hoth, M. (1995). Calcium and barium permeation through calcium release-activated calcium (CRAC) channels. *Pflugers Archiv* **430**(3):315-22.

Hou, X., Pedi, L., Diver, M.M. and Long, S.B. (2012). Crystal structure of the calcium release-activated calcium channel Orai. *Science* **338:**1308-1313.

Huang, W., Cane, M.C., Mukherjee, R., Szatmary, P., Zhang, X., Elliott, V., Ouyang, Y., *et al.* (2017). Caffeine protects against experimental acute pancreatitis by inhibition of inositol 1,4,5-trisphosphate receptor-mediated Ca2+ release. *Gut* **66:**301-313.

Husain, S. and Thrower, E. (2009). Molecular and cellular regulation of pancreatic acinar cell function. *Curr Opin Gastroenterol* **25:**466-71.

Irving, H.M., Samokhvalov, A.V. and Rehm, J. (2009). Alcohol as a risk factor for pancreatitis. A systematic review and meta-analysis. *Journal of the Pancreas* **10**(4):387-92.

Iwatsuki, N. and Petersen, O.H. (1977). Pancreatic acinar cells: localization of acetylcholine receptors and the importance of chloride and calcium for acetylcholine-evoked depolarization. *The Journal of Physiology* **269:**723-33.

Jaffe, N., Traggis, D., Das, L., Moloney, W.C., Hann, H.W., Kim, B.S. and Nair, R. (1971). L-Asparaginase in the treatment of neoplastic diseases in children. *Cancer Research* **31:**942-949.

Jairaman, A. and Prakriya, M. (2013). Molecular pharmacology of storeoperated CRAC channels. *Channels* **7:**402-414.

Johansson, K.A. and Grapin-Botton, A. (2002). Development and diseases of the pancreas. *Clinical Genetics* **62:**14-23.

Kambhampati, S., Park, W. and Habtezion, A. (2014). Pharmacologic therapy for acute pancreatitis.

Kaiser, A.M., Saluja, A.K., Sengupta, A., Saluja, M. and Steer, M.L. (1995). Relationship between severity, necrosis, and apoptosis in five models of experimental acute pancreatitis. *The American Journal of Physiology* **269:**1295-304.

Kamisawa, T., Wood, L.D., Itoi, T. and Takaori, K. (2016). Pancreatic cancer. *Lancet* **388:**73-85.

Kearney, S.L., Dahlberg, S.E., Levy, D.E., Voss, S. D., Sallan, S.E. and Silverman, L.B. (2009). Clinical course and outcome in children with acute lymphoblastic leukemia and asparaginase-associated pancreatitis. *Pediatric Blood and Cancer* **53:**162-167.

Kikuyama, M., Kamisawa, T., Kuruma, S., Chiba, K., Kawaguchi, S., Terada, S. and Satoh, T. (2018). Early diagnosis to improve the poor prognosis of pancreatic cancer. *Cancers* **10:**48.

Kim, K.D., Srikanth, S., Tan, Y.V., Yee, M.K., Jew, M., Damoiseaux, R., Jung, M.E., *et al.* (2014). Calcium signaling via Orai1 is essential for induction of the 186 nuclear orphan receptor pathway to drive Th17 differentiation. *The Journal of Immunology* **192:**110-22.

Kim, M.S., Hong, J.H., Li, Q., Shin, D.M., Abramowitz, J., Birnbaumer, L. and Muallem, S. (2009). Deletion of TRPC3 in mice reduces Store-Operated Ca2+ influx and the severity of acute pancreatitis. *Gastroenterology* **137:**1509-17.

Kim, J.Y., Kim, K.H., Lee, J.A., Namkung, W., Sun, A.Q., Ananthanarayanan, M., Suchy, F.J., *et al.* (2002). Transporter-mediated bile acid uptake causes Ca2+-dependent cell death in rat pancreatic acinar cells. *Gastroenterology* **122:**1941-1953.

Kirichok, Y., Krapivinsky, G. and Clapham, D.E. (2004). The mitochondrial calcium uniporter is a highly selective ion channel. *Nature* **427**(6972):360-4.

Knoderer, H.M., Robarge, J. and Flockhart, D.A. (2007). Predicting asparaginase-associated pancreatitis. *Pediatric Blood and Cancer* **49:**634-639.

Krishnan, K. (2017). Nutritional management of acute pancreatitis. *Current Opinion in Gastroenterology* **33:**102-106.

Krüger, B., Albrecht, E. and Lerch, M.M. (2000). The role of intracellular calcium signaling in premature protease activation and the onset of pancreatitis. *The American Journal of Pathology* **157**(1):43-50.

Kurre, H.A., Ettinger, A.G., Veenstra, D.L., Gaynon, P.S., Franklin, J., Sencer, S.F., Reaman, G.H., *et al.* (2002). A pharmacoeconomic analysis of pegaspargase versus native Escherichia coli L-asparaginase for the treatment of children with standard-risk, acute lymphoblastic leukemia: the Children's Cancer Group study (CCG-1962). *Journal of Pediatric Hematology/Oncology* **24:**175-181.

Kwan, C.Y. and Putney, J.W. (1990). Uptake and intracellular sequestration of divalent cations in resting and methacholine-stimulated mouse lacrimal acinar cells. Dissociation by Sr2+ and Ba2+ of agoniststimulated divalent cation entry from the refilling of the agonist-sensitive intracellular pool. *The Journal of Biological Chemistry* **265:**678-84.

Lacruz, R.S. and Feske, S. (2015). Diseases caused by mutations in ORAI1 and STIM1. *Annals of the New York Academy of Sciences* **1356:**45-79.

Lankisch, P.G., Apte, M. and Banks, P.A. (2015). Acute pancreatitis. *Lancet* **386:**85-96.

Laposata, E.A. and Lange, L.G. (1986). Presence of nonoxidative ethanol metabolism in human organs commonly damaged by ethanol abuse. *Science* **231**:497-499.

Laukkarinen, J.M., Weiss, E.R., van Acker, G.J.D., Steer, M.L. and Perides, G. (2008). Protease-activated receptor-2 exerts contrasting model-specific effects on acute experimental pancreatitis. *The Journal of Biological Chemistry* **283**(30):20703-12.

Lee, K.P., Choi, S., Hong, J.H., Ahuja, M., Graham, S., Ma, R., So, I., *et al.* (2014). Molecular determinants mediating gating of Transient Receptor Potential Canonical (TRPC) channels by stromal interaction molecule 1 (STIM1). *The Journal of Biological Chemistry.* **289:**6372-82.

Lee, M.G., Xu, X., Zeng, W., Diaz, J., Wojcikiewicz, R.J., Kuo, T.H., Wuytack, F., *et al.* (1997). Polarized expression of Ca2+ channels in pancreatic and salivary gland cells. Correlation with initiation and propagation of [Ca2+]i waves. *The Journal of Biological Chemistry* **272:**15765–70.

Le Gal, K., Ibrahim, M.X., Wiel, C., Sayin, V.I., Akula, M.K., Karlsson, C., Dalin, M.G., *et al.* (2015). Antioxidants can increase melanoma metastasis in mice. Science Translation Medicine **7:**308.

Leite, M.F., Dranoff, J.A., Gao, L. and Nathanson, M.H. (1999). Expression and subcellular localization of the ryanodine receptor in rat pancreatic acinar cells. *Biochem J* **337:**305-309.

Leo, S., Bianchi, K., Brini, M. and Rizzuto, R. (2005). Mitochondrial calcium signalling in cell death. *The Federatioon Of European Biochemical Soocieties Journal* **272:**4013-4022.

Lerch, M.M. and Gorelick, F.S. (2013). Models of acute and chronic pancreatitis. *Gastroenterology* **144**(6):1180- 1193.

Leung, P.S. and Ip, S.P. (2006). Pancreatic acinar cell: its role in acute pancreatitis. *The International Journal of Biochemistry and Cell Biology* **38:**1024-1030.

Li, J., Zhou, R., Zhang, J. and Li, Z.F. (2014). Calcium signalling of pancreatic acinar cells in the pathogenesis of pancreatitis. *World Journal of Gastroenterology* **20:**16146-16152.

Liou, J., Fivaz, M., Inoue, T. and Meyer, T. (2007). Live-cell imaging reveals sequential oligomerization and local plasma membrane targeting of stromal interaction molecule 1 after calcium store depletion. *Proceedings of the National Academy of Sciences USA.* **104:**9301-9306.

Liou, J., Kim, M.L., Heo, W.D., Jones, J.T., Myers, J.W., Ferrell, J.E. Jr. and Meyer, T. (2005). STIM is a Ca2+ sensor essential for Ca2+-store-depletion-triggered Ca2+ influx. *Current Biology* **15**(13):1235-41.

Litjens, T., Harland, M.L., Roberts, M.L., Barritt, G.J. and Rychkov, G.Y. (2004). Fast Ca(2+)-dependent inactivation of the store-operated Ca2+ current (ISOC) in liver cells: a role for calmodulin. *The Journal of Physiology* **558:**85-97.

Liu, X., Cheng, K.T., Bandyopadhyay, B.C., Pani, B., Dietrich, A., Paria, B.C., Swaim, W.D., *et al.* (2007). Attenuation of store-operated Ca2+ current impairs salivary gland fluid secretion in TRPC1(-/-) mice. *Proceedings of the National Academy of Sciences USA* **104**(44):17542-7.

Liu, X., Wang, W., Singh, B.B., Lockwich, T., Jadlowiec, J., O'Connell, B., Wellner, R., *et al.* (2000). Trp1, a candidate protein for the store-operated Ca(2+) influx mechanism in salivary gland cells. *The Journal of Biological Chemistry* **275**(5):3403-11.

Lloyd-Evans, E. and Platt, F.M. (2011). Lysosomal Ca(2+) homeostasis: role in pathogenesis of lysosomal storage diseases. *Cell Calcium* **50:**200-5.

Lloyd-Evans, E., Morgan, A.J., He, X., Smith, D.A., Elliot-Smith, E., Sillence, D.J., Churchill, G.C., *et al.,* (2008). Niemann-Pick disease type C1 is a sphingosine storage disease that causes deregulation of lysosomal calcium. *Nature Medicine* **14:**1247-55.

Logsdon, C.D. and Baoan, J. (2014). The role of protein synthesis and digestive enzymes in acinar cell injury. *Nature Reviews Gastroenterology and Hepatology* **10:**362-370.

Lopez, M.J. (2002). The changing incidence of acute pancreatitis in children: a single-institution perspective. *Journal of Pediatrics* **140:**622–624.

Low, J.T., Shukla, A. and Thorn, P. (2010). Pancreatic acinar cell: new insights into the control of secretion. *The International Journal of Biochemistry and Cell Biology* **42:**1586-9.

Luik, R.M., Wang, B., Prakriya, M., Wu, M.M. and Lewis, R.S. (2008). Oligomerization of STIM1 couples ER calcium depletion to CRAC channel activation. *Nature* **454**(7203):538-42.

Lur, G., Haynes, L.P., Prior, I.A., Gerasimenko, O.V., Feske, S., Petersen, O.H., Burgoyne, R.D. and Tepikin, A.V. (2009). Ribosome free terminals of rough ER allow formation of STIM1 puncta and segregation of STIM1 from IP(3) receptors. *Current Biology* **19:**1648-53.

Lur, G., Sherwood, M.W., Ebisui, E., Haynes, L., Feske, S., Sutton, R., Burgoyne, R.D., *et al.* (2011). InsP3receptors and Orai channels in pancreatic acinar cells: colocalization and its consequences. *Biochemical Journal* **436:**231-239.

Lytton, J., Westlin, M., Burk, S.E., Shull, G.E., and Maclennan, D.H. (1992). Functional comparisons between isoforms of the sarcoplasmic or endoplasmic reticulum family of calcium pumps. *The Journal of Biological Chemistry.* **267:**14483-14489.

Mangialavori, I., Ferreira-Gomes, M., Pignataro, M.F., Strehler, E.E. and Rossi, J.P.F.C. (2010). Determination of the dissociation constants for Ca2+ and calmodulin from the plasma membrane Ca2+ pump by a lipid probe that senses membrane domain changes. *The Journal of Biological Chemistry* **285**(1):123–30.

Manohar, M., Verma, A.K., Venkateshaiah, S.U., Sanders, N.L., Mishra, A. (2017). Pathogenic mechanisms of pancreatitis. *World Journal of Gastrointestinal Pharmacology and Therapeutics* **8:**10-25.

Majumder, S. and Chari, S.T. (2016). Chronic pancreatitis. *Lancet* **387:**1957-66.

Malo, A., Kruger, B., Seyhun, E., Schafer, C., Hoffmann, R.T., Goke, B., Kubisch, C.H. (2010). Tauroursodeoxycholic acid reduces endoplasmic reticulum stress, trypsin activation, and acinar cell apoptosis while increasing secretion in rat pancreatic acini. *The American Journal of Physiology* **299:**877-886.

Malosio, M. L., Giordano, T., Laslop, A. and Meldolesi, J. (2004). Dense-core granules: a specific hallmark of the neuronal/neurosecretory cell phenotype. *Journal of Cell Science* **117**:743-749.

Maruyama, Y., Inooka, G., Li, Y.X., Miyashita, Y. and Kasai, H. (1993). Agonist-induced localized Ca2+ spikes directly triggering exocytotic secretion in exocrine pancreas. *European Molecular Biology Organisation Journal* **12**(8):3017-22.

McCombs, J.E. and Palmer, A.E. (2008). Measuring calcium dynamics in living cells with genetically encodable calcium indicators. *Methods* **46:**152-159

Michelangeli, F. and East, J.M. (2011). A diversity of SERCA Ca2+ pump inhibitors. *Bichemical Society Transactions Trans* **39:**789-797.

Michikawa, T., Hirota, J., Kawano, S., Hiraoka, M., Yamada, M., Furuichi, T. and Mikoshiba, K. (1999). Calmodulin Mediates Calcium-Dependent Inactivation of the Cerebellar Type 1 Inositol 1,4,5-Trisphosphate Receptor. *Neuron* **23**(4):799-808.

Mikoshiba, K. (2007). IP3 receptor/Ca2? channel: from discovery to new signaling concepts. *J*ournal of *Neurochemistry* **102:**1426-1446.

Mikoshiba, K., Hisatsune, C., Futatsugi, A., Mizutani, A., Nakamura, T. and Miyachi, K. (2008). The role of Ca2+ signaling in cell function with special reference to exocrine secretion. *Cornea* **27:**S3-S8.

Mitchell, K.J., Pinton, P., Varadi, A., Tacchetti, C., Ainscow, E.K., Pozzan, T., Rizzuto, R. and Rutter, G.A. (2001). Dense core secretory vesicles revealed as a dynamic Ca2+ store in neuroendocrine cells with a vesicle-associated membrane protein aequorin chimaera. *Journal of Cell Biology* **155**:41-51.

Moccia, F., Zuccolo, E., Soda, T., Tanzi, F., Guerra, G., Mapelli, L., Lodola, F., *et al.* (2015). Stim and Orai proteins in neuronal Ca^{2+} signaling and excitability. *Frontiers in Cellular Neuroscience* **9:**153.

Mogami, H., Tepikin, A.V. and Petersen, O.H. (1998). Termination of cytosolic Ca2+ signals: Ca2+ reuptake into intracellular stores is regulated by the free Ca2+ concentration in the store lumen. *European Molecular Biology Organisation Journal* **17:**435-42.

Molino, M., Barnathan, E.S., Numerof, R., Clark, J., Dreyer, M., Cumashi, A., Hoxie, J.A., *et al.* (1997). Interactions of mast cell tryptase with thrombin receptors and PAR-2. *The Journal of Biological Chemistry* **272**:4043-4049.

Morinville, V.D., Barmada, M.M., Lowe, M.E. (2010). Increasing incidence of acute pancreatitis at an American pediatric tertiary care center: is greater awareness among physicians responsible? *Pancreas* **39:**5-8.

Mukherjee, R., Criddle, D.N., Gukovskaya, A., Pandol, S., Petersen, O.H. and Sutton, R. (2008). Mitochondrial injury in pancreatitis. *Cell Calcium* **44:**14-23.

Mukherjee, R., Mareninova, O.A., Odinokova, I.V., Huang, W., Murphy, J., Chvanov, M., Javed, M.A., *et al*. (2016). Mechanism of mitochondrial permeability transition pore induction and damage in the pancreas: inhibition prevents acute pancreatitis by protecting production of ATP. *Gut* **65:**1333-46.

Muller, H.J. and Boos, J. (1998). Use of L-asparaginase in childhood ALL. *Critical Reviews in Oncology/Hematology* **28:**97-113.

Nakai, J., Imagawa, T., Hakamat, Y., Shigekawa, M., Takeshima, H.and Numa, S. (1990). Primary structure and functional expression from cDNA of the cardiac ryanodine receptor/calcium release channel. *The Federation of European Biochemical Societies Journal* **271:**169-77.

Nakagawa, T., Shimizu, S., Watanabe, T., Yamaguchi, O., Otsu, K., Yamagata, H., Inohara, H., *et al.* (2005). Cyclophilin D-dependent mitochondrial permeability transition regulates some necrotic but not apoptotic cell death. *Nature* **434**(7033):652-8.

Nakamura, K., Hamada, K., Terauchi, A., Matsui, M., Nakamura, T., Okada, T. and Mikoshiba, K. (2013). Distinct roles of M1 and M3 muscarinic acetylcholine receptors controlling oscillatory and non-oscillatory [Ca2+]i increase. *Cell Calcium* **54:**111-119.

Nathanson, M.H., Fallon, M.B., Padfield, P.J. and Maranto, A.R. (1994). Localization of the type 3 inositol 1,4,5-trisphosphate receptor in the Ca2+ wave trigger zone of pancreatic acinar cells. *The Journal of Biological Chemistry* **269:**4693-4696.

Namkung, W., Han, W., Luo, X., Muallem, S., Cho, K.H., Kim, K.H. and Lee, M.G. (2004). Protease-activated receptor 2 exerts local protection and mediates some systemic complications in acute pancreatitis. *Gastroenterology* **126**(7):1844-59.

Nesvaderani, M., Eslick, G.D., Vagg, D., Faraj, S. and Cox, M.R. (2015). Epidemiology, aetiology and outcomes of acute pancreatitis: a retrospective cohort study. *International Journal of Surgery* **23:**68-74.

Norton, I.D., Apte, M.V., Haber, P.S., McCaughan, G.W., Pirola, R.C. and Wilson, J.S. (1998). Cytochrome P4502E1 is present in rat pancreas and is induced by chronic ethanol administration. *Gut* **42:**426-430.

Nydegger, A., Heine, R.G., Ranuh, R., Gegati-Levy, R., Crameri, J., Oliver, M.R. (2007). Changing incidence of acute pancreatitis: 10-year experience at the Royal Children's Hospital, Melbourne. *Journal of Gastroenterology and Hepatology* **22:**1313-1316.

Nystedt, S., Emilsson, K., Wahlestedt, C. and Sundelin, J. (1994). Molecular cloning of a potential proteinase activated receptor. *Proceedings of the National Academy of Sciences U.S.A*. **91:**9208-9212.

Opie, E.L. (1901). The etiology of acute hemorrhagic pancreatitis. *Bulletin of the Johns Hopkins Hospital* **12:**182–8.

Orabi, A.I., Muili, K.A., Javed, T.A., Jin, S., Jayaraman, T., Lund, F.E. and Husain, S.Z. (2013). Cluster of differentiation 38 (CD38) mediates bile acid-induced acinar cell injury and pancreatitis through cyclic ADP-ribose and intracellular calcium release. *The Journal of Biological Chemistry* **288:**27128-27137.

Osherovich L. (2013). Cracking pancreatitis. *Science-Business Exchange* **6:**30.

Owyang, C. (1996). Physiological mechanisms of cholecystokinin action on pancreatic secretion. *The American Journal of Physiology* **271:**G1-7.

Palade, G**.** (1975). Intracellular aspects of the process of protein synthesis. *Science* **189**(4200): 347-358.

Pandol, S.J., Lugea, A., Mareninova, O.A., Smoot, D., Gorelick, F.S., Gukovskaya, A.S. and Gukovsky, I. (2011). Investigating the pathobiology of alcoholic pancreatitis. *Alcoholism: Clinical and Experimental Research* **35**(5):830-7.

Pandol, S.J., Periskic, S., Gukovsky, I., Zaninovic, V., Jung, Y., Zong, Y., Solomon, T.E., *et al.* (1999). Ethanol diet increases the sensitivity of rats to pancreatitis induced by cholecystokinin octapeptide. *Gastroenterology* **117**(3):706-16.

Pandol, S.J., Saluia, A.K., Imrie, C.W. and Banks, P.A. (2007). Acute pancreatitis: bench to the bedside**.** *Gastroenterology* **132:**1127-51.

Parekh, A.B. and Penner, R. (1997). Store depletion and calcium influx. *Physiological Reviews* **77:**901-930.

Parekh, A.B. and Putney, J.W. Jr. (2005). Store-operated calcium channels. *Physiological Reviews* **85:**757-810.

Parekh, A.B. (2010). Store-operated CRAC channels: function in health and disease. *Nature Reviews Drug Discovery* **9:**399-410.

Park, M.K., Ashby, M.C., Erdemli, G., Petersen, O.H. and Tepikin, A.V. (2001). Perinuclear, perigranular and sub-plasmalemmal mitochondria have distinct functions in the regulation of cellular calcium transport. *European Molecular Biology Organisation Journal* **20:**1863-1874.

Park, C.Y., Hoover, P.J., Mullins, F.M., Bachhawat, P., Covington, E.D., Raunser, S., Walz, T., *et al.* (2009a). STIM1 clusters and activates CRAC channels via direct binding of a cytosolic domain to Orai1. *Cell* **136:**876-890.

Park, A., Latif, S.U., Shah, A.U., Tian, J., Werlin, S., Hsiao, A., Pashankar, D., *et al.* (2009b). Changing referral trends of acute pancreatitis in children: A 12-year single-center analysis*. Journal of Pediatric Gastroenterology and Nutrition* **49:**316-322.

Park, M.K., Petersen, O.H. and Tepikin, A.V. (2000). The endoplasmic reticulum as one continuous Ca2+ pool: visualization of rapid Ca2+ movements and equilibration. *European Molecular Biology Organisation Journal* **19:**5729-5739.

Parod, R.J. and Putney, J.W. (1978). The role of calcium in the receptor mediated control of potassium permeability in the rat lacrimal gland. *The Journal of Physiology* **281(**1):371-81.

Peel, S.E., Liu, B. and Hall, I.P. (2008). ORAI1 and store-operated calcium influx in human airway smooth muscle cells. *American Journal of Respiratory Cell and Molecular Biology* **38:**744-749.

Peery, A.F., Dellon, E.S., Lund, J., Crockett, S.D., McGowan, C.E., Bulsiewicz, W.J., Gangarosa, L.M., *et al.* (2012). Burden of gastrointestinal disease in the United States: 2012 update. *Gastroenterol* **143:**1179-87.

Peng, S., Gerasimenko, J.V., Tsugorka, T., Gryshchenko,O., Samarasinghe, S., Petersen, O.H. and Gerasimenko, O.V. (2016). Calcium and adenosine triphosphate control of cellular pathology: asparaginase-induced pancreatitis elicited via protease-activated receptor 2. *Philosophical Transactions of the Royal Society of London: Biological Sciences* **371:**20150423.

Peng, S., Gerasimenko, J.V., Tsugorka, T., Gryshchenko,O., Samarasinghe, S., Petersen, O.H. and Gerasimenko, O.V. (2018). Galactose protects against cell damage in mouse models of acute pancreatitis. *Journal of Clinical Investigations* **128**(9):3769-3778.

Perides, G., Laukkarinen, J.M., Vassileva, G. and Steer, M.L. (2010a). Biliary acute pancreatitis in mice is mediated by the G-protein-coupled cell surface bile acid receptor Gpbar1. *Gastroenterology* **138:**715-25.

Perides, G., van Acker, G.J.D., Laukkarinen, J.M. and Steer, M.L. (2010b). Experimental acute biliary pancreatitis induced by retrograde infusion of bile acids into the mouse pancreatic duct. *Nature Protocols* **5**(2):335-41.

Petersen, O.H. and Sutton, R. (2006). Ca2+ signalling and pancreatitis: effects of alcohol, bile and coffee. *Trends in Pharmacological Sciences* **27:**113-20.

Petersen, O.H. and Tepikin, A.V. (2008). Polarized calcium signaling in exocrine gland cells. *Annual Review of Physiology* **70:**273-99.

Petersen, O.H. and Ueda, N. (1976). Pancreatic acinar cells: the role of calcium in stimulus-secretion coupling. *The Journal of Physiology* **254:**583-606.

Petersen, O.H. (1992). Stimulus-secretion coupling: cytoplasmic calcium signals and the control of ion channels in exocrine acinar cells. *The Journal of Physiology* **448:**1-51.

Petersen, O.H. (2003). Localization and regulation of Ca2+ entry and exit pathways in exocrine gland cells. *Cell Calcium* **33**(5-6):337-44.

Petersen, O.H. (2005). Ca2+ signalling and Ca2+-activated ion channels in exocrine acinar cells. *Cell Calcium* **38:**171-200.

Petersen, O.H. (2012). Specific mitochondrial functions in separate sub-cellular domains of pancreatic acinar cells. *Pflugers Arciv* **464:**77-87.

Petersen, O.H. (2014). Can specific calcium channel blockade be the basis for a drug-based treatment of acute pancreatitis? *Expert Review of Gastroenterology and Hepatology* **8:**339-341.

Petersen, O.H., Gerasimenko, O.V. and Gerasimenko, J.V. (2011). Pathobiology of acute pancreatitis: focus on intracellular calcium and calmodulin**.** *Medicine Reports* **3:**15.

Petersen, O.H., Tepikin, A.V., Gerasimenko, J.V., Gerasimenko, O.V., Sutton, R. and Criddle, D.N. (2009). Fatty acids, alcohol and fatty acid ethyl esters: toxic Ca2+ signal generation and pancreatitis. *Cell Calcium* **45:**634-42.

Pevarello, P., Cainarca, S., Liberati, C., Tarroni, P., Piscitelli, F., Severi, E. (2014). Ca^{2+} releaseactivated Ca^{2+}channel inhibitors. *Pharmaceutical Patent Analyst* **3:**171-182.

Philpott, H.G. and Petersen, O.H. (1979). Extracellular but not intracellular application of peptide hormones activates pancreatic acinar cells. *Nature* **281:**684-86.

Prakriya, M. and Lewis, R.S. (2004). Store-operated calcium channels: properties, functions and the search for a molecular mechanism. *Advances in Molecular and Cell Biology* **32:**121-140.

Prakriya, M. and Lewis, R.S. (2006). Regulation of CRAC channel activity by recruitment of silent channels to a high open-probability gating mode. *The Journal of General Physiology* **128**(3):373-86.

Prakriya, M. and Lewis, R.S. (2015). Store-operated calcium channels. *Physiological Reviews* **95:**1383-1436.

Prakriya, M., Feske, S., Gwack, Y., Srikanth, S., Rao, A. and Hogan, P.G. (2006). Orai1 is an essential pore subunit of the CRAC channel. *Nature* **443**(7108):230-3.

Putney, J.W. (1977). Muscarinic, alpha-adrenergic and peptide receptors regulate the same calcium influx sites in the parotid gland. *The Journal of Physiology* **268**(1):139-49.

Putney, J.W. (1986). A model for receptor-activated calcium entry. *Cell Calcium* **7:**1-12.

Putney, J.W. (2007). Recent breakthroughs in the molecular mechanism of capacitative calcium entry (with thoughts on how we got here). *Cell Calcium* **42**(2):103-10.

Quesada, I., Chin, W.C. and Verdugo, P. (2003). ATP-independent luminal oscillations and release of Ca2+ and H+ from mast cell secretory granules: implications for signal transduction. Biophysical Journal **85:**963-970.

Quesada, I., Chin, W.C., Steed, J., Campos-Bedolla, P. and Verdugo, P. (2001). Mouse mast cell secretory granules can function as intracellular ionic oscillators. *Biophysical Journal* **80:**2133-2139.

Raja, R.A., Schmiegelow, K. and Frandsen, T.L. (2012). Asparaginase-associated pancreatitis in children. *British Journal of Haematology* **159:**18-27.

Raraty, M., Ward, J., Erdemli, G., Vaillant, C., Neoptolemos, J.P., Sutton, R. and Petersen, O.H. (2000). Calcium-dependent enzyme activation and vacuole formation in the apical granular region of pancreatic acinar cells. *Proceedings of the National Academy of Sciences USA* **97:**13126-31.

Reed, A.M., Husain, S.Z., Thrower, E., Alexandre, M., Shah, A., Gorelick, F.S. and Nathanson, M.H. (2011). Low extracellular pH induces damage in the pancreatic acinar cell by enhancing calcium signaling. *The Journal of Biological Chemistry* **286:**1919-1926.

Rice, L.V., Bax, H.J., Russell, L.J., Barrett, V.J., Walton, S.E., Deakin, A.M., Thomson, S.A., *et al.* (2013). Characterization of selective Calcium-Release Activated Calcium channel blockers in mast cells and T-cells from human, rat, mouse and guinea-pig preparations. *European Journal of Pharmacology* **704:**49-57.

Roberts, S.E., Williams, J.G., Meddings, D. and Goldacre, M.J. (2008). Incidence and case fatality for acute pancreatitis in England: geographical variation, social deprivation, alcohol consumption and aetiology – a record linkage study. *Alimentary Pharmacology and Therapeutics* **28**(7):931-41.

Roberts-Thomson, S.J., Peters, A.A., Grice, D.M. and Monteith, G.R. (2010). ORAI-mediated calcium entry: mechanism and roles, diseases and pharmacology. *Pharmacology and Therapeutics* **127**:121-30.

Röder, P.V., Wu, B., Liu, Y. and Han, W. (2016). Pancreatic regulation of glucose homeostasis. *Experimental and Molecular Medicine* **48:**e219.

Roos, J., DiGregorio, P.J., Yeromin, A.V., Ohlsen, K., Lioudyno, M., Zhang, S., Safrina, O., *et al.* (2005). STIM1, an essential and conserved component of store-operated Ca2+ channel function. *The Journal of Cell Biology* **169**(3):435-45.

Rosen, D., Lewis, A.M., Mizote, A., Thomas, J.M., Aley, P.K., Vasudevan, S.R., Parkesh, R., *et al.* (2009). Analogues of the nicotinic acid adenine dinucleotide phosphate (NAADP) antagonist Ned-19 indicate two binding sites on the NAADP receptor. *The Journal of Biological Chemistry* **284:**34930-34934.

Sadr-Azodi, O., Andrén-Sandberg, Å., Orsini, N. and Wolk, A. (2012). Cigarette smoking, smoking cessation and acute pancreatitis: a prospective population-based study. *Gut* **61:**262-7.

Sakurai, Y., Kolokolstov, A.A., Chen, C.C., Tidwell, M.W., Bauta, W.E., Klugbauer, N., Grimm, C., *et al.* (2015). Two-pore channels control Ebola virus host cell entry and are drug targets for disease treatment. *Science* **347:**6225.

Sankaran, S.J., Xiao, A.Y., Wu, L.M., Windsor, J.A., Forsmark, C.E. and Petrov, M.S. (2015). Frequency of progression from acute to chronic pancreatitis and risk factors: a meta-analysis. *Gastroenterology* **149:**1490-1500.

Schmiegelow, K., Müller, K., Mogensen, S.S., Mogensen, P.R., Wolthers, B.O., Stoltze, U.K., Tuckuviene, R., *et al.* (2017). Non-infectious chemotherapy-associated acute toxicities during childhood acute lymphoblastic leukemia therapy. *F1000Research* **6:**444.

Sclafani, A. and Ackroff, K. (2015). Flavor preference conditioning by different sugars in sweet ageusic Trpm5 knockout mice. *Physiology and Behaviour* **140:**156-163.

Shalbueva, N., Mareninova, O.A., Gerloff, A., Yuan, J., Waldron, R.T., Pandol, S.J., Gukovskaya, A.S., *et al.* (2013). Effects of oxidative alcohol metabolism on the mitochondrial permeability transition pore and necrosis in a mouse model of alcoholic pancreatitis. *Gastroenterology* **144**(2):437-446.

Sherwood, M.W., Prior, I.A., Voronina, S.G., Barrow, S.L., Woodsmith, J.D., Gerasimenko, O.V., Petersen, O.H., et al. (2007). Activation of trypsinogen in large endocytic vacuoles of pancreatic acinar cells. *Proceedings of the National Academy of Sciences USA* **104:**5674-5679.

Siech, M., Heinrich, P. and Letko, G. (1991). Development of acute pancreatitis in rats after single ethanol administration and induction of a pancreatic juice edema. *International Journal of Pancreatology* **8**(2):169-75.

Siegel, R.L., Miller, K.D. and Jemal, A. (2018). Cancer statistics. *A Cancer Journal for Clinicians* **68:**7-30.

Silverman, L.B., Gelber, R.D., Dalton, V.K., Asselin, B.L., Barr, R.D., Clavell, L.A., Hurwitz, C.A., *et al.* (2001). Improved outcome for children with acute lymphoblastic leukemia: results of DanaFarber Consortium Protocol 91-01. *Blood* **97:**1211-1218.

Singh, V.P., Bhagat, L., Navina, S., Sharif, R., Dawra, R.K. and Saluja, A.K. (2007). Protease-activated receptor-2 protects against pancreatitis by stimulating exocrine secretion. *Gut* **56**(7):958-64.

Singh, V.K., Moran, R.A., Afghani, E. and de-Madaria, E. (2015). Treating acute pancreatitis: what's new? *Expert Review of Gastroenterology and Hepatology* **9**(7):901-11.

Smyth, J.T., Dehaven, W.I., Bird, G.S., Putney, J.W. (2008). Ca2+-store-dependentand -independent reversal of Stim1 localization and function. *Journal of Cell Science* **121**:762-72.

Soh, U.J.K., Dores, M.R., Chen, B. and Trejo, J. (2010). Signal transduction by protease-activated receptors. *British Journal of Pharmacology* **160**(2):191-203.

Spanier, B.W., Dijkgraaf, M.G. and Bruno, M.J. (2008). Epidemiology, aetiology and outcome of acute and chronic pancreatitis: An update. *Best Practice and Research: Clinical Gastroenterology* **22:**45-63.

Stathopulos, P.B. and Ikura, M. (2013). Structure and function of endoplasmic reticulum STIM calcium sensors. *Current Topics in Membranes* **71:**59-93.

Stathopulos, P.B., Zheng, L., Li, G.Y., Plevin, M.J. and Ikura, M. (2008). Structural and mechanistic insights into STIM1-mediated initiation of store-operated calcium entry. *Cell* **110:**110-122.

Stewart, T.A., Yapa, K.T.D.S. and Monteith, G.R. (2015). Altered calcium signaling in cancer cells. B*iochimica et Biophysica Acta – Biomembranes* **1848**:2502-11.

Stiber, J., Hawkins, A., Zhang, Z.S., Wang, S., Burch, J., Graham, V., Ward, C.C., *et al.* (2008). STIM1 signalling controls store-operated calcium entry required for development and contractile function in skeletal muscle. *Nature Cell Biology* **10:**688-97.

Straub, S.V., Giovannucci, D.R. and Yule, D.I. (2000). Calcium wave propagation in pancreatic acinar cells. Functional interaction of inositol 1,4,5-trisphosphate receptors, ryanodine receptors and mitochondria. *The Journal of General Physiology* **116:**547-559.

Sun, S., Zhang, H., Liu, J., Popugaeva, E., Xu, N.J., Feske, S., White, C.L., *et al.* (2014). Reduced synaptic STIM2 expression and impaired store-operated calcium entry cause destabilization of mature spines in mutant presenilin mice. *Neuron* **82:**79-93.

Szabadkai, G., Simoni, A.M. and Rizzuto, R. (2003). Mitochondrial Ca2+ Uptake Requires Sustained Ca2+ Release from the Endoplasmic Reticulum. *The Journal of Biological Chemistry* **278:**15153-61.

Takemura, H., Hughes, A.R., Thastrup, O. and Putney, J.W. (1989). Activation of calcium entry by the tumor promoter thapsigargin in parotid acinar cells. Evidence that an intracellular calcium pool and not an inositol phosphate regulates calcium fluxes at the plasma membrane. *The Journal of Biological Chemistry* **264**(21):12266-71.

Takeshima, H., Nishimura, S., Matsumoto, T., Ishida, H., Kangawa, K., Minamino, N., Matsuo, H., *et al.* (1989). Primary structure and expression from complementary DNA of skeletal muscle ryanodine receptor. *Nature.* **339:**439-45.

Tepikin, A.V., Voronina, S.G., Gallacher, D.V. and Petersen, O.H. (1992). Pulsatile Ca2+ extrusion from single pancreatic acinar cells during receptor-activated cytosolic Ca2+ spiking. *The Journal of Biological Chemistry* **15:**14073-6.

Thorn, P., Lawrie, A.M., Smith, P.M., Gallacher, D.V. and Petersen, O.H. (1993). Local and global cytosolic Ca2+ oscillations in exocrine cells evoked by agonists and inositol trisphosphate. *Cell* **74:**661668.

Tian, C., Du, L., Zhou, Y. and Li, M. (2016). Store-operated CRAC channel inhibitors: opportunities and challenges. *Future Medicinal Chemistry* **8:**817-32.

Tinel, H., Cancela, J., Gerasimenko, J.V., Gerasimenko, O.V., Tepikin, A.V. and Peterson, O.H. (1999). Active mitochondria surrounding the pancreatic acinar granule region prevents spreading of inositol – evoked local cytosolic calcium signals. *European Molecular Biology Organisation Journal* **18:**4999- 5008.

Toescu, E.C., O'Neill, S.C., Petersen, O.H. and Eisner, D.A. (1992). Caffeine inhibits the agonist-evoked cytosolic Ca2+ signal in mouse pancreatic acinar cells by blocking inositol trisphosphate production. *The Journal of Biological Chemistry* **267:**23467-70.

Treepongkaruna, S., Thongpak, N., Pakakasama, S., Pienvichit, P., Sirachainan, N. and Hongeng, S. (2009). Acute pancreatitis in children with acute lymphoblastic leukemia after chemotherapy. *Journal of Pediatric Hematology/Oncology* **31:**812-815.

Vaeth, M., Zee, I., Concepcion, A.R., Maus, M., Shaw, P., Portal-Celhav, C., Zahra, A., *et al.* (2015). Ca2+ signaling but not store-operated Ca2+ entry is required for the function of macrophages and dendritic cells. *The Journal of Immunology* **195:**1202-17.

Van Kruchten, R., Braun, A., Feijge, M.A., Kuijpers, M.J., Riveragaldos, R., Kraft, P., Stoll, G., *et al.* (2012). Antithrombotic potential of blockers of store-operated calcium channels in platelets. *Arteriosclerosis, Thrombosis and Vascular Biology* **32:**1717-23.

Van Laethem, J.L., Robberecht, P., Résibois, A. and Devière, J. (1996). Transforming growth factor b promotes development of fibrosis after repeated courses of acute pancreatitis in mice. *Gastroenterology* **110:**576-582.

Varnai, P., Toth, B., Toth, D.J., Hunyady, L. and Balla, T. (2007). Visualization and manipulation of plasma membrane– endoplasmic reticulum contact sites indicates the presence of additional molecular components within the STIM1–Orai1 complex. *The Journal of Biological Chemistry* **282:**29678-29689.

Vervliet, T., Decrock, E., Molgó, J., Sorrentino, V., Missiaen, L., Levbaert, L., Smedt, H.D., *et al.* (2014). Bcl-2 binds to and inhibits ryanodine receptors. *Journal of Cell Science* **127**:2782-2792.

Vervliet, T., Parys, J.B. and Bultynck, G. (2016). Bcl-2 proteins and calcium signaling: complexity beneath the surface. *Oncogene* **35**:5079-5092.

Vervliet, T., Gerasimenko, J.V., Ferdek, P.E., Jakubowska, Petersen, O.H., Gerasimenko O.V. and Bultynck, G. (2018). BH4 domain peptides derived from Bcl-2/ Bcl-XL as novel tools against acute pancreatitis *Cell Death Discovery* **4:**58.

Vig, M., Dehaven, W.I., Bird, G.S., Billingsley, J.M., Wang, H., Rao, P.E., Hutchings, A.B., Jouvin, M.H., *et al.* (2008). Defective mast cell effector functions in mice lacking the CRACM1 pore subunit of store-operated calcium release-activated calcium channels. *Nature Immunology* **9:**89-96.

Vig, M., Peinelt, C., Beck, A., Koomoa, D.L., Rabah, D., Koblan-Huberson, M., Kraft, S., *et al.* (2006). CRACM1 is a plasma membrane protein essential for store-operated Ca2+ entry. *Science* **312**(5777):1220-3.

Vishy, M. (2016). Anatomy of the pancreas and spleen. *Surgery* **34:**261-265.

Voets, T., Prenen, J., Fleig, A., Vennekens, R., Watanabe, H., Hoenderop, J.G., Bindels, R.J., *et al.* (2001). CaT1 and the calcium release-activated calcium channel manifest distinct pore properties. *The Journal of Biological Chemistry* **276:**47767-47770.

Vonlaufen, A., Wilson, J.S. and Apte, M.V. (2008). Molecular mechanisms of pancreatitis: current opinion. *Journal of Gastroenterology and Hepatology* ***23*:**1339-1348.

Voronina, S., Collier, D., Chvanoy, M., Middlehurst, B., Beckett, A.J., Prior, I.A., Criddle, D.N., *et al.* (2015). The role of Ca^{2+} influx in endocytic vacuole formation in pancreatic acinar cells. *Biochemical Journal* **465:**405-412.

Voronina, S., Longbottom, R., Sutton, R., Petersen, O.H. and Tepikin, A. (2002a). Bile acids induce calcium signals in mouse pancreatic acinar cells. Implications for bile-induced pancreatic pathology. *The Journal of Physiology* **540**:49-55.

Voronina, S., Sukhomlin, T., Johnson, P.R., Erdemli, G., Petersen, O.H. and Tepikin, A. (2002b). Correlation of NADH and Ca2+ signals in mouse pancreatic acinar cells. *The Journal of Physiology* **539:**41-52.

Wakui, M., Osipchuk, Y.V. and Petersen, O.H. (1990). Receptor-activated cytoplasmic Ca2+ Spiking Mediated by Inositol trisphosphate is due to Ca2+-induced Ca2+ release. *Cell* **63:**1025-1032.

Wakui, M. and Petersen, O.H. (1990). Cytoplasmic Ca2+ oscillations evoked by acetylcholine or intracellular infusion of inositol trisphosphate or Ca2+ can be inhibited by internal Ca2+. *The Federation of European Biochemical Societies Journal* **263:**206-208.

Waldron, R.T., Chen, Y., Pham, H., Go, A., Su, H.Y., Hu, C., Wen, L., *et al.* (2019). The Orai Ca2+ channel inhibitor CM4620 targets both parenchymal and immune cells to reduce inflammation in experimental acute pancreatitis. *The Journal of Physiology* **597**:3085-3105.

Ward, J.B., Petersen, O.H., Jenkins, S.A. and Sutton, R. (1995). Is an elevated concentration of acinar cytosolic free ionised calcium the trigger for acute pancreatitis? *Lancet* **346**:1016-9.

Wen, Li., Voronia, S., Javed, M.A., Awais, M., Szatmary, P., Latawiec, D., Chvanov, M., *et al.* (2015). Inhibitors of ORAI1 prevent cytosolic calcium-associated injury of human pancreatic acinar cells and acute pancreatitis in 3 mouse models. *Gastroenterology* **149:**481-492.

Werner, J., Laposata, M., Fernandez-del Castillo, C., Saghir, M., Iozzo, R., Lewandrowski, K., Warshaw, A.L. (1997). Pancreatic injury in rats induced by fatty acid ethyl ester, a nonoxidative metabolite of alcohol. *Gastroenterology* **113**(1):286-94.

Wildi, S., Kleeff, J., Mayerle, J., Zimmermann, A., Böttinger, E.P., Wakefield, L., Büchler, M.W., *et al.,* (2007). Suppression of transforming growth factor b signalling aborts caerulein induced pancreatitis and eliminates restricted stimulation at high caerulein concentrations. *Gut* **56:**685-692.

Williams, J.A. (2001). Intracellular signalling mechanisms activated by cholecystokinin – regulating synthesis and secretion of digestive enzymes in pancreatic acinar cells. *Annual Review of Physiology* **63:**77-97.

Williams JA. (2008). Receptor-mediated signal transduction pathways and the regulation of pancreatic acinar cell function. *Current Opinion in Gastroenterology* **24**(5): 573-579.

Wolthers, B.O., Frandsen, T.L., Abrahamsson, J., Albertsen, B.K., Helt, L.R., Heyman, M., Jónsson, O.G., *et al.* (2017). Asparaginase-associated pancreatitis: a study on phenotype and genotype in the NOPHO ALL2008 protocol. *Leukemia* **31:**325-332.

Wu, B.U. and Banks, P.A. (2013). Clinical management of patients with acute pancreatitis. *Gastroenterology* **144:**1272-81.

Wu, M.M., Buchanan, J., Luik, R.M. and Lewis, R.S. (2006). Ca2+ store depletion causes STIM1 to accumulate in ER regions closely associated with the plasma membrane. *Journal of Cell Biology* **174:**803-813.

Yadav, D. and Lowenfels, A.B. (2013). The epidemiology of pancreatitis and pancreatic cancer. *Gastroenterology* **144:**1252-1261.

Yamasaki, M., Masgrau, R., Morgan, A., Churchill, G.C., Patel, S., Ashcroft, S.J.H. and Galione, A. (2004). Organelle selection determines agonist-specific Ca2+ signals in pancreatic acinar and beta cells. *Journal of Biological Chemistry* **279:**7234-7240.

Yamasaki, M., Thomas, J.M., Churchill, G.C., Garnham, C., Lewis, A.M., Cancela, J.M., Patel, S., *et al.* (2005). Role of NAADP and cADPR in the induction and maintenance of agonist-evoked Ca2+ spiking in mouse pancreatic acinar cells. *Current Biology* **15:**874-8.

Yang, S., Zhang, J.J. and Huang, X. Y. (2009). Orai1 and STIM1 are critical for breast tumor cell migration and metastasis. *Cancer Cell* **15:**124-34.

Yeromin, A., Zhang, S., Jiang, W., Yu, Y., Safrina, O. and Cahalan, M. (2006). Molecular identification of the CRAC channel by altered ion selectivity in a mutant of Orai. *Nature* **443:**226-229.

Yoo, S.H. (2000). Coupling of the IP3 receptor/Ca2+ channel with Ca2+ storage proteins chromogranins A and B in secretory granules. *Trends in Neurosciences* **23:**424-428.

Yoshino, T., Ishikawa, J., Ohga, K., Morokata, T., Takezawa, R., Morio, H., Okada, Y., *et al.* (2007). YM58483, a selective CRAC channel inhibitor, prevents antigen-induced airway eosinophilia and late phase asthmatic responses via Th2 cytokine inhibition in animal models. *European Journal of Pharmacology* **560:**225-233.

Yuan, J.P., Zeng, W., Huang, G.N., Worley, P.F., Muallem, S. (2007). STIM1 heteromultimerizes TRPC channels to determine their function as store-operated channels. *Nature Cell Biology* **9:**636-645.

Yule, D.I., Lawrie, A.M. and Gallacher, D.V. (1991). Acetylcholine and cholecystokinin induce different patterns of oscillating calcium signals in pancreatic acinar cells. *Cell Calcium* 12:145-51.

Zeiger, W., Ito, D., Swetlik, C., Oh-hora, M., Villereal, M.L. and Thinakaran, G. (2011). Stanniocalcin 2 is a negative modulator of store-operated calcium entry. *Molecular and Cell Biology* **31:**3710-22.

Zhang, S.L., Yeromin, A.V., Zhang, X.H.F., Yu, Y., Safrina, O., Penna, A., Stauderman, K.A., *et al.* (2006). Genome-wide RNAi screen of Ca(2+) influx identifies genes that regulate Ca(2+) release-activated Ca(2+) channel activity. *Proceedings of the National Academy of Sciences USA* **103**(24):9357-62.

Zhang, S., Yu, Y., Roos, J., Kozak, J., Deerinck, T., Ellisman, M., Stauderman, K., *et al*. (2005). STIM1 is a Ca2 sensor that activates CRAC channels and migrates from the Ca2 store to the plasma membrane. *Nature* **437:**902-905.

Zhang, X., Jin, T., Shi, N., Yao, L., Yang, X., Han, C., Wen, L., *et al.* (2019). Mechanisms of pancreatic injury induced by basic amino acids differ between l-Arginine, l-Ornithine, and l-Histidine. *Frontiers in Physiology* **9:**1922.

Zhou, Y., Meraner, P., Kwon, H.T., Machnes, D., Oh-hora, M., Zimmer, J., Huang, Y., *et al.* (2010). STIM1 gates the store-operated calcium channel ORAI1 in vitro. *Nature Structural Molecular Biology* **17**(1):112-6.

Zweifach, A. and Lewis, R.S. (1993). Mitogen-regulated Ca2+ current of T lymphocytes is activated by depletion of intracellular Ca2+ stores. *Proceedings of the National Academy of Sciences USA* **90:**6295-6299.

Zylińska, L. and Soszyński, M. (2000). Plasma membrane Ca2+-ATPase in excitable and nonexcitable cells. *Acta Biochimica Polonica* **47**(3):529-39.